

**GRAFT COPOLYMERIZATION OF**  
**p-BENZOPHENONEOXYCARBONYLPHENYL ACRYLATE**  
**ONTO**  
**HIGH DENSITY POLYETHYLENE**

**by**  
**UĞUR SOYKAN**

**THESIS SUBMITTED TO**  
**THE GRADUATE SCHOOL OF NATURAL AND APPLIED SCIENCES**  
**OF**  
**THE ABANT İZZET BAYSAL UNIVERSITY**  
**IN PARTIAL FULFILLMENT OF THE REQUIREMENTS FOR THE DEGREE OF**  
**MASTER OF SCIENCE**  
**IN**  
**THE DEPARTMENT OF CHEMISTRY**

**JANUARY 2013**

Approval of the Graduate School of Natural and Applied Sciences

Prof. Dr. Yaşar DÜRÜST

Director

I certify that this thesis satisfies all the requirements as a thesis for the degree of Master of Science.

Prof. Dr. Çetin BOZKURT

Head of Department

This is to certify that we have read this thesis and that in our opinion it is fully adequate in scope and quality, as a thesis for the degree of Master of Sciences.

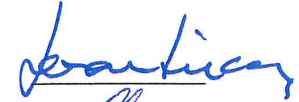


Yrd. Doç. Dr. Sedat ÇETİN

Advisor

Examining Committee Members

1- Prof. Dr. Teoman TİNÇER (M.E.T.U., CHEM.)



2- Prof. Dr. Zeki ÖKTEM (KIRIKKALE Ü., CHEM.)



3- Assist. Prof. Dr. Sedat ÇETİN (A.İ.B.Ü., CHEM.)



**ABSTRACT**

**GRAFT COPOLYMERIZATION OF**

**p-BENZOPHENONEOXYCARBONYLPHENYL ACRYLATE**

**ONTO**

**HIGH DENSITY POLYETHYLENE**

Soykan, Uğur

M.Sc., Department of Chemistry

Advisor: Yrd. Doç. Dr. Sedat ÇETİN

January 2013, 78 Pages

The monomer, p-benzophenoneoxycarbonylphenyl acrylate (BPOCPA) was synthesized by condensation reaction of p-acryloyloxybenzoyl chloride (ABC), prepared by refluxing p-acryloyloxybenzoic acid (ABA) in thionyl chloride, with p-hydroxybenzophenone (HBP). The synthesis of monomer was studied by trying various methods, and the maximum yield, 57%, was achieved by refluxing ABC and

HBP in xylene. Poly(p-benzophenoneoxycarbonylphenyl acrylate), poly(BPOCPA), was obtained by solution and bulk melt polymerization by the initiation of dicumyl peroxide (DCP).

The graft copolymerization of the monomer onto high density polyethylene (HDPE) was successfully conducted with bulk melt polymerization. The graft copolymerization was investigated at varying concentrations of BPOCPA in the reaction mixture (5%, 10%, 15%, 20%, 30%, and 40%) and at constant reaction temperature (140°C). The amount of grafting increased with increasing concentration of the monomer and reached the maximum, 14.2% poly(BPOCPA), at 30% BPOCPA in the reaction medium, and followed by a considerable decrease reducing to 5.79% poly(BPOCPA) at 40% BPOCPA. The maximum % grafting (percentage of grafted poly(BPOCPA) with respect to total poly(BPOCPA) in the product) was observed to be 85.41% at 10% BPOCPA mixture.

Poly(BPOCPA) and the graft coproducts were characterized by several techniques, DSC, SEM, FTIR, TG/IR systems and mechanical testing. In DSC studies, the crystalline melting temperature of poly(BPOCPA) was observed at 231°C, whereas, among the graft coproducts, it was detected only in the sample with 39.1% poly(BPOCPA) at 235°C.

The decomposition mechanism of poly(BPOCPA) and graft coproducts were studied by TG/IR. The polymers degraded predominantly by the decomposition of side groups giving mainly carbondioxide and the compounds containing phenolic and vinylic groups.

The mechanical properties of the graft coproducts studied at room temperature. An explicit improvement was detected particularly in tensile strength

and modulus. The maximum tensile strength and modulus were found as 26.0 and 605 MPa, respectively, revealed with the sample containing 9.32% poly(BPOCPA). The impact strength of the products increased initially with the percentage of poly(BPOCPA), and the maximum strength, 52.39 kJm<sup>-2</sup>, was achieved with the sample including 19.90% poly(BPOCPA), then followed by a dramatic decrease.

The tensile and impact fractured surfaces of the products studied by scanning electron microscopy (SEM) showed homogeneous structure without any phase separation. At low contents of poly(BPOCPA) the samples were mainly ductile while at high percentages they displayed brittle nature, with an increasing trend with the content.

**Key words:** Polyethylene, p-benzophenoneoxycarbonylphenyl acrylate, Poly(p-benzophenoneoxycarbonylphenyl acrylate), side-chain liquid crystalline polymers and graft copolymerization.

## ÖZET

### p-BENZOFENONOKSİKARBONİLFENİL AKRİLAT'IN

### YÜKSEK YOĞUNLUKLU POLİETİLEN ÜZERİNE

### AŞI POLİMERİZASYONU

Soykan, Uğur

Yüksek Lisans Tezi, Kimya Bölümü

Tez Danışmanı: Yrd. Doç. Dr. Sedat Çetin

Ocak 2013, 78 sayfa

p-Benzofenonoksikarbonilfenil akrilat (BPOCPA) monomeri p-akriloiloksibenzoik asitin (ABA) geri soğutucu altında tiyonil klorür içerisinde kaynatılmasıyla hazırlanan p-akriloiloksibenzoil klorürün (ABC) p-hidroksibenzofenon (HBP) ile kondensasyon tepkimesiyle sentezlendi. Monomerin sentezlenmesi farklı yöntemler denenerek çalışıldı ve maksimum verim, %57, ABC ve HBPnin ksilen içerisinde geri soğutucu altında kaynatılmasıyla elde edildi. Polip-

benzofenonoksikarbonilfenil akrilat, poly(BPOCPA), çözeltili ve dikünil peroksit (DCP) başlatıcısının kullanıldığı kütle polimerleşme ile elde edilmiştir.

BPOCPA'nın HDPE üzerine aşırı kopolimerleşmesi kütle polimerleşmesi ile başarılı bir şekilde gerçekleştirildi. Aşırı kopolimerleşme monomerin tepkime ortamındaki farklı derişimlerinde (% 5, 10, 15, 20, 30 ve %40) ve 140°C sabit tepkime sıcaklığında çalışıldı. Takılma miktarı monomer derişiminin artmasıyla arttı ve %30 BPOCPA derişiminde maksimum takılmadan (%14,2) sonra hızlı bir şekilde azalarak %40 BPOCPA'da %5,79 poli(BPOCPA)'ya düştü. Maksimum aşılama (ürünlerde toplam poli(BPOCPA) miktarına göre takılan poli(BPOCPA) yüzdesi), %10 BPOCPA tepkime karışımında %85,41 olarak bulunmuştur.

Poli(BPOCPA) ve aşırı ürünler DSC, SEM, FTIR, TG/IR sistemleri ve mekanik test yöntemleriyle karakterize edildi. DSC ölçümlerinde, 231°C de gözlenen poli(BPOCPA)'nın kristal erime sıcaklığı aşırı ürünler arasında sadece %39,1 poli(BPOCPA) içeren örnekte 235°C de kaydedilmiştir.

Poli(BPOCPA) ve aşırı ürünlerin ısı kararlılığı ve bozunma mekanizması termogravimetri ve FTIR (TG/IR) sistemi ile çalışıldı. Bozunma genelde yan grupların başlıca karbondioksit ve fenolik ve vinilik gruplar içeren bileşiklere parçalanmasıyla gerçekleştiği görülmüştür.

Aşırı ürünlerin mekanik özellikleri oda sıcaklığında çalışıldı. Özellikle gerilim direnci ve modül değerlerinde önemli iyileşme görüldü. %9,32 poli(BPOCPA) içeren örnek ile maksimum gerilim direnci ve modül değeri sırasıyla 26,0 ve 605 MPa olarak kaydedildi. Ürünlerin çarpma direnci, örneklerde poli(BPOCPA) yüzdesi ile artarak %19,90 poli(BPOCPA) ile maksimum dirence (52,39 kJm<sup>-2</sup>) ulaşıktan sonra hızlı bir düşüş göstermiştir.

Ürünlerin gerilim ve çarpma etkisiyle kırılan yüzeylerinin taramalı elektron mikroskobu ile incelenmesinde elde edilen ürünlerin faz ayrımı olmadan homojen yapı oluşturduğu gözlenmiştir. Düşük poli(BPOCPA) içeren örneklerde çoğunlukla sünek, yüksek içerikli ürünlerde ise poli(BPOCPA) yüzdesi ile artan kırılma yapı gözlenmiştir.

**Anahtar Kelimeler:** Polietilen, p-benzofenonoksikarbonilfenil akrilat, poli(p-benzofenonoksikarbonilfenil akrilat), yan-zincir sıvı kristal polimerler, aşı kopolimerizasyonu



*TO MY FAMILY AND MY LOVE*

## ACKNOWLEDGEMENTS

I would like to express my deepest gratitude to my advisor Yrd. Doç. Dr. Sedat ÇETİN for his inspiration, endless support, guidance, encouragement, patience and his enthusiasm throughout this study that helps me flourish my polymer vision and polymer love throughout the research.

I wish to express my sincere thanks to my precious and lovely family, my love, Derya UĞUR and my brother-in-law, Cem BIYIKLI for their unshakable faith in me and her willingness to endure with me the vicissitudes of my endeavor.

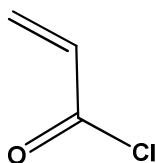
I would like to thank also jury members, Prof. Dr. Teoman TİNÇER and Prof. Dr. Zeki ÖKTEM for their cooperation and suggestions for this study.

I would gratefully like to extend my sincere thanks to Yrd. Doç. Dr. Gürcan YILDIRIM, Fırat KARABOĞA, Ali Yiğit KUTLUCA, Mehmet AVCI, Özgür İŞGÜDER, Salih SEKİTMEN and Musa DOĞRUER, who act as my brother all parts of my life.

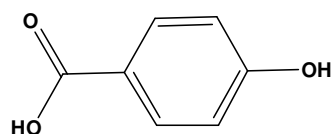
I would also like to thank my best friends Behiye ÖZTÜRK ŞEN and Ayşen ÇETİN for their support, and help in experimental process. I wish to express my sincere thanks to Metin ALKAN for preparation of desired glasswares.

Gratitude is also extended to the Department of Chemistry of A.İ.B.U. for providing the necessary equipment and chemicals which made this work possible, and all the members of the department who aided in the completion of the work.

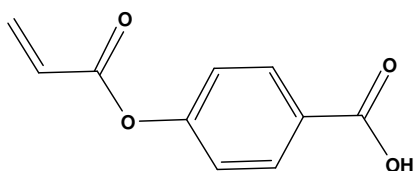
## FORMULAE



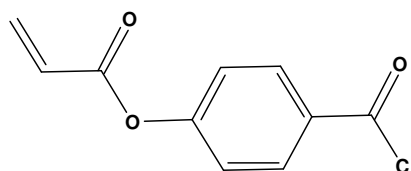
**Acryloyl Chloride**



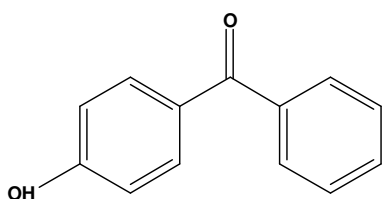
**p-Hydroxybenzoic Acid**



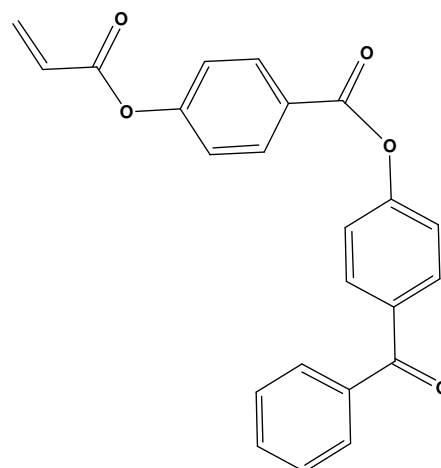
**p-Acryloyloxybenzoic Acid (ABA)**



**p-Acryloyloxybenzyl Chloride (ABC)**



**4-Hydroxybenzophenone (HBP)**



**p-Benzophenoneoxycarbonylphenyl  
Acrylate (BPOCPA)**

## TABLE OF CONTENTS

<b>ABSTRACT .....</b>	<b>iii</b>
<b>ÖZET.....</b>	<b>vi</b>
<b>ACKNOWLEDGEMENTS.....</b>	<b>x</b>
<b>FORMULAE .....</b>	<b>xi</b>
<b>TABLE OF CONTENTS.....</b>	<b>xii</b>
<b>LIST OF TABLES .....</b>	<b>xvi</b>
<b>LIST OF FIGURES .....</b>	<b>xvii</b>
<b>ABBREVIATIONS .....</b>	<b>xxii</b>
<b>CHAPTER 1 .....</b>	<b>1</b>
<b>INTRODUCTION.....</b>	<b>1</b>
1.1. General Review on HDPE, LCPs and Their Blends .....	2
1.1.1. High-Density Polyethylene (HDPE).....	2
1.1.2. Liquid Crystalline Polymers, LCPs .....	5
1.1.3. Blends and Combining Thermoplastics with LCPs .....	7
1.2. Reinforcement of Polyolefins with LCPs.....	11
1.3. Graft Copolymerization.....	13
1.4. Side-Chain Liquid Crystal, Poly(p-Benzophenoneoxycarbonylphenyl Acrylate).....	15
1.4.1. Side Chain Liquid Crystals, SCLCPs.....	15
1.4.2 Poly(p-Benzophenoneoxycarbonylphenyl Acrylate), Poly(BPOCPA) .	17
1.5. Aim of the Work.....	18

<b>CHAPTER 2 .....</b>	<b>19</b>
<b>EXPERIMENTAL DETAILS .....</b>	<b>19</b>
2.1. Chemicals and Materials Used .....	19
2.1.1. Solvents and Reagents.....	19
2.1.2. Preparation of Powder High Density Polyethylene .....	19
2.2. Synthesis of p-Benzophenoneoxycarbonylphenyl Acrylate, BPOCPA .....	20
2.2.1. Preparation of p-Acryloyloxybenzoic Acid, ABA.....	20
2.2.2. Preparation of p-Acryloyloxybenzoyl Chloride, ABC .....	21
2.2.3. Preparation of p-Benzophenoneoxycarbonylphenyl Acrylate .....	21
2.3. Polymerization of the Monomer, BPOCPA .....	23
2.4. Graft Copolymerization of BPOCPA.....	24
2.5. Characterization and Instruments .....	26
2.5.1. FTIR Measurements.....	26
2.5.2. <sup>1</sup> H NMR Measurements .....	26
2.5.3. Differential Scanning Calorimeter (DSC) Analysis.....	26
2.5.4. TG/IR Measurements .....	27
2.5.5. Mechanical Properties.....	27
2.5.6. Scanning Electron Microscope (SEM) Study .....	28
2.5.7. Elemental Analysis of the Monomer .....	28
<b>CHAPTER 3 .....</b>	<b>29</b>
<b>RESULTS AND DISCUSSION .....</b>	<b>29</b>
3.1. Characterizations .....	29
3.1.1. Characterization of High Density Polyethylene.....	29
3.1.2. Characterization of p-Acryloyloxybenzoic Acid .....	30
3.1.3. Characterization of p-Acrloyloxybenzoyl Chloride.....	31

3.1.4. Characterization of p-Benzophenoneoxycarbonylphenyl Acrylate .....	32
3.1.5. Characterization of Poly(p-Benzophenoneoxycarbonylphenyl Acrylate) .....	34
3.1.6 Graft Copolymerization of BPOCPA onto HDPE.....	36
3.1.7. Characterization of the Graft Copolymerization Products.....	39
3.2. TG/IR Analysis of the Products .....	43
3.2.1. TG/IR Analysis of Poly(BPOCPA) .....	43
3.2.2. TG/IR Analysis of the Graft Copolymerization Products.....	50
3.3. Mechanical Properties of the Polymers.....	57
3.4. SEM Analysis of the Polymers .....	63
<b>CHAPTER 4 .....</b>	<b>72</b>
<b>CONCLUSION.....</b>	<b>72</b>
<b>REFERENCES.....</b>	<b>74</b>

## LIST OF TABLES

Table 1.1. Typical values of major polyethylene types .....	4
Table 2.1. The content of poly(BPOCPA) in the graft copolymerization products with concentration of BPOCPA in the reaction mixture ... ..	38
Table 3.1. Ultimate tensile strength of the products with % poly(BPOCPA) in samples .....	60
Table 3.2. Young's modulus of the products with % poly(BPOCPA) in samples .....	61
Table 3.3. Impact strength of HDPE and the products with % poly(BPOCPA) in samples. NB denotes 'Not Broken' samples .....	62

## LIST OF FIGURES

Figure 1.1. Arrangements of phase sequences in LCPs .....	6
Figure 1.2. Orientability of a rigid rod in simple shear and uniaxial extensional flow fields. ....	9
Figure 1.3. The structure of a graft copolymer .....	14
Figure 1.4. Possible SCLCPs (a) rod-like terminal, (b) disc-like, (c) rod-like lateral.....	16
Figure 2.1. Reaction between p-hydroxybenzoic acid and acryloyl chloride.....	20
Figure 2.2. Reaction between p-acryloyloxybenzoic acid and thionyl chloride.....	21
Figure 2.3. Reaction between p-hydroxybenzophenone and p-acryloyloxybenzoyl chloride.....	23
Figure 2.4. Graft copolymerization between BPOCPA and HDPE.....	25
Figure 3.1. FTIR spectrum of the virgin HDPE.....	29
Figure 3.2. DSC thermogram of the virgin HDPE.....	30
Figure 3.3. FTIR spectrum of BPOCPA .....	32
Figure 3.4. Proton scheme of BPOCPA.....	33
Figure 3.5. The <sup>1</sup> H-NMR spectrum of BPOCPA.....	33
Figure 3.6. DSC thermogram of BPOCPA .....	34
Figure 3.7. FTIR spectrum of poly(BPOCPA) .....	35
Figure 3.8. DSC thermogram of poly(BPOCPA) .....	36



Figure 3.9. Dependence of percent grafting on concentration of BPOCPA in reaction mixture .....	38
Figure 3.10. FTIR spectrum of the product with 13.66% poly(BPOCPA).....	39
Figure 3.11. FTIR spectrum of the product with 39.10% poly(BPOCPA).....	40
Figure 3.12. DSC thermogram of the product with 39.10% poly(BPOCPA).....	41
Figure 3.13. DSC thermogram of the product 13.66% poly(BPOCPA).....	42
Figure 3.14. DSC thermogram of a) annealed HDPE and b) the sample of HDPE with 2% DCP heated to 140°C .....	42
Figure 3.15. TGA thermogram of poly(BPOCPA) in nitrogen. ....	45
Figure 3.16.a. FTIR spectrum of the decomposition products formed at 322°C in nitrogen. ....	45
Figure 3.16.b and c. FTIR spectrum of the decomposition products formed at b) 378°C, and c) 405°C in nitrogen.....	46
Figure 3.16.d. FTIR spectrum of the decomposition products formed at 530°C in nitrogen. ....	47
Figure 3.17. TGA thermogram of poly(BPOCPA) in air.....	48
Figure 3.18.a. FTIR spectrum of the decomposition products formed at 284°C in air.....	48
Figure 3.18.b and c. FTIR spectra of the decomposition products formed at b) 385°C, and c) 450°C in air.....	49
Figure 3.18.d. FTIR spectrum of the decomposition products formed at 492°C in air.....	50
Figure 3.19. TGA thermogram of the product with 13.66% poly(BPOCPA) in nitrogen. ....	51

Figure 3.20. TGA thermogram of the product with 39.10% poly(BPOCPA) in nitrogen. ....	51
Figure 3.21.a. FTIR spectrum of the decomposition products formed at 364°C during the heating of product containing 13.66% poly(BPOCPA) in nitrogen. ....	52
Figure 3.21.b and c. FTIR spectra of the decomposition products formed at b) 447°C, and c) 572°C during the heating of product containing 13.66% poly(BPOCPA) in nitrogen.....	53
Figure 3.22.a and b. FTIR spectra of the decomposition products formed at a) 281°C, and b) 350°C during the heating of product containing 39.10% poly(BPOCPA) in nitrogen.....	54
Figure 3.23. TGA thermogram of the product with 13.66% poly(BPOCPA) in air.....	55
Figure 3.24. TGA thermogram of the product with 39.10% poly(BPOCPA) in air.....	55
Figure 3.25. FTIR spectrum of the decomposition products formed at 326°C during the heating of the product containing 13.66% poly(BPOCPA) in air. ....	56
Figure 3.26. FTIR spectrum of the decomposition products formed at 381°C during the heating of the product containing 13.66% poly(BPOCPA) in air. ....	56
Figure 3.27. Stress-strain curve of HDPE and the graft copolymerization products with the content of 4.97, 9.32, 13.66, 19.90, 28.28 and 39.10% poly(BPOCPA).....	58

Figure 3.28. Magnified stress-strain curve of HDPE and the graft copolymerization products with the content of 4.97, 9.32, 13.66, 19.90, 28.28 and 39.10% poly(BPOCPA). .....	59
Figure 3.29. Dependence of ultimate strength on the content of poly(BPOCPA).....	60
Figure 3.30. Dependence of Young's modulus on the content of poly(BPOCPA). ...	61
Figure 3.31. Dependence of impact strength on the content of poly(BPOCPA). .....	63
Figure 3.32. SEM photograph of poly(BPOCPA)-g-PE (4.97% poly(BPOCPA)), after obtained from tensile test.....	64
Figure 3.33. SEM photograph of poly(BPOCPA)-g-PE (9.32% poly(BPOCPA)), after obtained from tensile test .....	65
Figure 3.34. SEM photograph of poly(BPOCPA)-g-PE (13.66% poly(BPOCPA)), after obtained from tensile test .....	65
Figure 3.35. SEM photograph of poly(BPOCPA)-g-PE (13.66% poly(BPOCPA)), after obtained from tensile test .....	66
Figure 3.36. SEM photograph of poly(BPOCPA)-g-PE (19.90% poly(BPOCPA)), after obtained from tensile test .....	66
Figure 3.37. SEM photograph of poly(BPOCPA)-g-PE (28.28% poly(BPOCPA)), after obtained from tensile test. ....	67
Figure 3.38. SEM photograph of poly(BPOCPA)-g-PE (28.28% poly(BPOCPA)), after obtained from tensile test. ....	67
Figure 3.39. SEM photograph of poly(BPOCPA)-g-PE (39.10% poly(BPOCPA)), after obtained from tensile test.. .....	68
Figure 3.40. SEM photograph of poly(BPOCPA)-g-PE (13.66% poly(BPOCPA)), after obtained from impact test.....	69

Figure 3.41.	SEM photograph of poly(BPOCPA)-g-PE (13.66% poly(BPOCPA)), after obtained from impact test.....	69
Figure 3.42.	SEM photograph of poly(BPOCPA)-g-PE (13.66% poly(BPOCPA)), after obtained from impact test.....	70
Figure 3.43.	SEM photograph of poly(BPOCPA)-g-PE (28.28% poly(BPOCPA)), after obtained from impact test.....	70
Figure 3.44.	SEM photograph of poly(BPOCPA)-g-PE (39.10% poly(BPOCPA)), after obtained from impact test.....	71

## ABBREVIATIONS

**HDPE:** High Density Polyethylene

**TP:** Thermoplastic

**LCP:** Liquid Crystalline Polymer

**ABA:** p-Acryloyloxybenzoic Acid

**ABC:** p-Acryloyloxybenzoyl Chloride

**BPOCPA:** p-Benzophenoneoxycarbonylphenyl Acrylate

**DCM:** Dicumyl Peroxide

**Poly(BPOCPA):** Poly(p-Benzophenoneoxycarbonylphenyl Acrylate)

**Poly(BPOCPA)-g-HDPE:** Poly(p-Benzophenoneoxycarbonylphenyl Acrylate)-graft-High Density Polyethylene

**DSC:** Differential Scanning Calorimetry

**TG/IR:** Thermogravimetry/Infrared Spectroscopy

**FTIR:** Fourier Transform Infrared Spectrometry

**SEM:** Scanning Electron Microscopy

## **CHAPTER 1**

### **INTRODUCTION**

Polymers are vital parts of our daily life wherever we look. Their consumption is continuously growing up owing to increasing demand for using in many application areas [1] and these forces out the scientists to improve their properties. The modification of polymers possesses an importance because it presents a relatively easy and economical way of production of new materials to expand the the range of polymer applications. Therefore, for many years, polyolefins and their copolymers have received increased research interest regarding the functionalized and engineered polyolefins modified and with superior properties for new materials and with the advantage of having simple chemical structures and fascinating hierarchical structural organizations possible [2].

The modification of polymers by grafting or copolymerization is important because the modified properties induce macromolecules to have raised intermolecular interactions and possible crosslinking. The surface chemistry and physics of polymers can also be altered by several surface modifying techniques such as surface coating, degradation, hydrolysis, and radiation induced, photochemistry-induced, or catalytic-initiated graft copolymerization. On the other hand, a remarkable approach has been revealed in the modification of polymeric material by graft copolymerization for producing functional polyolefines. Depending on this

intention, varying functional groups can be grafted and thus some desirable properties may be imparted into the polymer by graft copolymerization without a change in the architecture of the polymer backbone, which presents a commercial importance in polymer applications. Besides the enhancement in compatibility for blends and composites, tensile strength, modulus, abrasion resistance, adhesion and also thermal and photochemical stability may be improved by grafting [3].

## **1.1. General Review on HDPE, LCPs and Their Blends**

### **1.1.1. High-Density Polyethylene, HDPE**

Polyethylene (PE) is one of the most commonly utilized thermoplastic polymers in wide range of applications. PE plastics acquire a good reputation in vast areas owing to the fact that they have the generally advantageous properties of toughness, good barrier properties to moisture or else. In addition that, not only PE has ease manufacture process due to their relatively low melting point ranges [4] but also it is the least costly of the major synthetic polymers [5]. Polyethylene owing to being regarded as high molecular weight paraffin may be expected as a rather inert material. Its high chemical resistance which leads to be processed in a variety of ways (blown film, pipe extrusion, blow molding, injection molding, etc.) into myriad shapes and devices and its remarkable flexibility makes it indispensable for the plastic industry [5]. It is unaffected by most acids, alkalis and aqueous solutions and its electrical insulating properties are outstanding. However, the practical applications of PE materials are restricted owing to lack of chemical functionality, difficulty in dyeing, low strength and modulus, low melting and sticking temperature, inadequate compatibility with other synthetic polymers. To improve this

commodity polymer via the chemical modification of PE by introduction of functional groups into macromolecules, by grafting of functional compounds to PE backbone, and reinforcement of PE by fibers, the importance of which is still in progress today.

The monomer is derived from either modifying natural gas (a methane, ethane, propane mix) or from the catalytic cracking of crude oil into gasoline and it polymerized to give PE [6]. The original polyethylene (LDPE: low density polyethylene) has been supplemented with two other extensively-used types –high-density polyethylene (HDPE) and linear low-density polyethylene (LLDPE). Other classifications are occasionally used for particular specialized polyethylene polymers such as very-low-density polyethylene (VLDPE), medium-density polyethylene (MDPE), ultra high molecular weight polyethylene (UHMWPE). That is, industrial polyethylenes are commonly classified and named using acronyms that incorporate resin density or molecular weight. When considering the density of polyethylene which is inverse proportional to chain branching, the types of polyethylenes obtained from various commercial processes differ in the degree of branching which leads several properties of polymers. The presence of branches reduces the ability of polymer chains to pack together closely and regularly, and thus is responsible for the difference in the degree of crystallinity, which also controls the plastics' melting point ranges. The more highly branched polymers have the lower density, crystalline melting point, stiffness, surface hardness, and softening temperature and greater permeability to gases and vapors [7]. Typical values of PE parameters are listed in the following table [5]:



Table 1.1. Typical values of major polyethylene types

	Density, g/cm <sup>3</sup>	Degree of Crystallinity, %	Melting Point Range, °C	Molecular Weight
LDPE	0.915-0.940	45-55	105-115	10,000-50,000
LLDPE	0.915-0.926	30-45	112-124	50,000-200,000
HDPE	0.940-0.970	70-90	120-130	250,000-500,000
UHMWPE	0.940-0.965	60-85	130-140	500,000-1,000,000

Among the three types of commercially PE, high density (linear) polyethylene is produced by four methods. Three of them involve solution or slurry processes by which differ mainly in the nature of the catalyst used. Ziegler processes involve the operation generally at high pressures slightly above atmospheric (2-4 atm) and the temperatures of 50-75°C. The catalyst of the process is usually based on titanium tetrachloride/aluminium alkyl. Ziegler-Natta catalyst is carried out by slurry and gas phase processes. Philips processes involve the use of chromium oxide catalyst on silica or silica/alumina support. Phillips process takes place at a temperature between 85-110°C. The catalysts of the Philips processes lead to almost completely linear polyethylene chains containing up to three methyl groups per 1000 carbon atoms without any ethyl or butyl branches [8]. Standard Oil processes are similar to Philips processes, in which the pressures of 40-100 atm are employed in the temperature region of 200-300°C. The catalyst of the method consists of a metal oxide such as molybdenum trioxide on a support which may be alumina, titanium dioxide or zirconium dioxide. The polyethylene obtained by the Standard Oil processes, as in Philips processes, is almost completely linear. In Union Carbide

process, on the other hand, ethylene is polymerized in the gas phase. Pressures of 7-20 atm and temperatures of about 100°C are used. In the polymerization supported organochromium compounds such as chromacene are employed.

Under these manufacture conditions; HDPE clearly possesses larger density and degree of crystallinity, great chain length and molar mass about many hundred thousands. This rigid, short chain branching and rough polymer has extraordinary impact strength, high modulus, yield and tensile properties relative to LLDPE and MDPE. That it becomes one of the best known impact-resistant thermoplastics available and self-lubricating characteristics and quickly spring back to its original shape easily is remarkable. Furthermore, HDPE has more opacity property and very good chemical resistance to corrosives, while certain hydrocarbons cause only a light surface swelling at moderate temperature. Moisture and water (including saltwater) have no affect on HDPE [9]. Because of the fact that it has linear structure with little entanglements in the melt, HDPE molecules have a tendency to be aligned in the direction of flow when processed in the melt. While cooling, speedy crystallization and high shrinkage occur because of this orientation [6-9].

### **1.1.2. Liquid Crystalline Polymers, LCPs**

The liquid crystal state is a distinct phase of matter observed between the crystalline (solid) and isotropic (liquid) states. Liquid crystalline polymers (LCPs) are the kind of polymers composed of extended, rod-like and rigid molecules. The polymers that form liquid crystal organization in solution are called lyotropic LCPs, whereas those that form from melt in a certain temperature range are termed as thermotropic LCPs. There exist many types of liquid crystal states that based on the

degree of order in the system and primarily can be classified into three groups due to their arrangements as nematic, smectic and cholesteric.

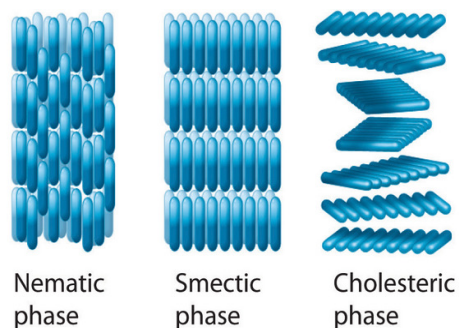


Figure 1.1. Arrangements of phase sequences in LCPs [10]

The molecules of the liquid crystalline polymer exist as associated in an ordered manner and form elongated domain in which the rigid molecules are found to be parallel with each other [11]. Liquid crystalline polymers are also classified as main chain LCPs when rigid elements, the mesogenic units are incorporated into the backbone molecule. When mesogenic units are attached to the molecules as side groups they are classified as side chain LCPs. Moreover, combined chain LCPs were also reported in which the mesogenic units are present as a part of the backbone and as side groups attached to the molecule [12]. Liquid crystalline polymers may be crosslinked to each other to form a network that retains the liquid crystal feature. The liquid crystal networks deform when a stress is applied as rubber does. They exhibit rubber elasticity [13].

This ordered structure can be distorted not only in fluid but also solid states. When the liquid crystals expose to external force which is able to make significant distortion or deformation to liquid crystals, the order of molecule will become

higher. As long relaxation are combined with orientation decompose of LCPs, the order may be retained upon coagulation or solidification in lyotropic or thermotropic LCPs. At this point, the high moduli and strength are obtained from considerably crystalline products by means of performing a large scale orientation state [14-15] and extension in rigid chain molecules. Chain extended liquid crystalline polymers have priority on chain folded semicrystalline commodity polymer.

Main factor affecting properties of LCPs is orientability of the material in the fluid state. Flow field, especially uniaxial extensional flow field dominates the formation of oriented LCP fibrils. In addition, Lewis and Fellers revealed that elongation flow is extraordinarily influential upon orientation enhancement [16].

### **1.1.3. Blends and Combining Thermoplastics with LCPs**

Polymer blends are mixtures of at least two macromolecular species, polymers and/or copolymers. Blending has been one of the most appealing subjects in recent times so as to obtain new materials with specific properties without the need to synthesis, to improve specific aspects such as impact strength and solvent resistance and to benefit the manufacturer by offering improved processability, product uniformity, and scrap reduction. Therefore, much attention has been paid to marketable thermoplastic blends which could be formed from thermotropic liquid crystalline polymers (LCPs) and thermoplastic (TP) matrices in order to keep up with this trend toward specialization in the polymer products in industry. The key benefits expected from the use of LCPs as blend components are the distinct reduction of the melt viscosity, with consequent upgrading of processability, and the reinforcing

effect granted by the immiscible LCP particles, which can attain oriented fibrillar morphology when the blend is processed under elongational flow conditions [17-18]

When blends contain thermotropic liquid crystalline polymers and thermoplastic are considered, the effective aspect was revealed in literature that LCPs exhibit very high mechanical properties as a result of their stiff molecular backbones their relative simplicity so as to orient and their ability to maintain its orientation for about several minutes in the melt state [19-21].

LCPs can also function as a processing aid by reducing the viscosity of thermoplastic matrix during compounding, thereby easing the processability of thermoplastics. Moreover, the mesogenic phase such as nematic units have high degree of long-range order that enabling them to orient along the flow direction during processing. This leads to the formation of fine fibrils at an appropriate range of LCP concentration under certain processing conditions. The fine fibrils reinforce the matrix of thermoplastics effectively, giving rise to the development of polymer composites that commonly known as in situ composites [22].

Qin and co-workers [23–24] is one of the groups who has been actively investigating on such blends ranging from the type of LCP used, the effects of LCP content, extrusion and drawing conditions on the fibrillation process. It was reported that when the LCP consists of rigid aromatic segments, fibril formation would take place.

When mentioning about reinforcing PE by blending it with LCPs, the subject focuses on the successful phase compatibility and interfacial adhesion of these two structurally unlike polymers [25]. The addition of compatibilizing agents into

intrinsically immiscible polymer blends can have a substantial merit to solve this problem [26].

On the other hand, there are several factors that affect the ability of LCPs to reinforce commodity plastics as flow field, processing temperature, concentration and dispersion of LCP, miscibility of the components and effect of compatibilizers [27].

During processing, the high orientability and the high shear thinning characteristics of thermotropic LCPs (TLCP) are unique and beneficial for polymers. In addition to Ide and Ophir research [28] revealed that molecular orientation within neat LCPs is strongly affected by uniaxial extensional flow field, orientation of mesogenic moieties of LCPs occur readily under a flow field during melt processing. The molecular orientation of a rigid mesogen rod in simple shear and uniaxial extensional or elongational flow fields is depicted in Figure 1.2.

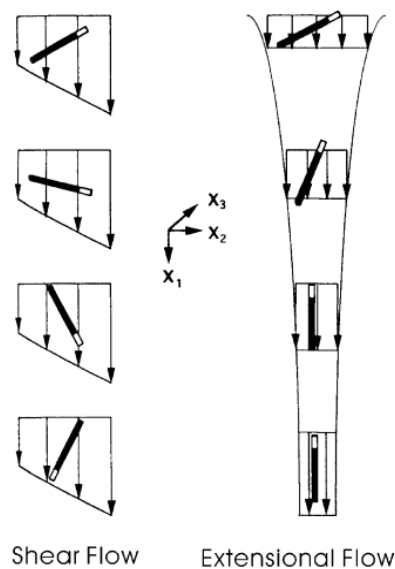


Figure 1.2. Orientability of a rigid rod in simple shear and uniaxial extensional flow fields [29]

Temperature must also be adjusted satisfactorily during processing of blends. In order to form reinforcing fibrillar structure of LCPs, high temperature is generally necessary. Though 300°C and above temperature could be seen eligible for LCPs process, some resin product could face degradation at this temperature. Once the processing temperature of each material suitably adjusted, fibrillar structure with flourished mechanical properties can be seen clearly [27].

Besides, Leng Y. and co-workers [30] revealed that mechanical test results generally indicate that the tensile modulus and strength decrease with increasing processing temperature. Tensile modulus moderately decreases when the temperature increases from 280 to 320°C. Effects of temperature, however, are more obvious on tensile strength than on the elastic modulus. Moreover, Yan et. al. demonstrated that the storage modulus and loss modulus dramatically decreased with the rise of the test temperature [31].

Correspondingly, blends processed at higher temperature have better mechanical properties than blends processed at lower temperature. This consequence can be indicated depending on two factors. Firstly, larger hydrodynamic stresses at lower temperatures supply opportunity needed to deform smaller LCP droplets [32]. Secondly, the effects of flow field and processing temperature, concentration of LCP within a polymer matrix has to be regarded as a critical issue in creation of a fibrous morphology [32-33]. Blizard and Baird [33] research is one of the example at this point by mentioning blends of a LCP based on poly(ethyleneterephthalate)/p-hydroxybenzoic acid (PET/PHB) with polycarbonate or nylon 6.6 matrices. LCPs with lower concentration have droplet morphology, while fibrous structure was obtained at higher concentrations.

## **1.2. Reinforcement of Polyolefins with LCPs**

Reinforcement of the polymers to enhance some properties of the material is one of the most important and popular methods of production of several kinds of polymeric materials which must possess the necessary mechanical and physical properties for any given practical application [34].

The incorporation of a liquid crystalline polymer (LCP) into a thermoplastic matrix has vital role for blend which called as self-reinforced or in-situ composites. It was used more commonly for glass-reinforced composites, such as recyclability, improved appearance and lower processing energy requirements. The parameter affecting the capacity of LCPs to reinforce thermoplastics is the creation of oriented fibers of LCPs. Therefore; a uniaxial extensional flow field plays a crucial role in the reinforcement of blends, leading to fiber formation with high aspect ratios [35].

When considering blends studied commonly, lots of the thermoplastics are not compatible with the widespread thermotropic LCPs (TLCP). As a consequence, the main restriction in order to obtain TLCP–polymer blends is clearly that the interfacial adhesion between the TLCP and matrix polymer is usually insufficient [36-37] The interfacial adhesion between immiscible polymers may be get better either by adding a third interfacially active polymer, called a compatibilizer, or by promoting a chemical reaction between the two polymers that effectively forms graft copolymer in situ that serves as the compatibilizer, an approach termed as reactive compatibilization [38].



In recent investigations, the behavior and reinforcement of the mechanical properties of the composites of high-density polyethylene has been examined widely with the use of UHMWPE sheet, hydroxyapatite (HA), nanoclay and Nylon-6 as improving elements [39-42].

Faruk, O. and Matuana, L.M [41] has studied on reinforcement of HDPE matrix with nanoclay by using matrix in the manufacture of the wood-plastic composites (melt blending process). The experimental results indicated that the flexural properties of HDPE/wood-flour composites could be considerably improved with a proper combination of the coupling agent content and nanoclay type in the composites.

Zhou et. al. [43] has clearly studied on ultra-high-molecular-weight polyethylene/liquid crystalline polymer composites (coded as UHMWPE/LCP) compatibilized with polyethylene-grafted maleic anhydride (PE-g-MAH). It was found that the incorporation of PE-g-MAH as a compatibilizer contributes to significant increasing in the tensile strength and wear resistance of UHMWPE–matrix composites blended with LCP, which is closely related to the crosslinking reinforcing action of the compatibilizer.

One of the most frequently used polyolefines among the plastic materials is explicitly polypropylene because of its easy processing and economy compared to the other engineering polymers. Several studies on the modification of polypropylene exist to improve its some mechanical properties. PP/LCP blends also draw attention due to flourish modulus.

Thomas and co-workers [44] studied on blends of polyamide 12 (PA12) and isotactic polypropylene (PP) with the presence and absence of a compatibilizer. They concluded that compatibilisation of the blends vastly enhanced the morphology of the blends by significantly reducing the average particle size as well as inter particle distance and increasing the interfacial area per unit volume although incompatibility with a two-phase non-uniform unstable morphology is main problem owing to high interfacial tension and coalescence effects.

### 1.3. Graft Copolymerization

A copolymer can be regarded as polymer derived from two (or more) monomeric species, as opposed to a homopolymer where only one monomer is used [45]. Because of the fact that the copolymer consists of at least two types of constituent units (also structural units), copolymers can be classified based on how these units are arranged along the chain [46]. These include:

- 1) A-A-B-A-B-A-B-B-B-A-B-A-A → Random Copolymer
- 2) A-B-A-B-A-B-A-B-A-B-A-B-A → Alternating Copolymer
- 3) A-A-A-A-B-B-B-B-B-A-A-A-A → Block Copolymer

Graft copolymers are a special type of branched copolymer in which the side chains are structurally distinct from the main chain. A graft copolymer contains a long sequence of one monomer (often referred to as the *backbone polymer*) with one

or more branches (grafts) of long sequences of a second monomer. [45]. Schematically, the structure of a graft copolymer can be illustrated as below.

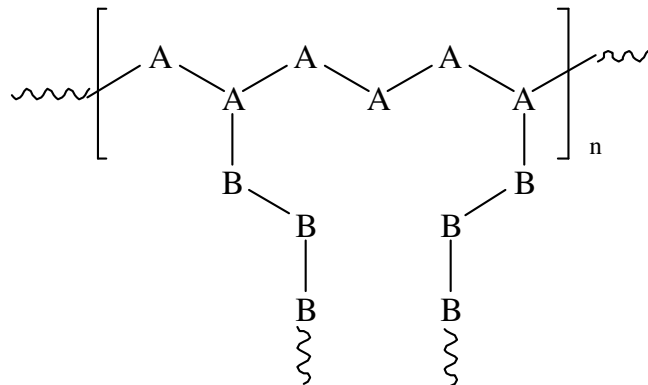
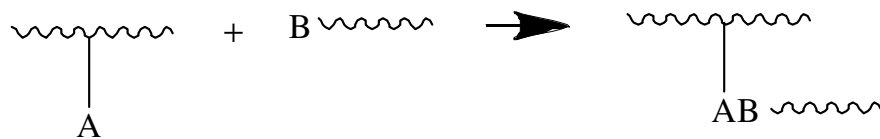


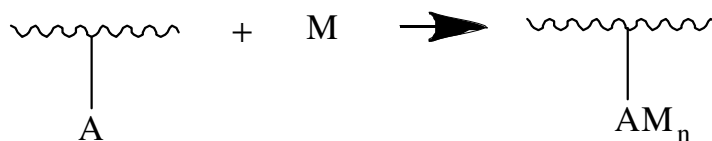
Figure 1.3. The structure of a graft copolymer

Three methods exist for synthesizing graft copolymers [45]:

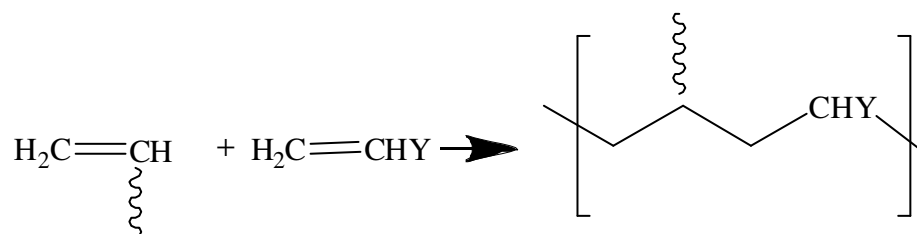
- 1) *Grafting onto* involves the reaction between functional groups on two different polymers:



- 2) *Grafting from* involves a polymer with functional groups that initiate polymerization of monomer:



3) *Grafting through* involves the polymerization (or copolymerization) of a macro monomer, usually a vinyl macro monomer:



Grafting can be accomplished by using several methods such as chemical methods, enzymatic methods and radiation induction [47-49]. Radiation induced graft copolymerization is the most commonly used method owing to several reasons such as enabling both bulk and surface copolymerization, processing in wide range of temperature with varying sizes of grafting component and easy controlling of polymerization rate.

Mai and co-workers [50] demonstrated a flexible approach for preparing the well modified UHMWPE fibers thanks to UV-induced sequential surface grafting polymerization. The widely improved interfacial bonding strength of UHMWPE fibers was achieved.

#### **1.4. Side-Chain Liquid Crystal, Poly(p-Benzophenoneoxycarbonylphenyl Acrylate)**

##### **1.4.1. Side Chain Liquid Crystals, SCLCPs**

The liquid crystal state is a kind of state whose order is between the crystal solid and isotropic liquid states. In the crystal state, there is a long range order in position and orientation, while in the liquid state, there is no long range ordering.

Side-chain liquid-crystalline polymers (SCLCPs) have been the subject of intensive research during the last decades. They represent a combination of liquid-crystalline behavior and polymeric properties, in another word, combine the anisotropy of liquid crystalline mesogens with the mechanical properties of polymers [51].

Systematic investigation of the synthesis of side-chain LCPs began only after Finkelmann and co-workers [52]. They proposed that a flexible spacer should be inserted between the polymeric backbones and mesogenic side groups to decouple the motions of the backbone and side groups in the liquid-crystalline state. On the basis of the spacer model, side-chain LCPs containing rod-like (terminal or lateral) and disk-like mesogens exists. Possible architectures of SCLCPs could be shown as:

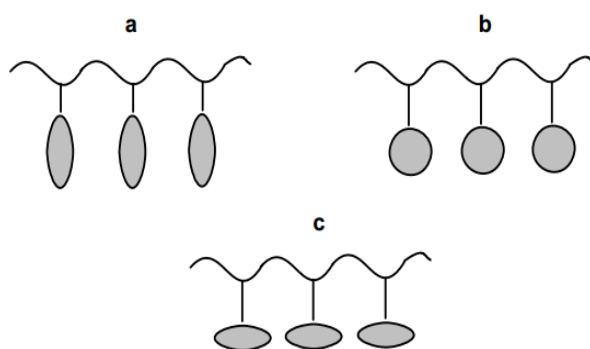


Figure 1.4. Possible SCLCPs (a) rod-like terminal, (b) disc-like, (c) rod-like lateral

Majority of the side chain liquid crystal materials were made by two synthetic routes: free radical polymerization of acrylic type monomers, bearing mesogenic moieties [53-54] and hydrosilylation of mesogenic terminal alkenes with linear poly [(methylhydro)siloxanes] copolymers bearing alkylhydrosiloxane monomeric units [53,55] or polymer systems modified with reactive Si-H bonds [56].

According to the ways in which the side chains are connected to the backbone, they are classified into two main categories: *The end-on side chain liquid-crystalline polymers* in which the side chains are terminally attached to backbone, and *the side-on (laterally attached) side chain liquid-crystalline polymers* [57]. Recently, *shoulderly-attached liquid-crystalline polymers* were synthesized in which the side chain attachment is offset from the centre of the side chains [58].

SCLCPs have been highly developed because of the proposal and wide range usages. So far, various potential applications have been considered for the side-chain LCs. Broadly speaking, applications fall into the following fields, optical data storage, non-linear optics, stationary phases for gas chromatography, supercritical-fluid chromatography, high-performance liquid chromatography, solid polymer electrolytes, separation membranes and display materials [51].

#### **1.4.2. Poly(p-Benzophenoneoxycarbonylphenyl Acrylate) Poly(BPOCPA)**

Although scientists give wide attention to our starting product, ABA, [59-61] unfortunately, a few researches about poly(p-benzophenoneoxycarbonylphenyl acrylate, (poly(BPOCPA))) have been made up to now.

Sesha Sainath et. al. [62] attempted to study on the polymerization of p-benzophenoneoxycarbonylphenyl acrylate and they had reported that the synthesis and mesophase properties of polyacrylates and polymethacrylates in which the pendant aromatic mesogenic group is attached to the polymeric backbone either directly or via an ethyleneoxy or benzoyloxy unit.

In addition, they have analyzed the phase transitions of poly(BPOCPA) as an example of transition behavior of side chain pendant aromatic mesogenic group polymer. According to their results, poly(BPOCPA) was non-crystalline, more specifically, glassy nematic order due to the fact that the DSC thermogram of BPOCPA shows T<sub>g</sub> at 69°C, an endotherm at 202°C corresponding to liquid crystal-isotropization transition (T<sub>i</sub>), the presence of T<sub>g</sub> and absence of crystal to melting transition (T<sub>m</sub>) [62]. Merely; the examination of thermal and characteristic properties exists in literature.

As far as we know, there is no research on the blends and graft copolymerization of poly(p-benzophenoneoxycarbonylphenyl acrylate) onto HDPE, and on mechanical properties of the obtained copolymers with varying in monomer composition and processing conditions.

### **1.5. Aim of the Work**

The objective of this study is to investigate the synthesis and polymerization of p-benzophenoneoxycarbonylphenyl acrylate and to carry out its graft copolymerization of onto HDPE. By the presumed mesomorphic properties of the polymer, obtained by polymerization of p-benzophenoneoxycarbonylphenyl acrylate, the improvement in properties of the HDPE was mainly aimed by graft copolymerization. It was planned to get an improvement in processability and dispersion of the reinforcing liquid crystalline polymer phase in the products.

## CHAPTER 2

### EXPERIMENTAL DETAILS

#### 2.1. Chemicals and Materials Used

##### 2.1.1. Solvents and Reagents

Acetone, dimethyl formamide, ethanol, ethyl methyl ketone, hexane, triethyl amine, xylene (Merck A.G.), dichloromethane, methanol, dimethyl sulfoxide, (VWR A.G.) and ethylacetate (Riedel-de Haen A.G.) were used without any purification.

The main chemicals acryloyl chloride, p-hydroxybenzoic acid, thionyl chloride (Merck A.G.) and 4-hydroxybenzophenone (Alfa Aesar A.G.), for the synthesis of p-benzophenoneoxycarbonylphenyl acrylate, were used without any purification. The initiator, dicumyl peroxide (DCP) (Merck A.G.) was used as received.

##### 2.1.2. Preparation of Powder High Density Polyethylene

High density polyethylene (HDPE), coded as S 0464, was supplied by PETKIM, Turkish Petrochemical Industry.

HDPE was dissolved in boiling xylene (138-139°C) by refluxing and precipitated by adding analytical grade ethanol. The precipitate was collected,



filtered and dried in vacuum at 40°C and ground by cooling in liquid nitrogen. The powder HDPE was used in the graft copolymerization experiments.

## 2.2. Synthesis of p-Benzophenoneoxycarbonylphenyl Acrylate, BPOCPA

### 2.2.1. Preparation of p-Acryloyloxybenzoic Acid, ABA

p-Acryloyloxybenzoic acid, ABA, was prepared by condensation of acryloyl chloride with p-hydroxybenzoic acid in alkaline medium (Figure 2.1) as described by Sessa Sainath et. al. [62] 69.0 g (0.5 mol) p-hydroxybenzoic acid was added to a solution of 40 g (1 mol) NaOH in 500 mL of distilled water in a flask equipped with a magnetic stirrer. The solution was cooled to 0-5°C, and then 43 mL (0.5 mol) of acryloyl chloride was added dropwise by stirring about 1 h. The stirring continued at 0-5°C for 1 h and then for another 1 h at room temperature. The precipitate was formed by the additional of cool diluted HCl then; it was filtered and washed with water. ABA was purified by 3-4 times repeated recrystallizations from acetone. The yield was 75 wt%, in good agreement with the literature [63].

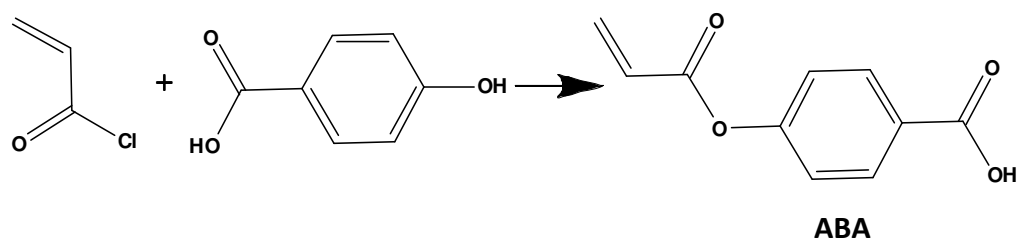


Figure 2. 1. Reaction between p-hydroxybenzoic acid and acryloyl chloride

### 2.2.2. Preparation of p-Acryloyloxybenzoyl Chloride, ABC

p-Acryloyloxybenzoyl chloride, ABC, was prepared by refluxing ABA, prepared in the previous stage, with thionyl chloride as reported by Sesha Sainath et. al. [62] ABA (25 g) was refluxed with 250 mL of thionyl chloride in presence of a trace amount of dimethylformamide for 8 hours, and then the excess of thionyl chloride was removed by vacuum distillation. The product was purified by repeated recrystallizations from dichloromethane in which the solubility of ABC was lowered by adding hexane until turbidity. The yield was 98 wt%. The plain reaction was illustrated in Figure 2.2.

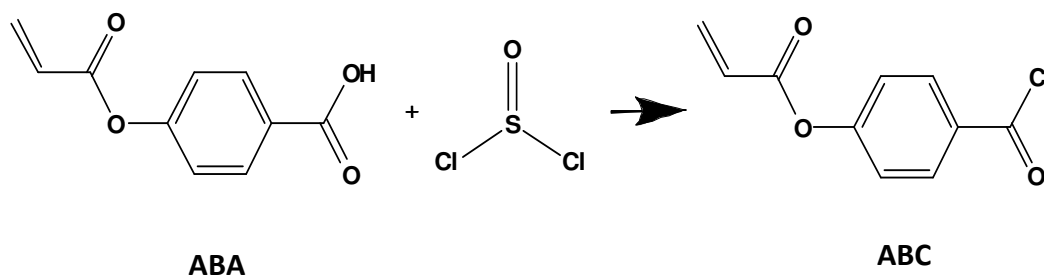


Figure 2.2. Reaction between p-acryloyloxybenzoic acid and thionyl chloride

### 2.2.3. Preparation of p-Benzophenoneoxycarbonylphenyl Acrylate

p-Benzophenoneoxycarbonylphenyl acrylate (BPOCPA) was prepared by condensation of 4-acryloyloxybenzoyl chloride, prepared in the previous stage, with p-hydroxybenzophenone, HBP. The condensation reaction was carried out by both as described by Sesha Sainath et. al. [62] by refluxing ABC and HBP in xylene.

As described by Sesha Sainath et. al. (62), 25.0 g, (0.126 mol) HBP and triethylamine 12 mL (7.5 g, 0.126 mol) were dissolved in 150 mL of ethyl methyl ketone (EMK), and the solution was cooled to 0-5°C in ice bath. Then, 26.5 g, (0.126 mol) ABC dissolved in 150 mL of EMK was added dropwise with stirring at the same temperature. After stirring at room temperature for another 5 hours, the solid quaternary ammonium salt was filtered off and washed with excess amount of EMK. The organic solution was also washed successively with 5% aqueous NaOH solution, diluted HCl and distilled water. The product was precipitated by further addition of distilled water and collected by filtering. The product, then, was recrystallized repeatedly from ethanol and ethylacetate and purified by column chromatography by utilizing dichloromethane as a mobile phase and silica gel as a stationary phase. The yield was approximately 16 wt%.

Alternatively, the novel effective synthesis method for the monomer was accomplished by refluxing ABC and HBP in xylene. 25.0 g (0.126 mol) HBP and 26.5 g, (0.126 mol) ABC were refluxed in 250 mL of xylene (137-138°C) for about 3-4 days. The dark brown-black impurity formed during refluxing as a suspension in the reaction medium was settled down by adding a small amount of hexane, and the solution containing the monomer above the impurity was separated. The monomer, BPOCPA was precipitated from the solution by cooling, and purified by repeated recrystallizations from ethanol and ethylacetate. The yield was 57 wt%. The synthesis method was also examined by using dioxane, dimethyl sulfoxide and dimethyl formamide instead of xylene but was not successful. The simplified reaction for the preparation of the monomer was shown as following, Figure 2.3.

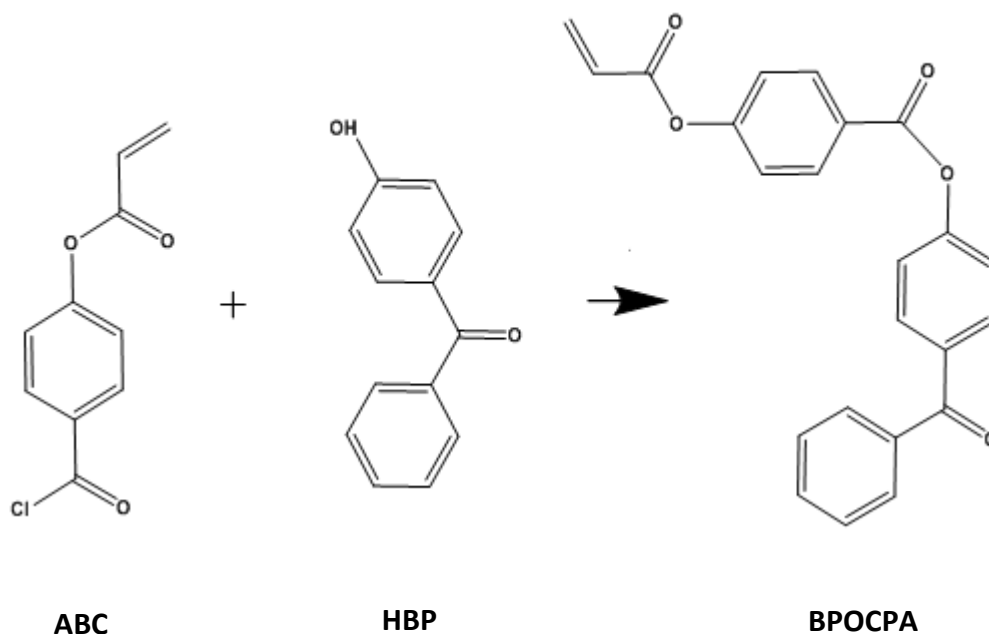


Figure 2.3. Reaction between p-hydroxybenzophenone and p-acryloyloxybenzoyl chloride

### 2.3. Polymerization of the Monomer, BPOCPA

The bulk melt polymerization of the monomer was carried out with the use of initiator, dicumyl peroxide, DCP. The mixture of BPOCPA (melt at 131°C) and DCP (2% with respect to weight of monomer) was heated to 140°C in vacuum keeping the temperature constant for 60 minutes. The product, poly(BPOCPA), was washed repeatedly with EMK, DMSO and methanol to remove residual monomer and any soluble parts, and then dried in vacuum. The yield was 94.91 wt%.

Solution polymerization of BPOCPA was carried out by using benzoyl peroxide, BPO, initiator. The solution of BPOCPA in DMF and DMSO containing 2 % BPO (with respect to weight of BPOCPA) was heated to 100°C in vacuum keeping the temperature constant for 60 minutes. The product, poly(BPOCPA) was

precipitated by adding methanol. After filtering, the product was washed repeatedly with methanol and ethyl methyl ketone to remove remaining unpolymerized monomer residue and other soluble products, and dried in vacuum at 40°C. The yield was 54.07 wt% in DMF and 43.67 wt% in DMSO.

The solubility of polyBPOCPA was tested in common conventional solvents such as DMF, DMSO, acetone, ethanol, ethyl acetate, but it was found to be soluble only in hot DMF (152-154°C) and DMSO (189°C).

#### **2.4. Graft Copolymerization of BPOCPA**

Graft copolymerization was carried out by bulk melt polymerization at 140°C at which both PE and BPOCPA melt at about 131°C. The polymer PE in powder form, monomer BPOCPA and initiator (DCP) were mixed in desired proportions in a mortar with hand grinding extensively, and the mixture was transferred to the tube-like reaction flask. The flask, then, evacuated, sealed and heated up to the pre-set temperature by keeping the temperature constant for a certain reaction time period (1 hour). At the end of the reaction time the flask was cooled to room temperature and crack-opened. The reaction products were first washed with EMK to remove soluble products, especially not grafted residual monomer and then with DMSO at room temperature by keeping in it for a day. After these washings the obtained products contained both grafted and ungrafted poly(BPOCPA). But, to determine the amount of grafted poly(BPOCPA) onto PE, the samples were washed with hot DMF to remove the ungrafted homopolymer.

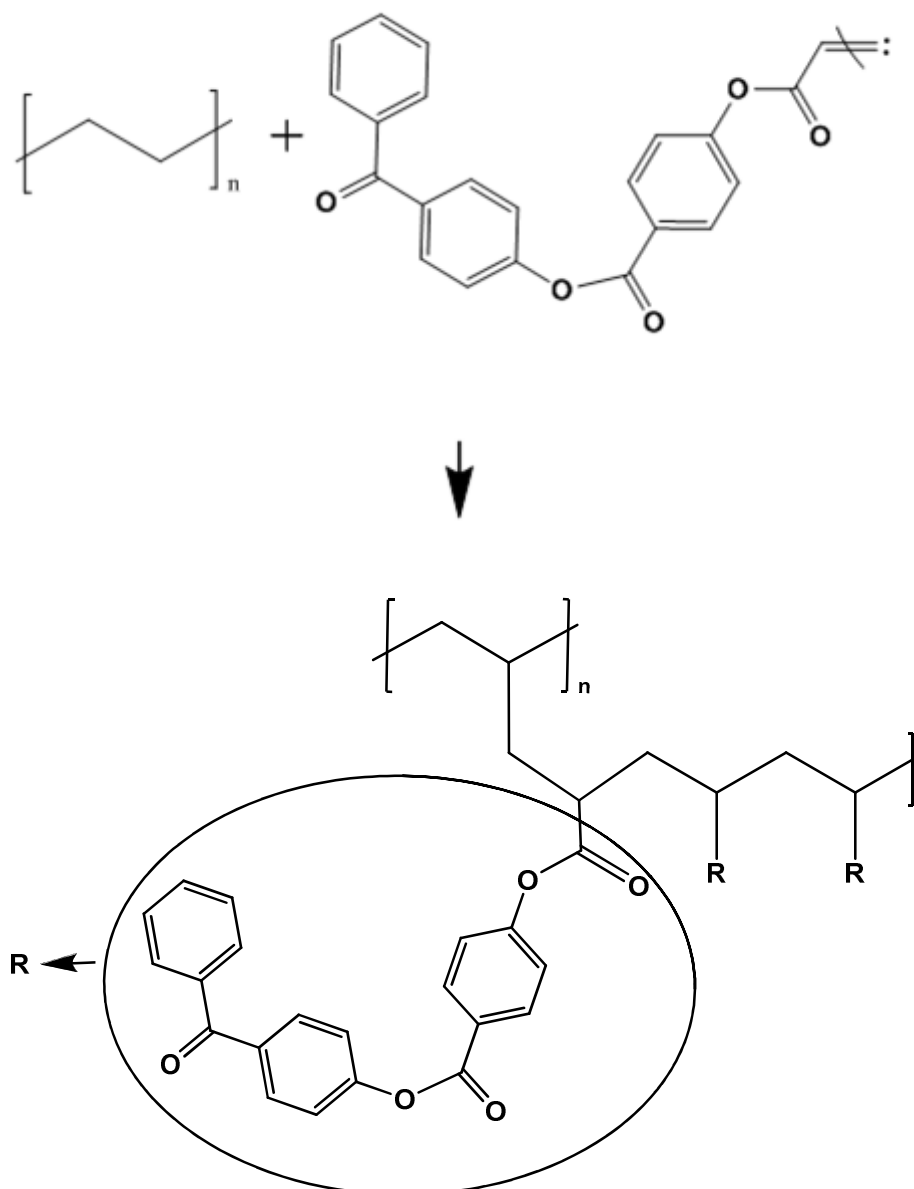


Figure 2.4. Graft copolymerization between BPOCPA and HDPE

Finally, the products were rewashed extensively with methanol several times to ensure the removal of DMSO and DMF, and then, dried in vacuum at 40°C for 4-5 hours. The amount of poly(BPOCPA) in the products, grafted or present as a homopolymer, was calculated gravimetrically and expressed as a percentage of

poly(BPOCPA) by weight in the products. The simplified graft copolymerization reaction between BPOCPA and HDPE is shown in Figure 2.4.

## **2.5. Characterization and Instruments**

### **2.5.1. FTIR Measurements**

FTIR characterization of HDPE, monomer and the products were done with the Shimadzu 8400 S FTIR spectrophotometer. FTIR spectra of the samples were obtained from KBr pellets prepared from approximately 3 mg sample in 100 mg spectroscopic grade KBr.

### **2.5.2. <sup>1</sup>H-NMR Measurements**

ABA, ABC and the BPOCPA were characterized by using a Bruker-Spectrospin Avance DPX 400 Ultra-shield <sup>1</sup>H-NMR spectrometer with a frequency of 400 MHz.

### **2.5.3. Differential Scanning Calorimeter (DSC) Analysis**

DSC analyses of HDPE, ABA, BPOCPA and the graft copolymerization products were carried out with a Setaram DSC 131 Differential Scanning Calorimeter, under nitrogen atmosphere, with a heating rate of 10°C/min, and sample size was varied between 5-15 mg. The glass transition temperature ( $T_g$ ) and melting points ( $T_m$ ) were determined from the obtained thermograms.

#### **2.5.4. TG/IR Measurements**

The TG/IR analysis of poly(BPOCPA) and poly(BPOCPA)-g-PE samples was carried out by a TG/IR system, which combined with a Perkin Elmer Pyris 1 TGA Thermogravimetric Analyzer and a Perkin Elmer Spectrum One FTIR Spectrometer (Central Research Laboratory, METU). Samples of about 10 mg were pyrolysed in the TG analyzer, and the evolved gases were led to the Perkin Elmer Spectrum One FTIR Spectrometer directly through a connected heated gas line to obtain FTIR spectra. The thermogravimetry tests were performed in both air and nitrogen atmosphere in the temperature range from 25 to about 600°C with the heating rate of 10°C/min.

#### **2.5.5. Mechanical Properties**

Tensile properties of HDPE and the products were determined by LLYOD LR5K Mechanical Tester at room temperature. The test samples were prepared by micro-injection molding at 275°C with the thickness of 3 mm, width of 7 mm and gauge length of 62 mm, respectively. Crosshead speed and gauge length in testing were 5 cm/min and 1 cm. The tensile strengths and moduli were directly obtained from the stress-strain curves by the provided software of the instrument. A minimum five specimens were tested for each composition.

The impact strength of the test samples prepared as for tensile tests were determined by Coesfeld Material Test Pendulum Impact Tester at room temperature.



### **2.5.6. Scanning Electron Microscope (SEM) Study**

Morphological properties of tensile and impact fractured surfaces were studied by using scanning electron microscope, JEOL 6390-LV, operated at 20 kV, with a resolution power of 3 nm.

### **2.5.7. Elemental Analysis of the Monomer**

Elemental analysis of the monomer in terms of C% and H% was done with the use of Eurovector EuroEA Elemental Analyser by utilizing benzamide, nicotinamide and urea as blank in N<sub>2</sub> medium.

## CHAPTER 3

### RESULTS AND DISCUSSION

#### 3.1. Characterizations

##### 3.1.1. Characterization of High Density Polyethylene

FTIR spectrum of high density polyethylene (HDPE) is given in Figure 3.1. The spectrum indicated the absorption bands of stretching vibrations of  $\text{CH}_2$  group at  $2932$  and  $2846\text{ cm}^{-1}$  and the bands due to bending vibrations of  $\text{CH}_2$  at  $1557$  and  $1472\text{ cm}^{-1}$ . The bending vibrations of C-C group were observed at  $723\text{ cm}^{-1}$ .

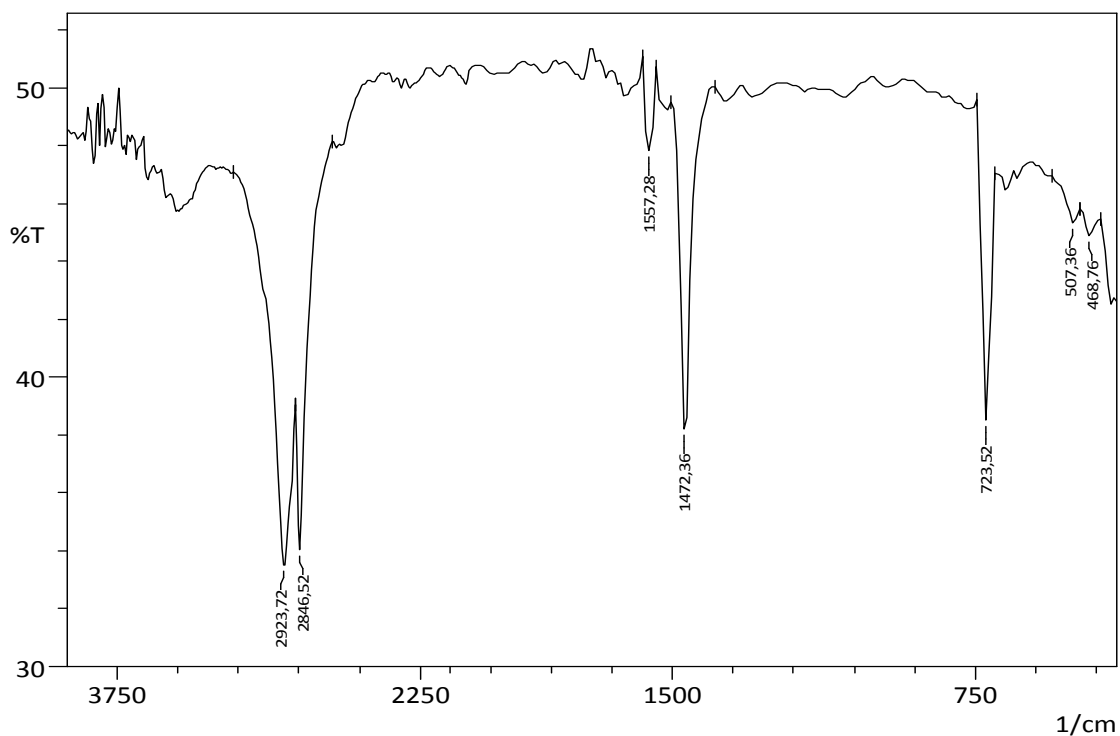


Figure 3.1. FTIR spectrum of the virgin HDPE

DSC melting point of powdered HDPE was found to be around 130-131°C in N<sub>2</sub> atmosphere with a heating rate of 10°C/min, Figure 3.2.

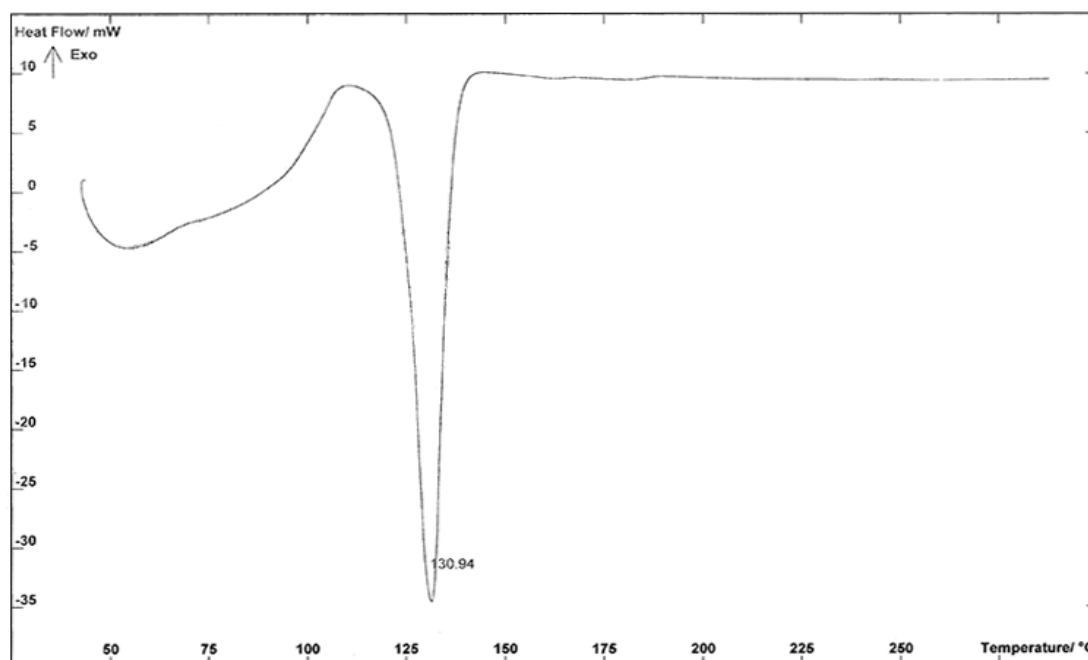


Figure 3.2. DSC thermogram of the virgin HDPE

### 3.1.2. Characterization of p-Acryloyloxybenzoic Acid

ABA prepared for the synthesis of BPOCPA was characterized by FTIR and <sup>1</sup>H-NMR spectroscopy and DSC analysis. The results showed good agreement with the literature [3].

The FTIR spectrum of ABA showed broad bands between 3200-2500 cm<sup>-1</sup> due to the carboxylic acid O-H and C-H stretching vibrations. The strong band due to characteristic C=O stretching vibrations of ester group was observed at 1742 cm<sup>-1</sup>. A strong band at 1688 cm<sup>-1</sup> was due to C=O stretching vibrations of aryl carboxylic acids. The bands at 1600 and 1500 cm<sup>-1</sup> were assigned to C=C stretching vibrations

of aromatic compounds. The four bands at 800, 909, 939 and 987  $\text{cm}^{-1}$  were arisen from vinylic C-H out-of-plane bending vibrations.

The  $^1\text{H-NMR}$  spectrum of ABA showed a quartet at  $\delta$  6.3 and doublets at  $\delta$  6.0 and  $\delta$  6.6 corresponding to three protons of  $\text{CH}_2=\text{CH-}$ , and two doublets at  $\delta$  7.1 and  $\delta$  8.1 corresponding to four protons of the  $\text{C}_6\text{H}_4$ - group.

DSC melting point of ABA was 199-200 $^\circ\text{C}$  in  $\text{N}_2$  atmosphere with a heating rate of 10 $^\circ\text{C}/\text{min}$ .

### 3.1.3. Characterization of p-Acryloyloxybenzoyl Chloride

ABC prepared for the synthesis of BPOCPA was characterized by FTIR and  $^1\text{H-NMR}$  spectroscopies and DSC analysis.

The FTIR spectrum of ABC pointed out aromatic C-H stretching vibrations as broad bands at about 3103 and 3076  $\text{cm}^{-1}$ . The strong band owing to characteristic C=O stretching vibrations of ester group was observed at 1741  $\text{cm}^{-1}$ . The bands at 1660 and 1500  $\text{cm}^{-1}$  were assigned to C=C stretching vibrations of aromatic compounds. The bands at 796, 844, 896 and 981  $\text{cm}^{-1}$  were due to vinylic C-H out-of-plane bending vibrations. The strong band at 644  $\text{cm}^{-1}$  is responsible for the C-Cl bending vibration.

The  $^1\text{H-NMR}$  spectrum of ABC showed a quartet at  $\delta$  6.03 and doublets at  $\delta$  6.10 and  $\delta$  5.5 corresponding to three protons of vinylic group,  $\text{CH}_2=\text{CH-}$ , and two doublets at  $\delta$  7.50 and  $\delta$  8.12 matching up to four protons of the  $\text{C}_6\text{H}_4$ - group.

DSC melting point of ABC was found as 57°C in N<sub>2</sub> atmosphere with a heating rate of 10°C/min.

### 3.1.4. Characterization of p-Benzophenoneoxycarbonylphenyl Acrylate

FTIR spectrum of BPOCPA indicated strong absorption bands at 1741 and 1730 cm<sup>-1</sup> due to C=O stretching vibrations of ester groups. The strong band at 1651 cm<sup>-1</sup> is due to C=O ketone stretching vibrations of the pendant benzophenone moiety. The bands at 1599 and 1504 cm<sup>-1</sup> are assigned to aromatic stretching vibrations of C=C bonds in the structure. The strong bands at 1207 and 1276 cm<sup>-1</sup> are corresponding to ester C-O-C stretching vibrations. The absorption bands because of monosubstituted aromatic C-H bending vibrations are observed between 1000 and 1200 cm<sup>-1</sup>. The moderate bands in between 823-1001 cm<sup>-1</sup> represent the vinylic C-H out-of-plane bending vibrations as shown in Figure 3.3.

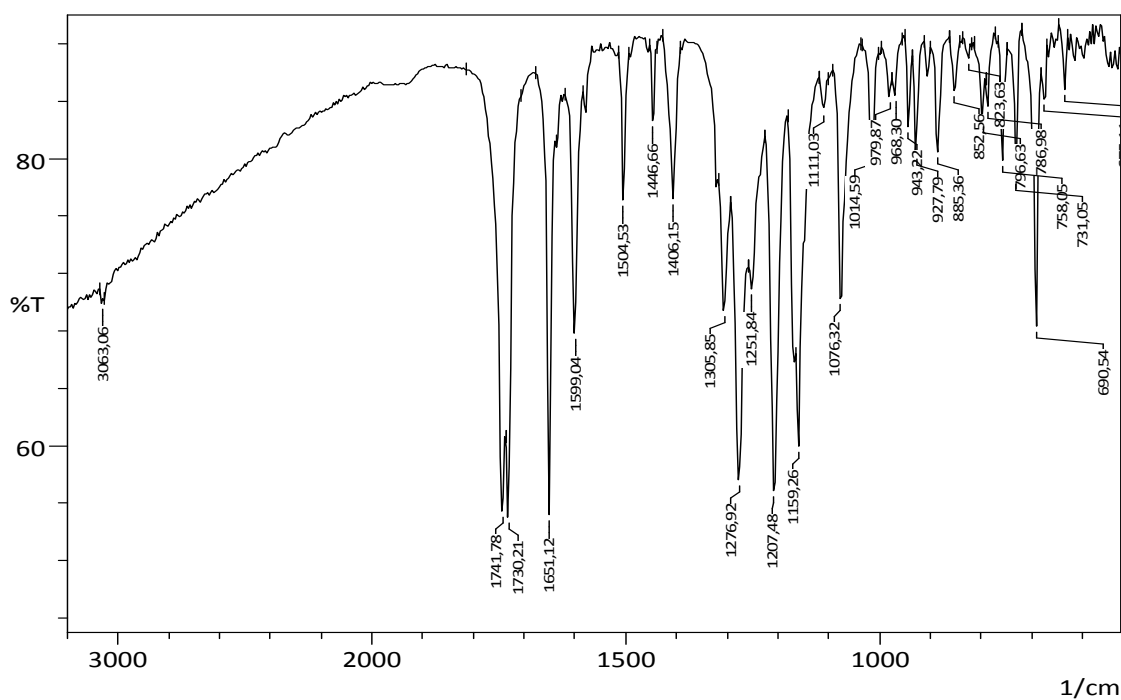


Figure 3.3. FTIR spectrum of BPOCPA

The  $^1\text{H-NMR}$  spectrum of BPOCPA containing  $\text{H}_a$ ,  $\text{H}_b$ ,  $\text{H}_c$ ,  $\text{H}_d$ ,  $\text{H}_e$ ,  $\text{H}_f$ ,  $\text{H}_g$ ,  $\text{H}_h$ ,  $\text{H}_i$ , and  $\text{H}_j$  protons shown schematically in Figure 3.4 is given in Figure 3.5. It displayed a doublet at  $\delta$  6.2 corresponding to  $\text{H}_b$  proton of vinylic group, one triplet at  $\delta$  6.45 corresponding to vinylic  $\text{H}_a$  proton. The doublet at  $\delta$  6.6 is responsible for  $\text{H}_a$ - $\text{H}_c$  trans coupling of vinylic group. The five doublets at  $\delta$  7.45, 7.50, 7.76, 7.86 and 8.21 are assigned to  $\text{H}_d$ ,  $\text{H}_f$ ,  $\text{H}_e$ ,  $\text{H}_g$ ,  $\text{H}_h$  protons which correspond single O-coupling of the  $\text{C}_6\text{H}_4$ -groups in structure. The two triplets at  $\delta$  7.57 and 7.68 are corresponding to  $\text{H}_j$  and  $\text{H}_i$  protons that have double O-coupling of  $\text{C}_6\text{H}_4$ -groups in molecule.

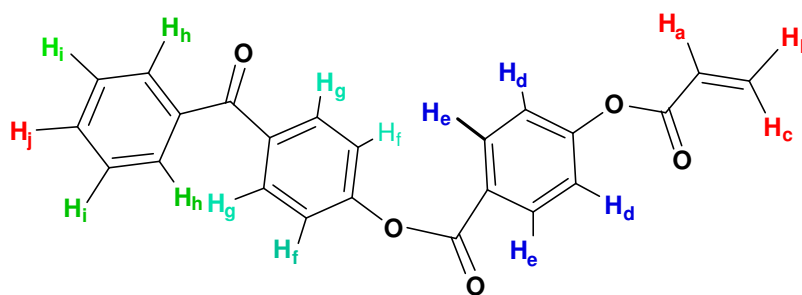


Figure 3.4. Proton scheme of BPOCPA

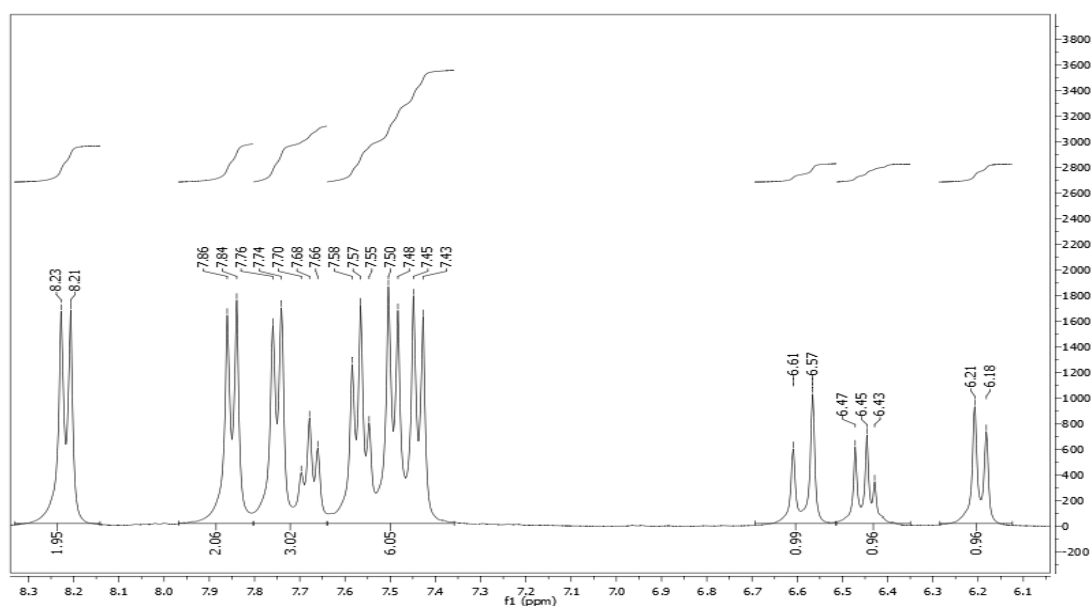


Figure 3.5. The  $^1\text{H-NMR}$  spectrum of BPOCPA

DSC melting point of BPOCPA was found as 131.06°C in N<sub>2</sub> atmosphere with a heating rate of 10°C/min, Figure 3.6.

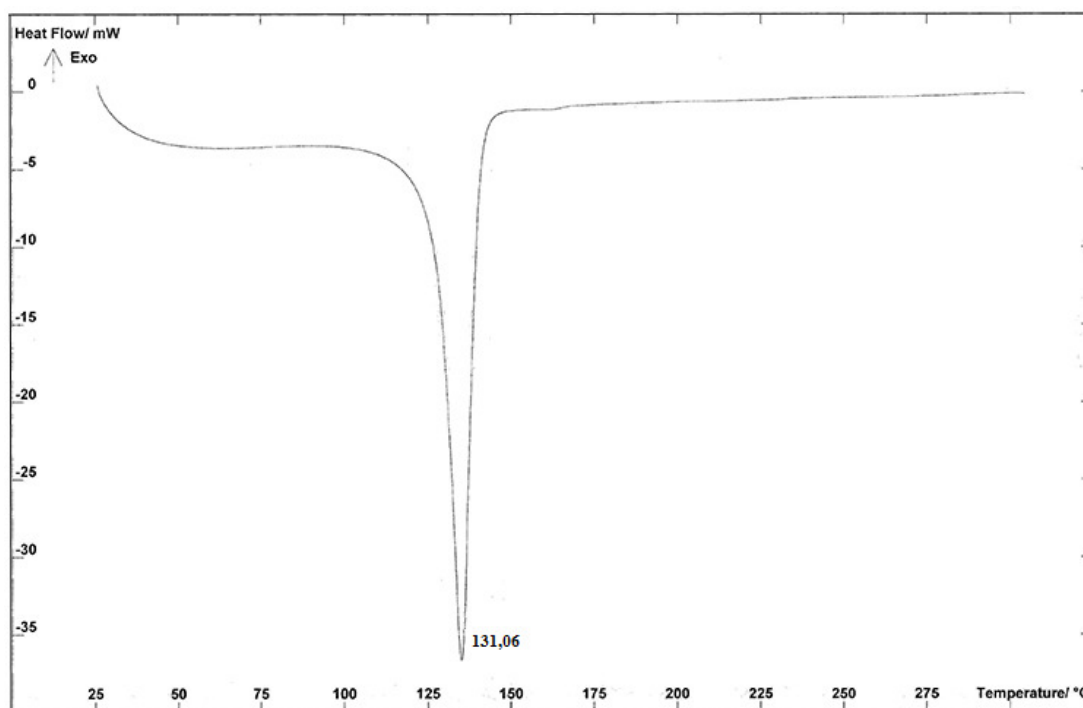


Figure 3.6. DSC thermogram of BPOCPA

Elemental analysis of monomer yielded the C and H contents of BPOCPA as 71.397 wt% and 3.554 wt%, respectively.

### 3.1.5. Characterization of Poly(p-Benzophenoneoxycarbonylphenyl Acrylate)

FTIR spectrum of bulk melt homopolymer poly(BPOCPA) is shown in Figure 3.7. The moderate band at 3063 cm<sup>-1</sup> is due to aromatic C-H stretching vibrations. C=O stretching vibrations of ester groups are observed at 1741 and 1730 cm<sup>-1</sup>. The strong band at 1651 cm<sup>-1</sup> is assigned to ketone C=O stretching vibrations between two phenyl groups. The stretching bands at 1599 and 1504 cm<sup>-1</sup> are in

charge of aromatic compounds which contain C=C bonds in the structure. The strong bands at 1207 and 1276  $\text{cm}^{-1}$  are corresponding to ester C-O-C stretching. The absorption bands because of monosubstituted aromatic C-H bending vibrations are observed between 1000 and 1200  $\text{cm}^{-1}$ . The four bands at 979, 968, 943, 904 and  $\text{cm}^{-1}$  observed in the spectrum of the monomer BPOCPA due to vinylic C-H out-of-plane bending vibrations disappeared in the spectrum of poly(BPOCPA), Figure 3.7. In polymer, all bands are broadened with respect to monomer.

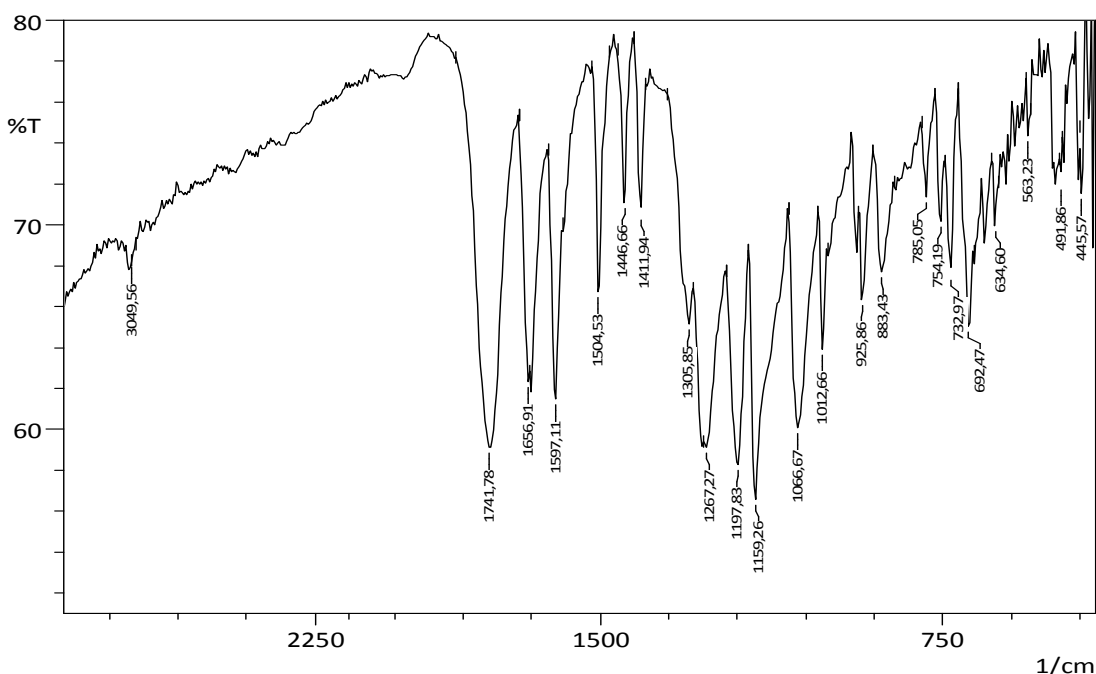


Figure 3.7. FTIR spectrum of poly(BPOCPA)

In the DSC study of poly(BPOCPA), the thermogram obtained with a heating rate of 10°C/min in N<sub>2</sub> atmosphere showed two endotherms at 198 and 231°C, Figure 3.8. In advance, the mesomorphic behavior of poly(BPOCPA) was studied by Sesha Sainath et al. [62] and the endotherm observed at 202°C in DSC thermogram was assigned to liquid crystal-isotropization transition. But, any endotherm corresponding



to crystal melting and thus melting temperature was not reported. With the same line of reasoning the smaller endotherm observed at 198°C may be attributed to the reported liquid crystal-isotropization temperature. The larger endotherm at 231°C, on the other hand, is apparently exhibiting the melting of crystalline domains. In addition, the endothermic shift observed at about 75°C may be ascribed to glass transition temperature, which was reported as 69°C by Sesha Sainath et al. [62], Figure 3.8.

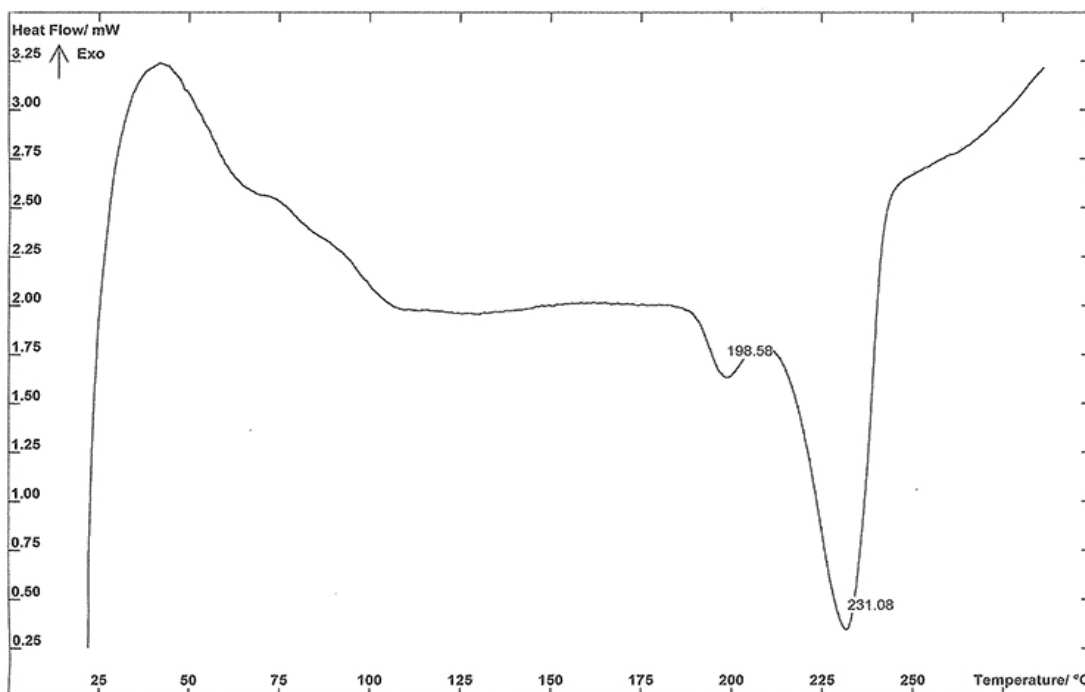


Figure 3.8. DSC thermogram of poly(BPOCPA)

### 3.1.6 Graft Copolymerization of BPOCPA onto HDPE

Graft copolymerization of BPOCPA onto PE with DCP, induced thermally, was studied at 140°C, above the crystalline melting temperature of both HDPE and BPOCPA (both are melting at about 131°C), by preparing the mixtures of six

different compositions of BPOCPA with PE. The amount of grafting was determined gravimetrically by washing the products with hot DMF to remove the homopolymer ungrafted onto PE and other remaining residuals. The results were recorded as the percentage of grafted poly(BPOCPA) and as the total percentage of poly(BPOCPA) involving both the grafted and ungrafted poly(BPOCPA) present as a homopolymer in the products, Table 2.1. The extent of grafting increased with increasing concentration of BPOCPA and reached the maximum value, 14.22%, at 30% BPOCPA in the reaction medium, which was followed by a dramatic decrease reducing to 5.79% poly(BPOCPA) at 40% BPOCPA, Figure 3.9. Regarding this result and the percent grafting which raised up to 85.41% at 10% BPOCPA, followed by a decreasing trend, it can be concluded that the grafting took place via the radicals forming on PE chains rather than propagating poly(BPOCPA) radicals, owing to appearingly steric hindrance. Accordingly, at lower concentrations of BPOCPA for a constant amount of DCP in reaction medium, more radicals formed on PE chains due to the direct reactions between PE chains and the radicals of the initiator, thus, high percentages of grafting were obtained. The increase of the extent of grafting with the concentration of BPOCPA presumably resulted from propagating poly(BPOCPA) units grafted onto PE chains, leading to high content of grafted poly(BPOCPA).

The percentage of grafted poly(BPOCPA) present in the products was calculated by using the following equation;

$$\% \text{ Poly(BPOCPA)} = (W_{\text{initial}} - W_{\text{final}}) \times 100 / W_{\text{initial}}$$

where,  $W_{\text{initial}}$  and  $W_{\text{final}}$  denote the weight of reaction mixture and of product after solvent washing, respectively.

Table 2.1. The content of poly(BPOCPA) in the graft copolymerization products with concentration of BPOCPA in the reaction mixture

% BPOCPA in rxn. Mixture	5%	10%	15%	20%	30%	40%
%Total Poly(BPOCPA) in products	4.97	9.32	13.66	19.90	28.28	39.10
% Grafted Poly(BPOCPA) in products	2.23	7.96	10.25	10.52	14.22	5.79
% Grafting	44.87	85.41	75.04	52.86	50.28	14.81

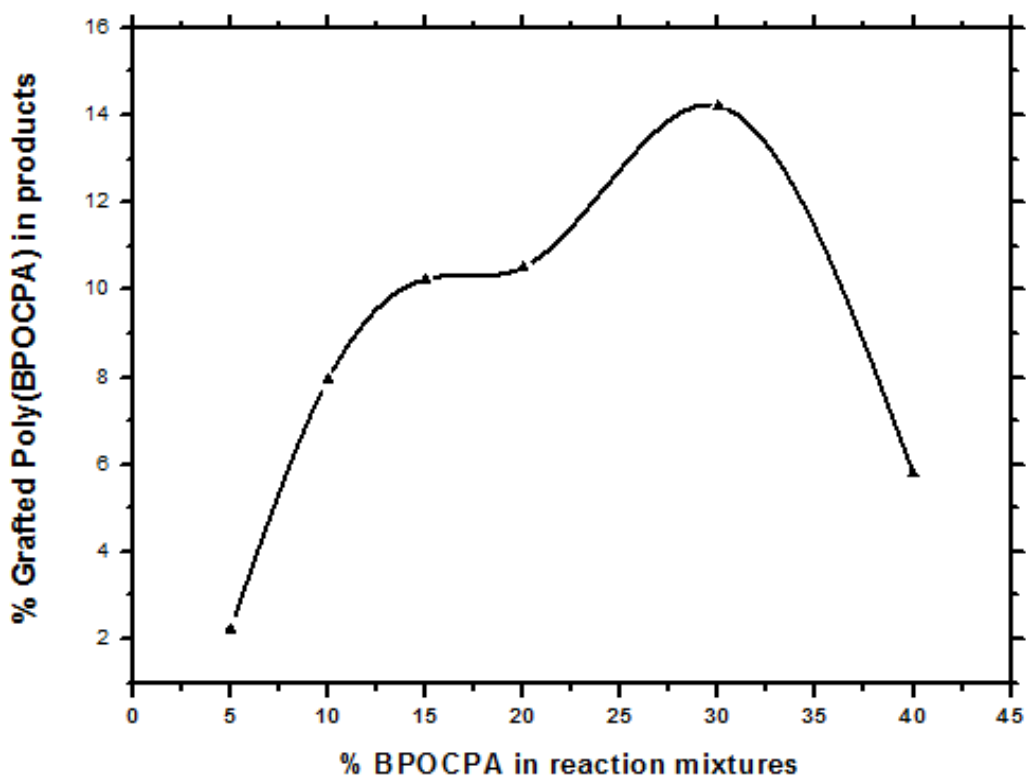


Figure 3.9. Dependence of percent grafting on concentration of BPOCPA in reaction mixture

### 3.1.7. Characterization of the Graft Copolymerization Products

FTIR spectra of the graft copolymerization products showed the characteristic absorption bands of poly(BPOCPA) due to aromatic, carbonyl and ester groups and of the aliphatic groups due to PE and main chain of poly(BPOCPA). The absorption bands at 904, 823, 796  $\text{cm}^{-1}$  were not seen in the spectra, of which monomer BPOCPA had, Figure 3.10. The characteristic bands of poly(BPOCPA) became more stronger as its content increased in the products as observed at about 1473, 731, 717  $\text{cm}^{-1}$  in the spectra, Figure 3.10,11.

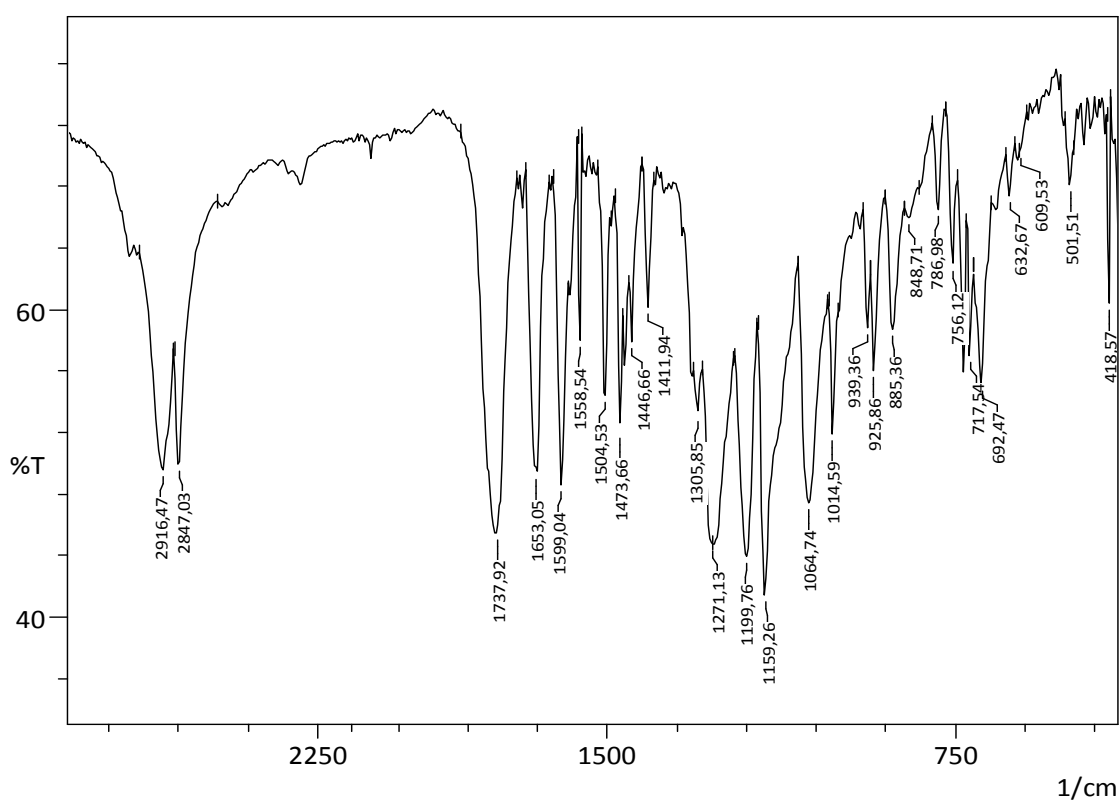


Figure 3.10. FTIR spectrum of the product with 13.66% poly(BPOCPA)

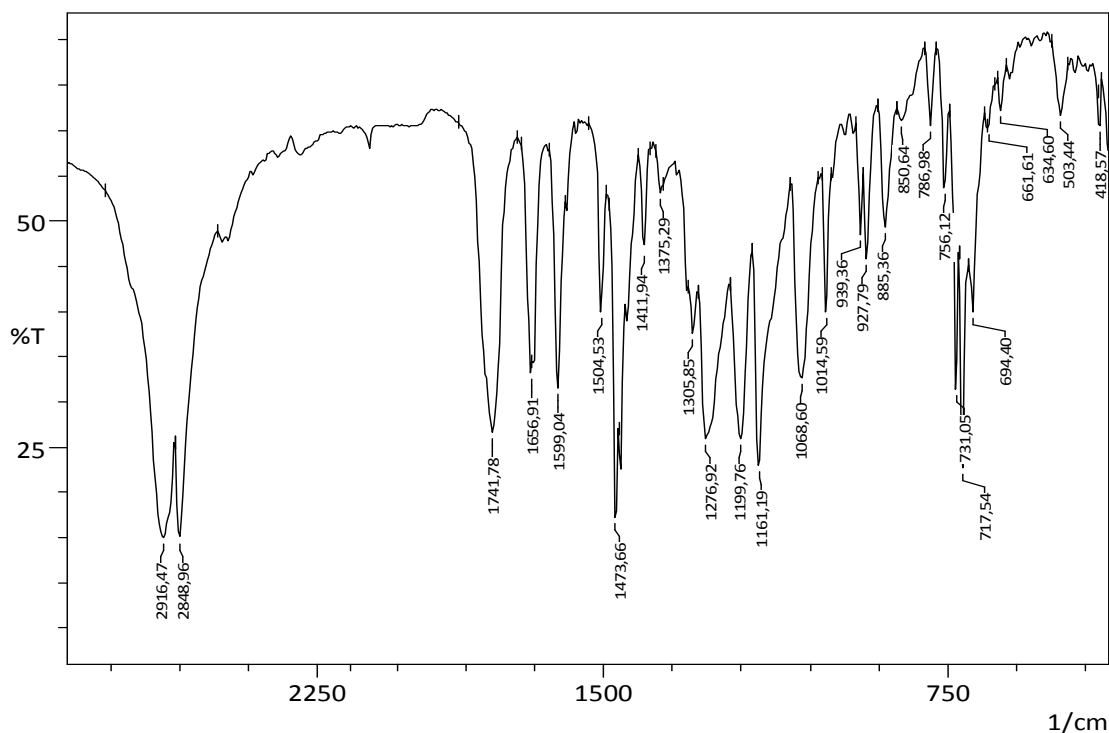


Figure 3.11. FTIR spectrum of the product with 39.10% poly(BPOCPA)

NMR analysis of the graft copolymerization products could not be carried out because of insolubility of the products in any solvent.

In order to find out the effect of graft copolymerization of BPOCPA onto HDPE on the thermal behavior of the graft copolymerization products the samples were analyzed by DSC. The endotherm corresponding to the crystalline melting of poly(BPOCPA) was observed but weakly at 235°C only in the thermogram of the sample with 39.1% poly(BPOCPA) among the products, Figure 3.12. The peak was not detected for the other products although it was observed as a massive endotherm in the thermogram of the homopolymer poly(BPOCPA). In the graft coproducts PE chains are probably interrupting the ordering of poly(BPOCPA) units and thus preventing the formation of poly(BPOCPA) crystals, resulting in an amorphous structure. On the other hand, the crystalline melting temperature of PE was observed

to increase slightly when compared to virgin PE (melting at about 131°C). Especially, the melting at 137-138°C was striking, observed with 13.66% poly(BPOCPA), Figure 3.13. The melting temperature in the other products was seen at 135°C in the sample with 9.32% poly(BPOCPA) and at 134°C in the samples with 4.97, 19.90, 28.28 and 39.10% poly(BPOCPA). In order to unfold the effect of the graft copolymerization on the melting temperature of PE, a PE sample was annealed at 140°C for 1 hour in vacuum, and a mixture of PE and DCP (2% with respect to weight of PE) was heated at 140°C for 1 hour in vacuum, as in graft copolymerization experiments. However, PE melting temperature of both samples was observed to remain almost unchanged at about 131°C (the same as virgin PE had), Figure 3.14. Accordingly, the poly(BPOCPA) units in the graft coproducts are presumably helping and enhancing the ordering of PE chains in the crystalline domains, thus giving rise to an increase in the crystalline melting temperatures.

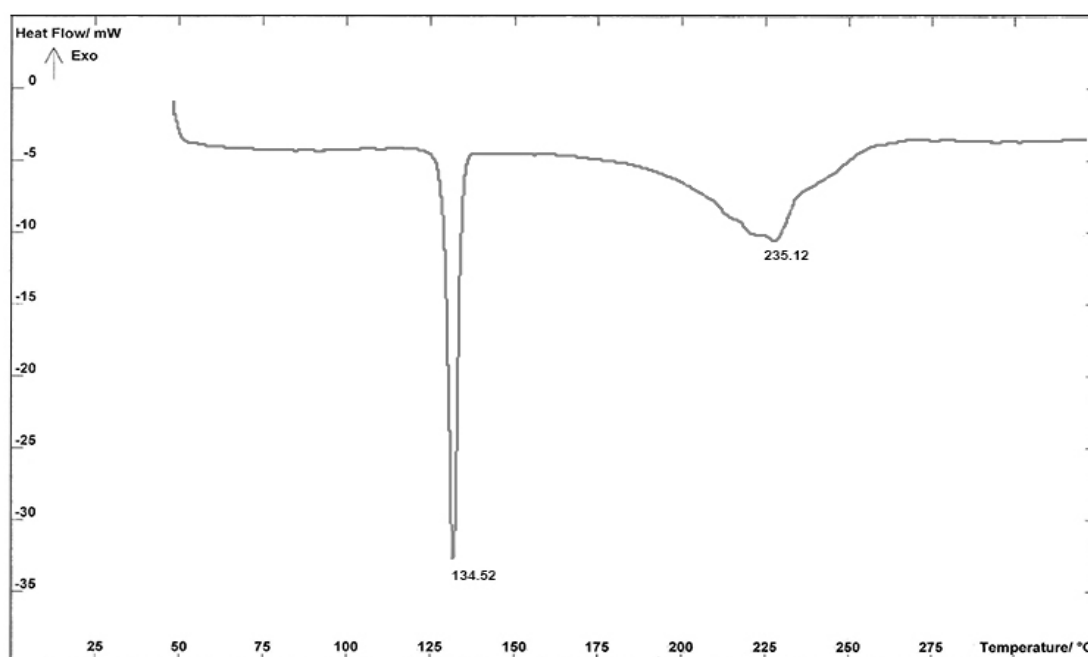


Figure 3.12. DSC thermogram of the product with 39.10% poly(BPOCPA)

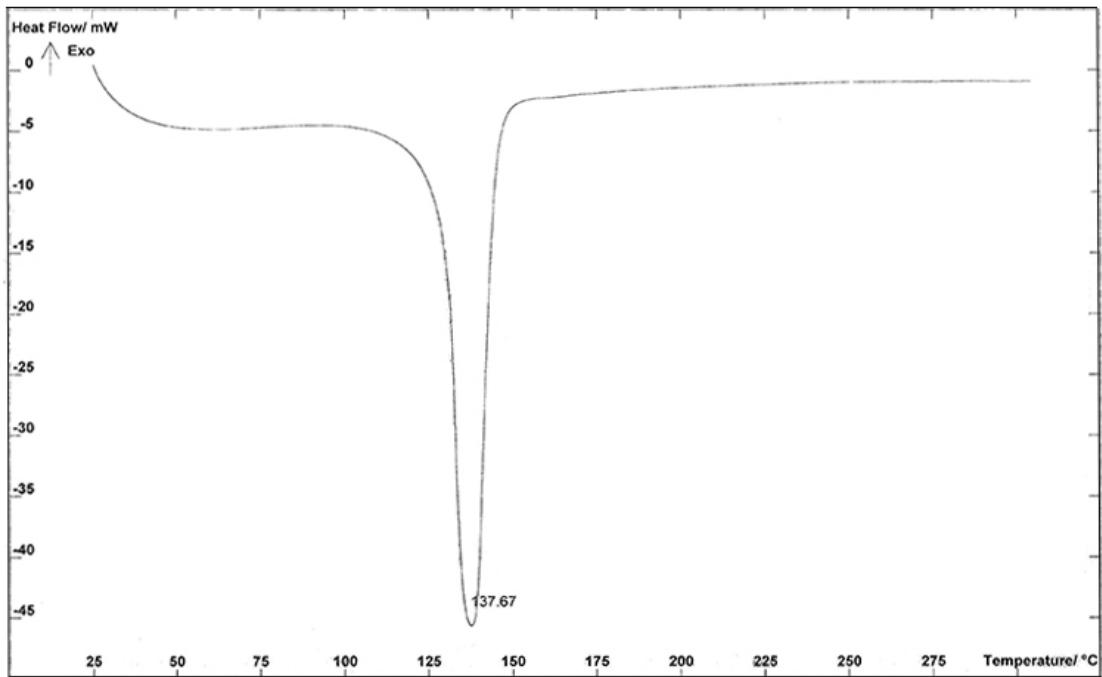


Figure 3.13. DSC thermogram of the product with 13.66% poly(BPOCPA)

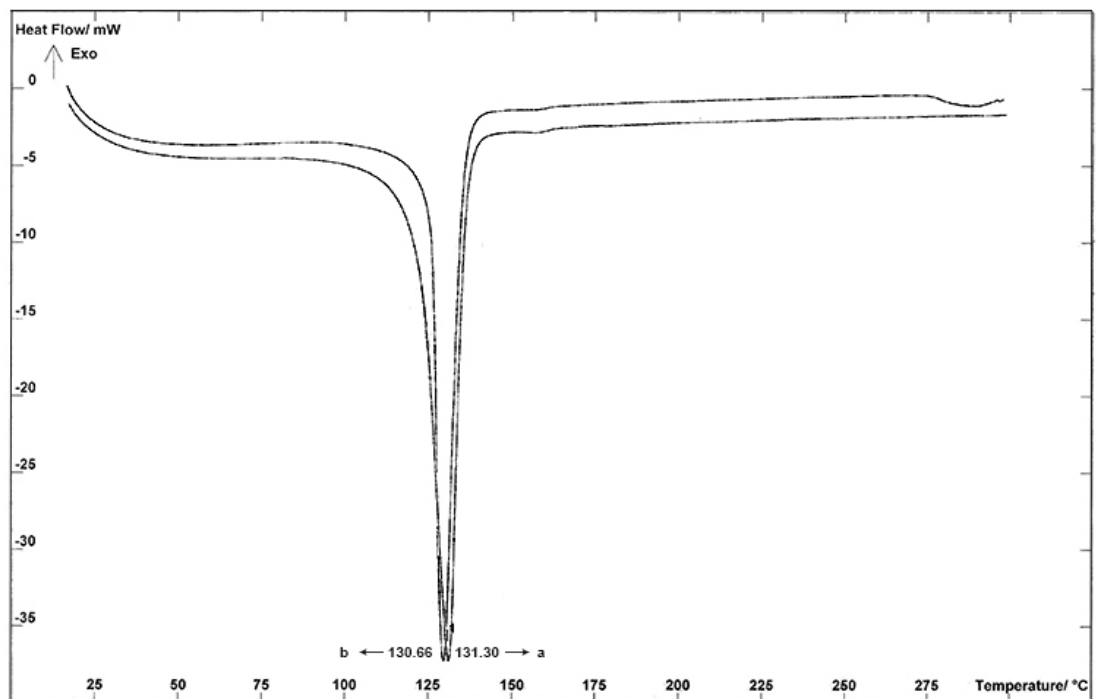


Figure 3.14. DSC thermogram of a) annealed HDPE and b) the sample of HDPE with 2% DCP heated to 140°C

### **3.2. TG/IR Analysis of the Products**

The mesomorphic behavior of poly(BPOCPA) was investigated by Sesha Sainath et al. [62], and it was reported to exhibit nematic phase between 145-199°C. Also, its initial decomposition temperature was reported to occur at 255°C. However, in DSC studies, although the smaller endotherm observed at 198°C was ascribed to liquid crystal-isotropization temperature by considering the study of Sesha Sainath et al.[62], any significant heat flow around 255°C, that could be responsible for decomposition of the polymer, was not detected in the thermogram, Figure 3.8. But, after completing the melting endotherm, the heat flow underwent an exothermic nature especially after about 265-266°C. It appears that thermal stability is also important for the processing of the graft coproduct, poly(BPOCPA)-g-PE. Therefore, in order to clarify the thermal behavior of the polymers at the temperatures that the mesomorphic state was observed and to comprehend the optimum conditions at which the polymers are stable for processing, decomposition and thermal behavior of poly(BPOCPA) and the graft copolymers were studied by DSC and TG/IR system, which combines thermogravimetric analyzer and FTIR spectrometer.

#### **3.2.1. TG/IR Analysis of Poly(BPOCPA)**

Thermogravimetric analysis of poly(BPOCPA) produced by DCP initiator carried out in N<sub>2</sub> showed that very slight weight loss started to be seen around 250°C, soon after completing the melting with regard to the DSC thermogram. The expressive weight loss, but with a slow rate, due to decomposition commenced at about 275-280°C. It became significant especially after 300°C and continued to 620°C, Figure 3.15. The rate of the loss was maximum in the region of 340-380°C as



revealed from the thermogram. The decomposition products were also analyzed by FTIR spectrometer combined with the thermogravimetric analyzer, and the spectra showed the similar absorption bands throughout the heating. In early stages of the decomposition, however, the absorption bands in the spectra were weak and imperceptible, Figure 3.16.a. The indicative and significant bands were observed markedly when the decomposition was fast, Figure 3.16.b. The formation of carbon dioxide started with the high rates of decomposition and continued until the end of the heating, apparently detected with the C=O stretching bands at 2355, 2353  $\text{cm}^{-1}$  and around 2311  $\text{cm}^{-1}$ , Figure 3.16.a, b, c and d. The spectrum taken at 378°C, Figure 3.16.b, most of the absorption bands of which were commonly observed in the other spectra, Figure 3.16. c and d, indicated the band at about 3644  $\text{cm}^{-1}$ , may be due to phenolic O-H stretching, the formation and assignment of which were reported in a similar analysis [4], the bands at about 3072 and 3038  $\text{cm}^{-1}$  possibly due to aromatic C-H stretching, the band at 1678  $\text{cm}^{-1}$  probably due to vinylic C=C stretching and the bands at 1606, 1512 and 1428  $\text{cm}^{-1}$  seemingly due to aromatic C=C stretching vibrations. The bands at 1266 and 1168  $\text{cm}^{-1}$  were attributed to C-O stretching vibrations. The bands at 933, 844 and 698  $\text{cm}^{-1}$  are probably corresponding to vinylic C-H out-of-plane bending vibrations. In accordance with the thermogram, while the absorption bands were observed markedly and significantly in high rates of decomposition, they weakened at high temperatures, through the end of the heating, especially after about 500°C, Figure 3.16.d.

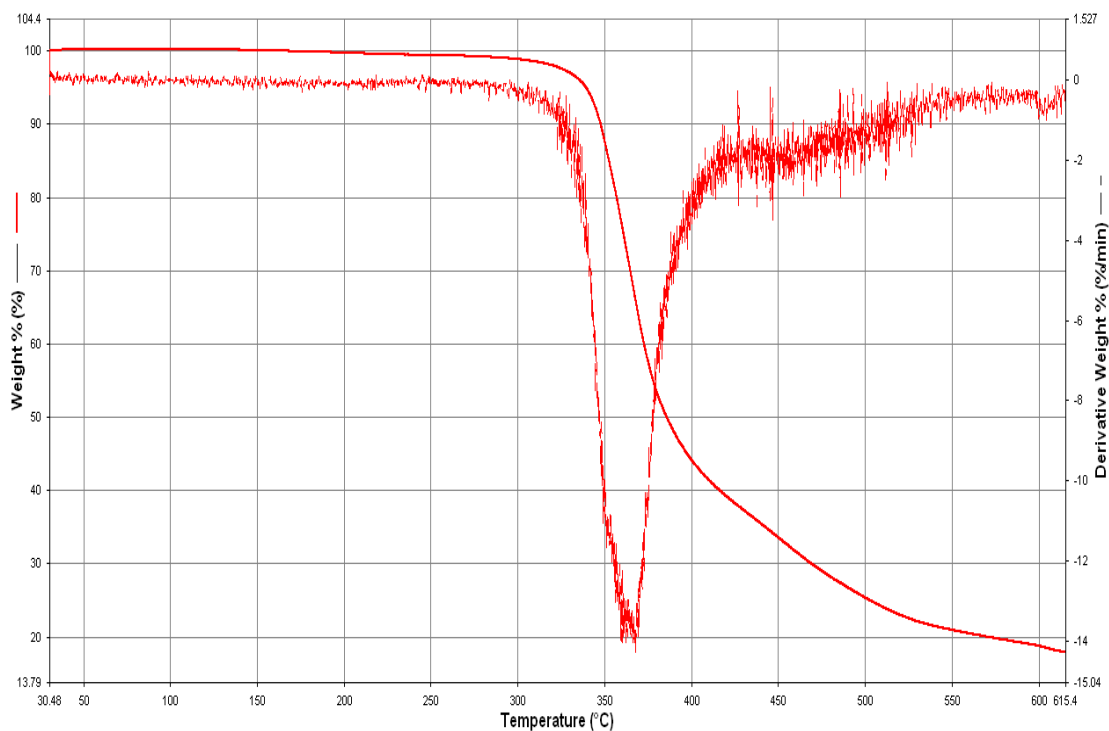


Figure 3.15. TGA thermogram of poly(BPOCPA)

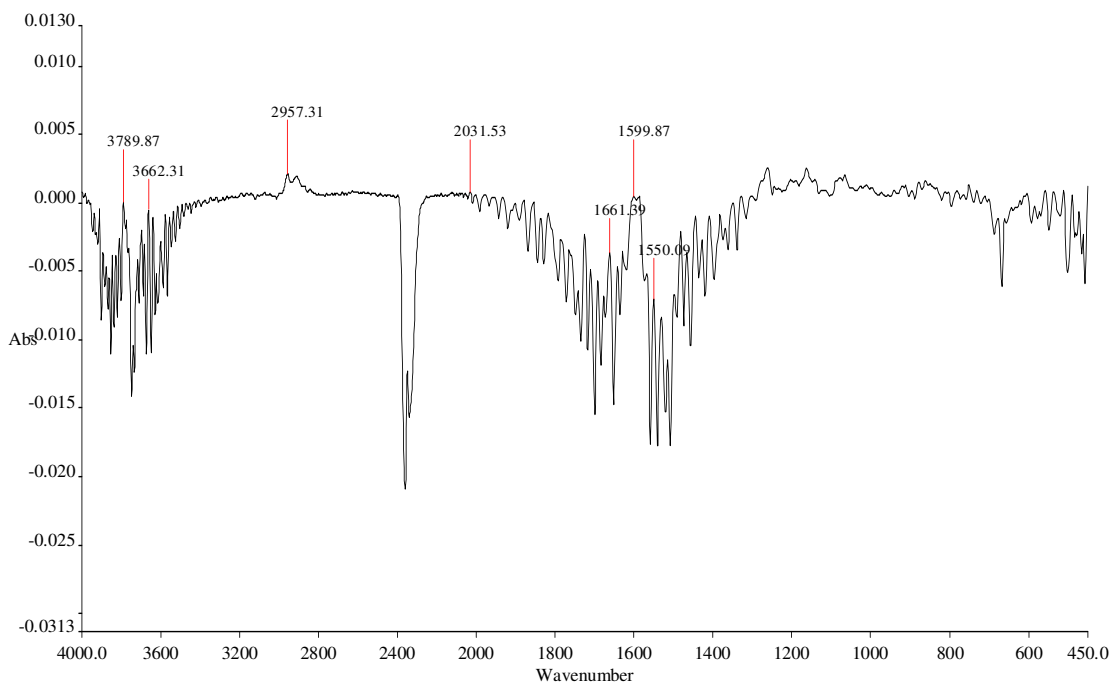


Figure 3.16.a. FTIR spectrum of the decomposition products formed at 322°C in nitrogen

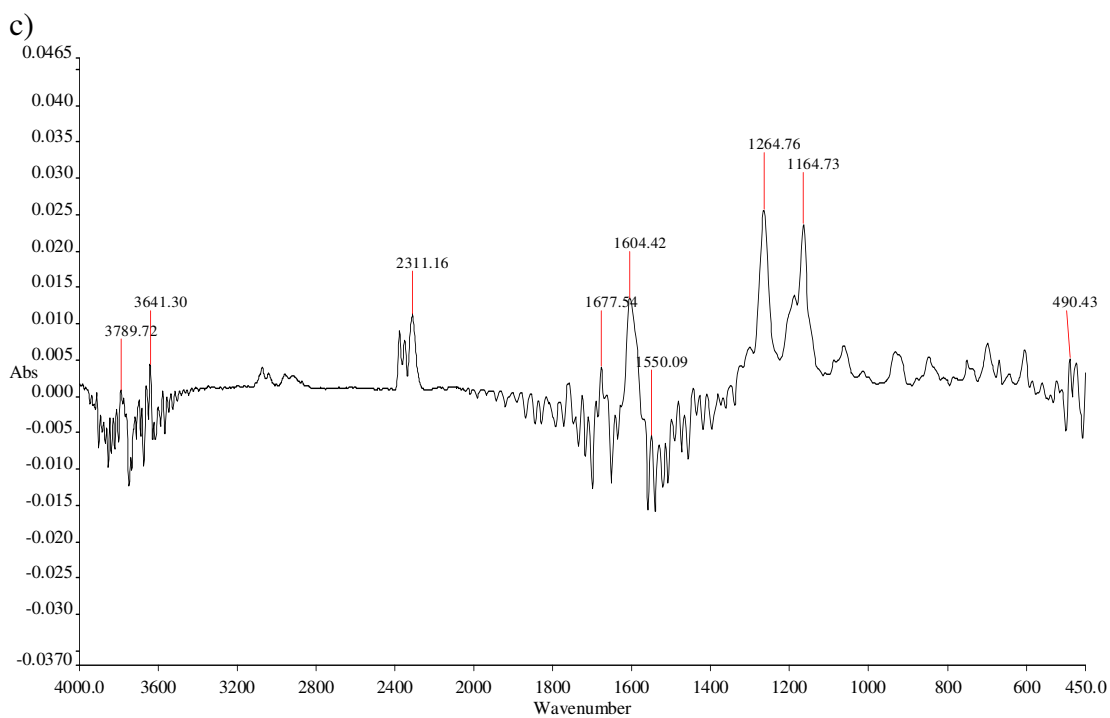
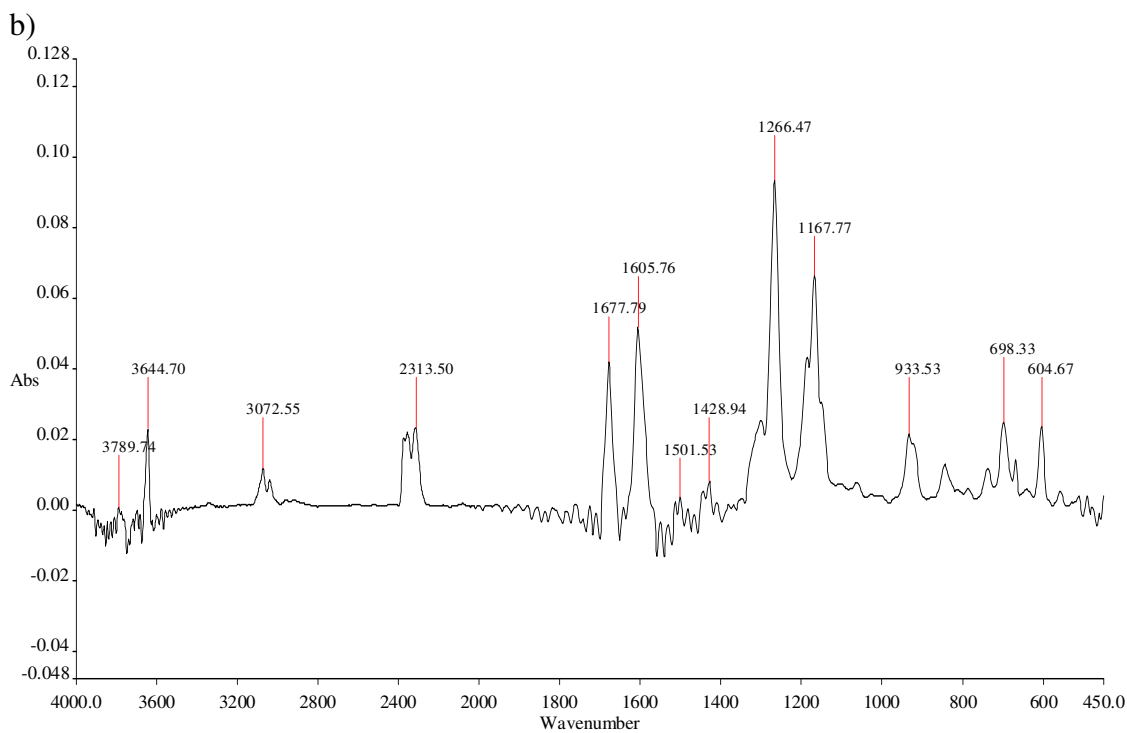


Figure 3.16.b and c. FTIR spectrum of the decomposition products formed at b) 378°C, and c) 405°C in nitrogen

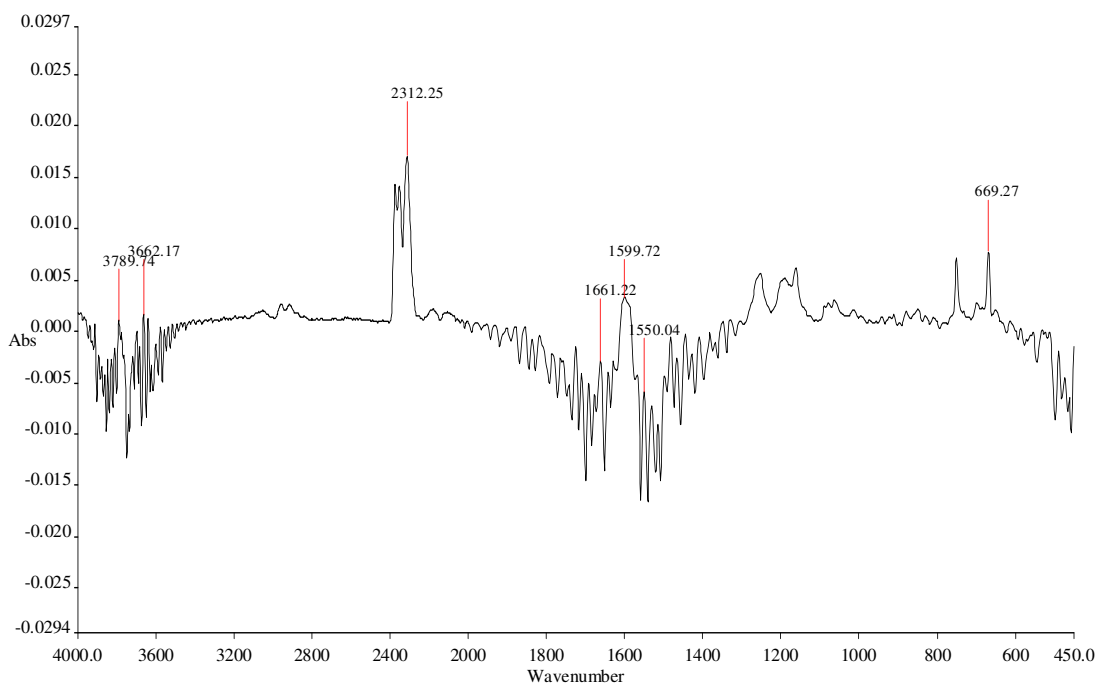


Figure 3.16.d. FTIR spectrum of the decomposition products formed at 530°C in nitrogen

Poly(BPOCPA) was also tested in air. The similar decomposition mechanism and trend were found with respect to that seen in nitrogen, Figure 3.17. The significant weight loss due to decomposition started to appear again especially after 300°C. But, at relatively earlier stages of the decomposition, between 280-300°C, the absorption bands of the decomposition products in the FTIR spectra, in contrast, were more massive and stronger, with a numerous peaks that could not be defined, newly forming around the bands that formerly observed in nitrogen. On the other hand, at higher temperatures the newly forming and undefinable bands diminished and vanished, and at high rates of weight loss, especially above 350°C, almost the same absorption bands were observed in the spectra with respect to that observed in nitrogen. The only additionally observed band is that seen at about 1757 and 1737

$\text{cm}^{-1}$ , which was ascribed to carboxylic and esteric  $\text{C}=\text{O}$  stretching vibrations respectively, Figure 3.18.a, b, c and d.

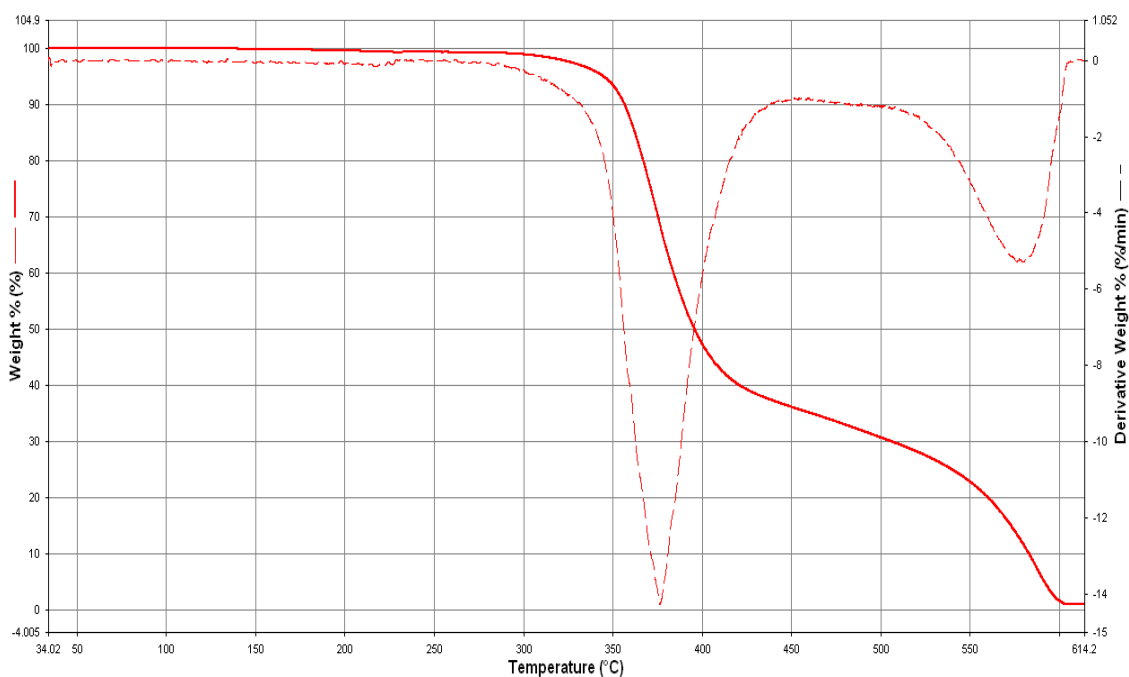


Figure 3.17. TGA thermogram of poly(BPOCPA) in air

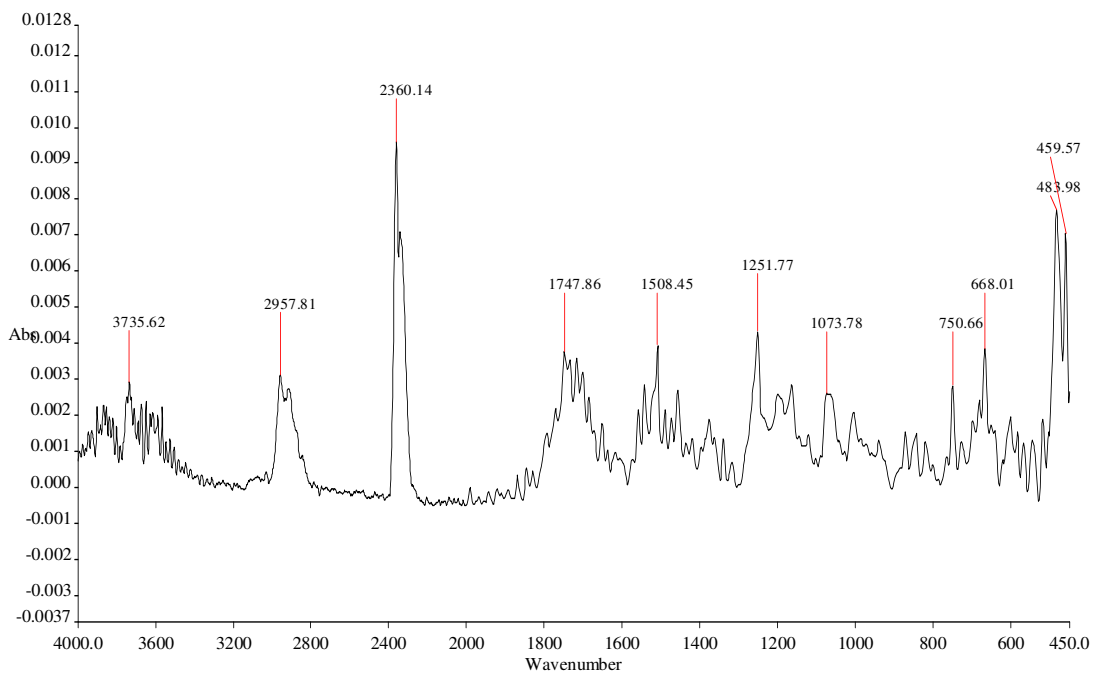


Figure 3.18.a. FTIR spectrum of the decomposition products formed at 284°C in air

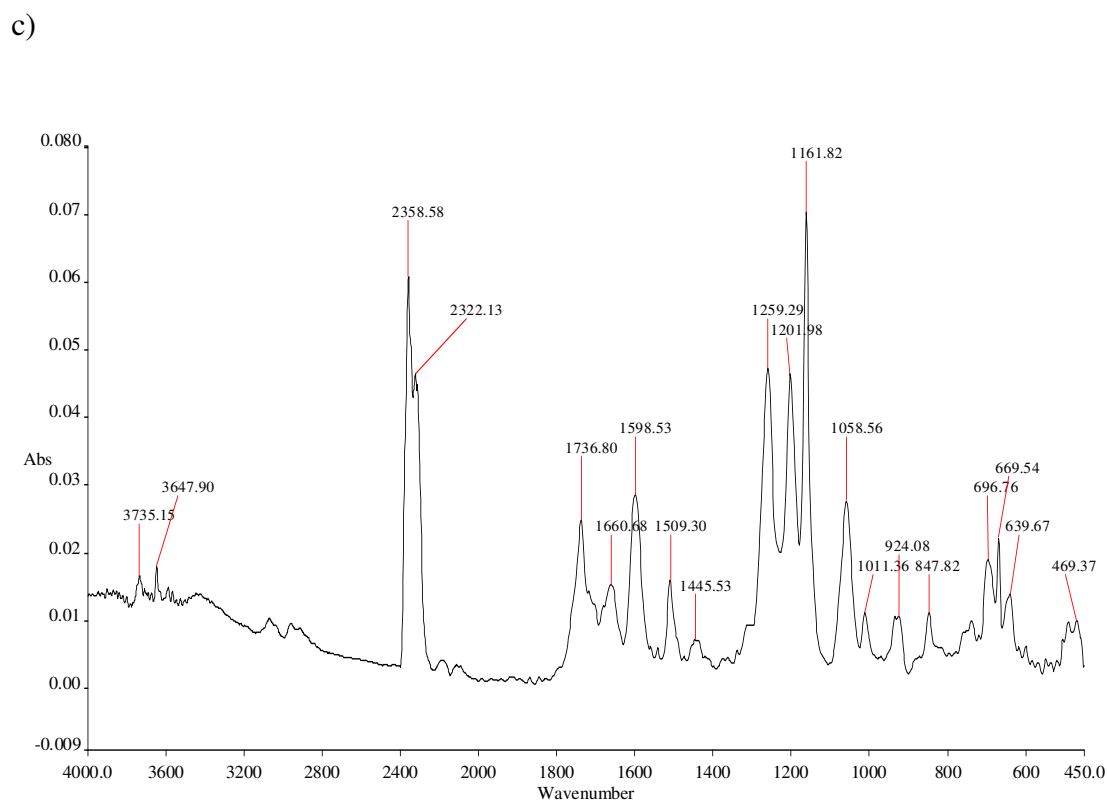
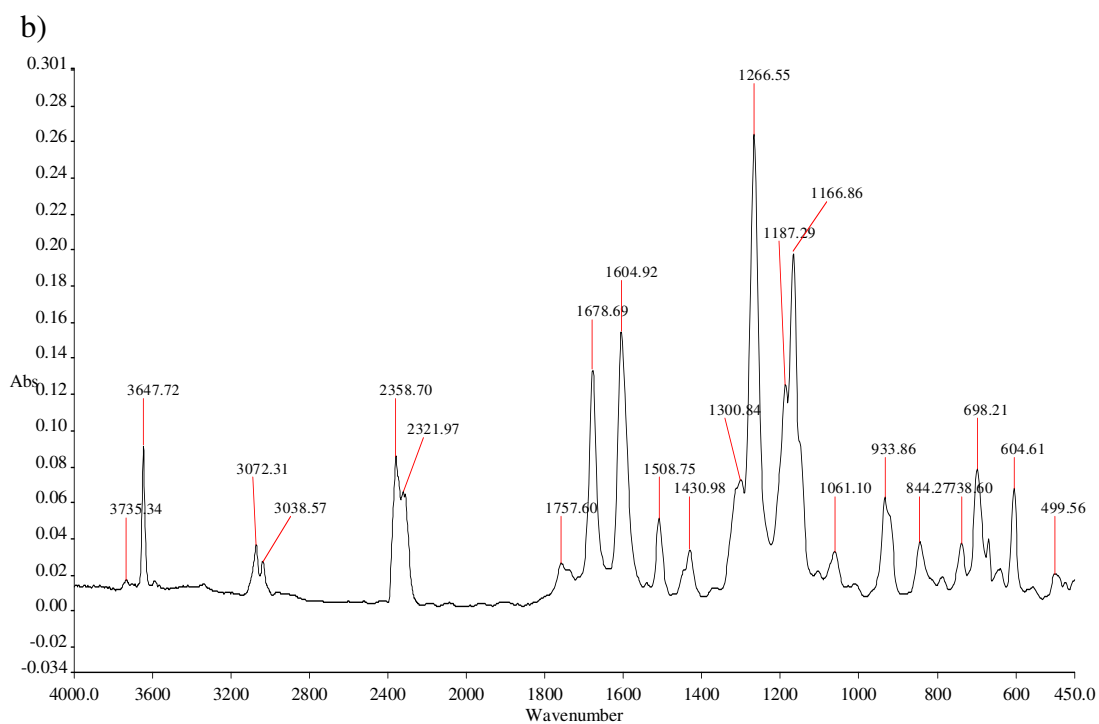


Figure 3.18.b and c. FTIR spectra of the decomposition products formed at b) 385°C, and c) 450°C in air

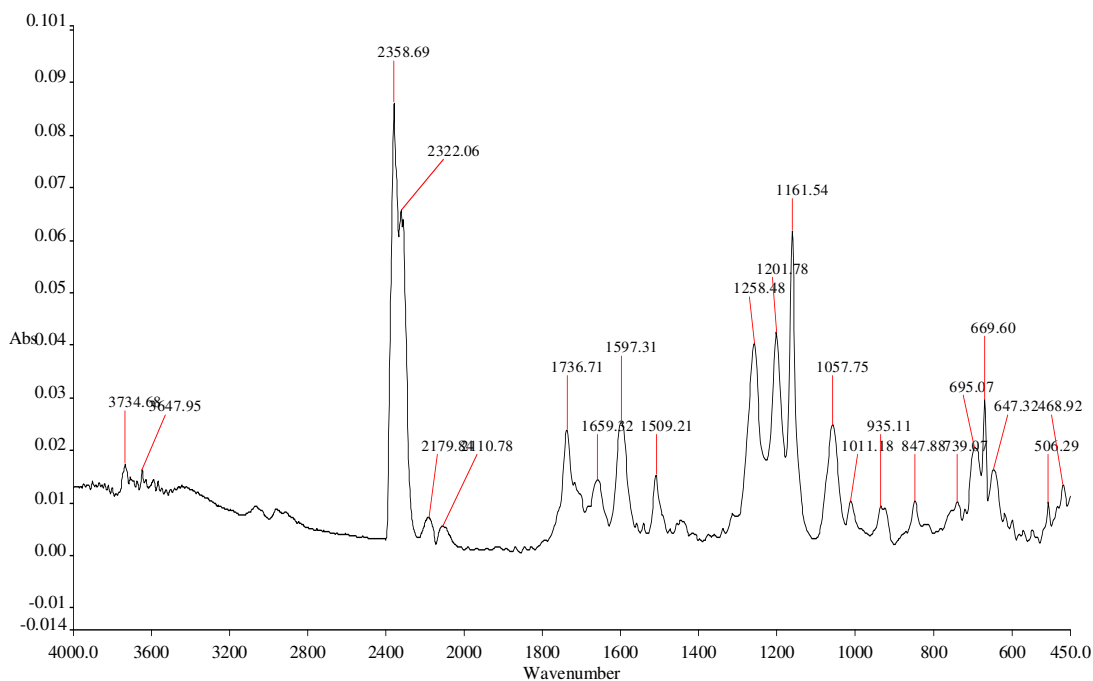


Figure 3.18.d. FTIR spectrum of the decomposition products formed at 492°C in air

### 3.2.2. TG/IR Analysis of the Graft Copolymerization Products

Thermogravimetric analysis of the 13.66% and 39.10% BPOCPA products carried out in N<sub>2</sub> atmosphere displayed that the first weight loss started at about 275°C in the former, and at about 250°C in the latter sample and continued to about 500°C and 600°, respectively, Figure 3.19 and 3.20. The weight loss was 10% at about 400°C and 15% at about 435°C for the former sample, while the same losses were reached at earlier temperatures, about 335 and 350°C, respectively, for the latter. When compared to that also revealed for the homopolymer, it can be concluded that the weight loss due to decomposition has been explicitly retarded by PE, and the effect were weakening with the increase of the percentage of poly(BPOCPA), accordingly with the decrease of PE percentage, in the products. The 15% loss in the former was followed by rapid loss with respect to earlier trend, proceeding until about 500°C, at which the loss was 96-97%. For the latter sample,

the similarly high rate of the loss was observed between about 450-500°C, above which the weight loss, 86-87% at about 500°C, slowed down.

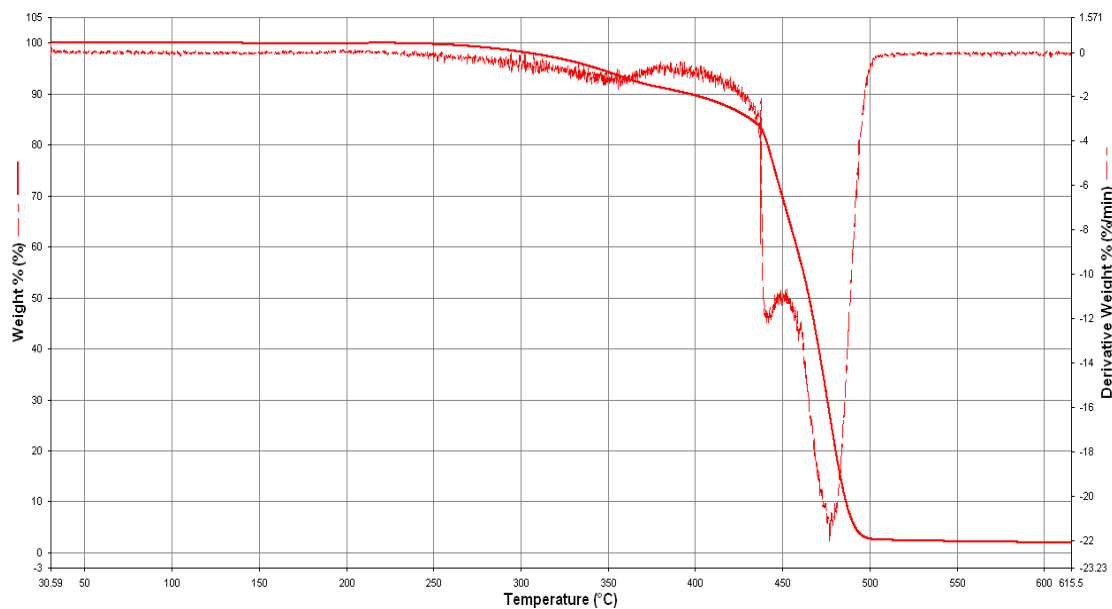


Figure 3.19. TGA thermogram of the product with 13.66% poly(BPOCPA) taken in nitrogen

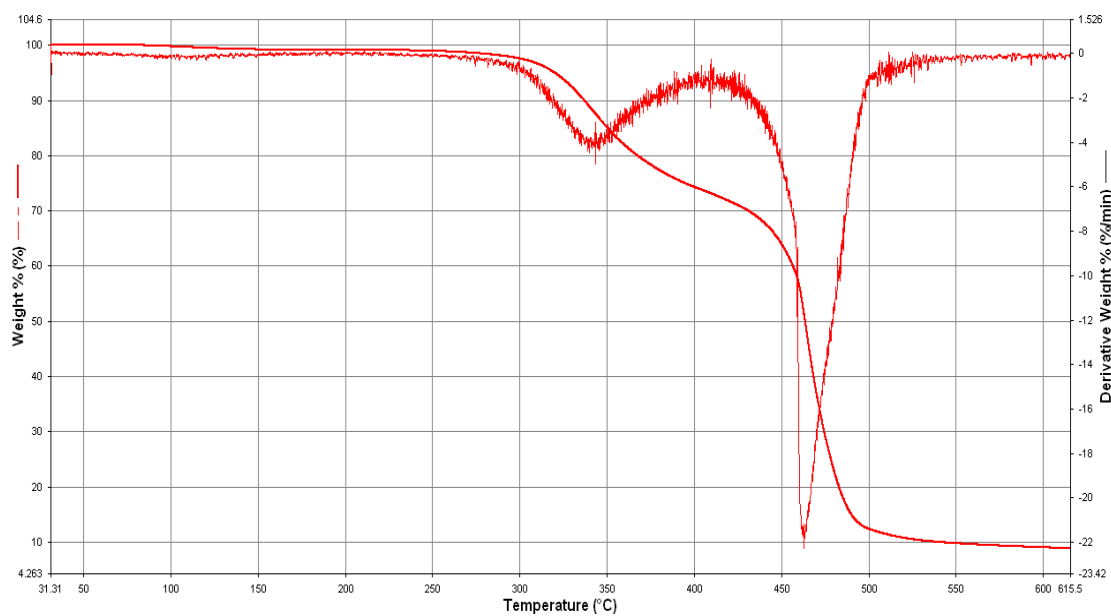


Figure 3.20. TGA thermogram of the product with 39.10% poly(BPOCPA) in nitrogen



FTIR analysis of the decomposition products exhibited the similar decomposition mechanism with respect to that observed for homopolymer, poly(BPOCPA). The formation of CO<sub>2</sub> in the analysis of 13.66% BPOCPA product, however, was seen between about 450-500°C, along which the weight loss rate was maximum, and at temperatures above 600°C, Figure 3.21.a, b and c, while it started to appear at lower temperatures, at about 350°C, in the analysis of the homopolymer and 39.10% BPOCPA product, Figure 3.22.b. In addition, the absorption bands at about 2932, 2925 and 2854 cm<sup>-1</sup>, ascribed to the C-H stretching vibrations of CH<sub>2</sub> group, were differently observed from the homopolymer at temperatures above 350°C, growing up with temperature, in the spectra of the former sample, Figure 3.21.b. They were detected, however, at all stages of the decomposition, even at about 280°C, in spectra of the latter, Figure 3.22.a and b.

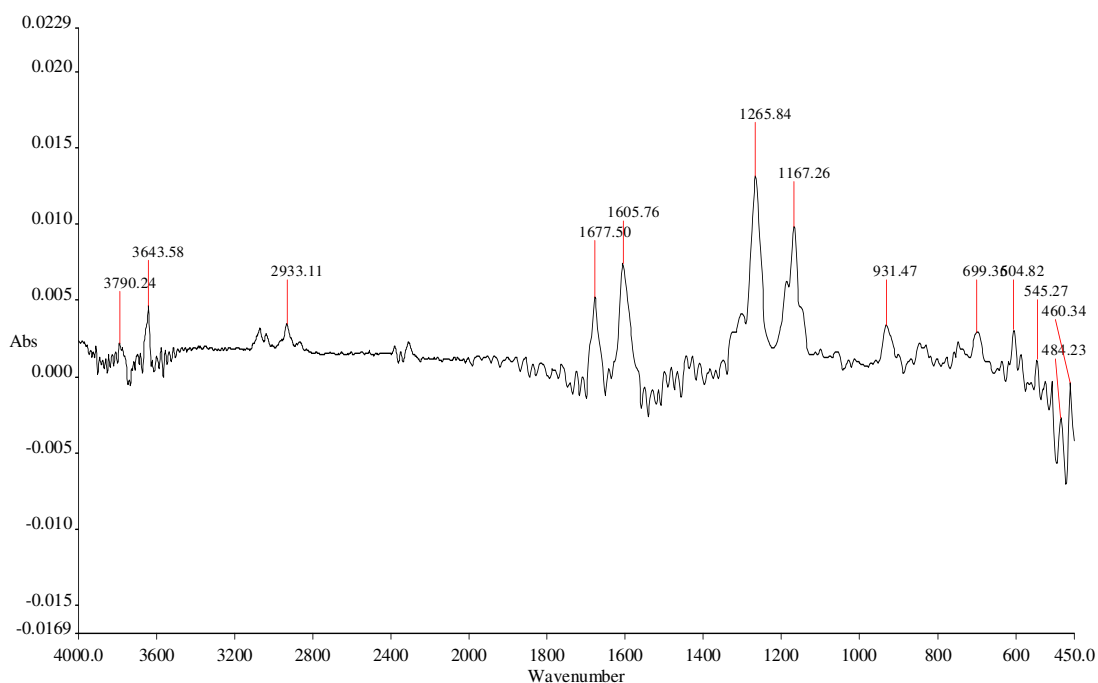


Figure 3.21.a. FTIR spectrum of the decomposition products formed at 364°C during the heating of the product containing 13.66% poly(BPOCPA) in nitrogen

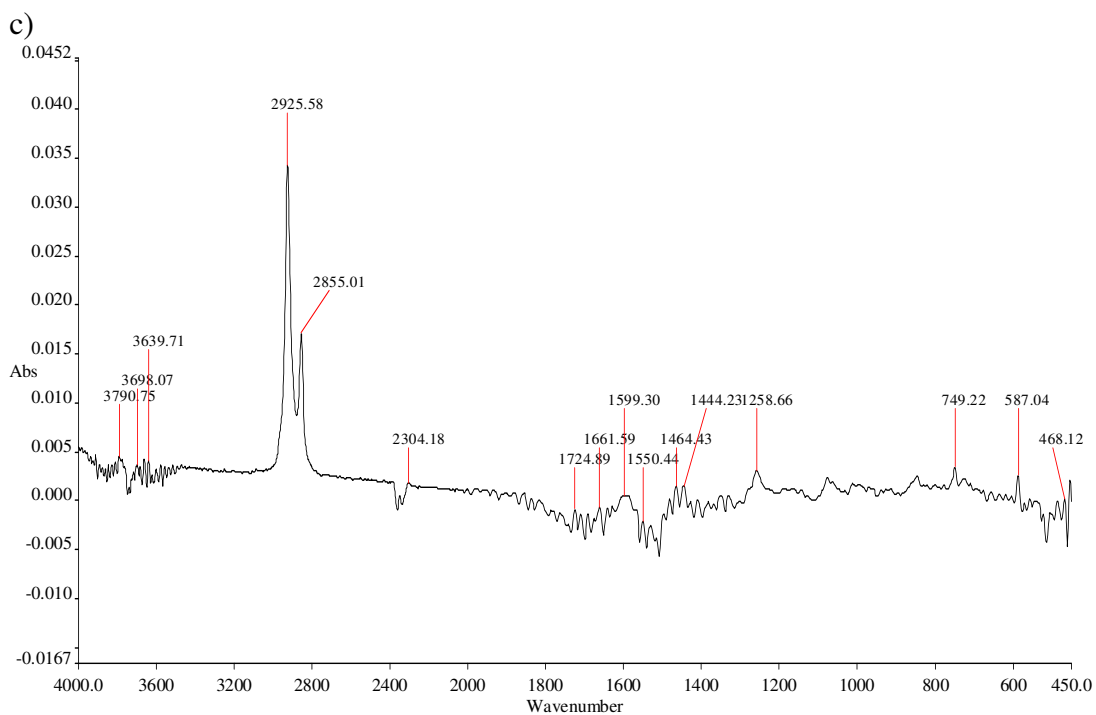
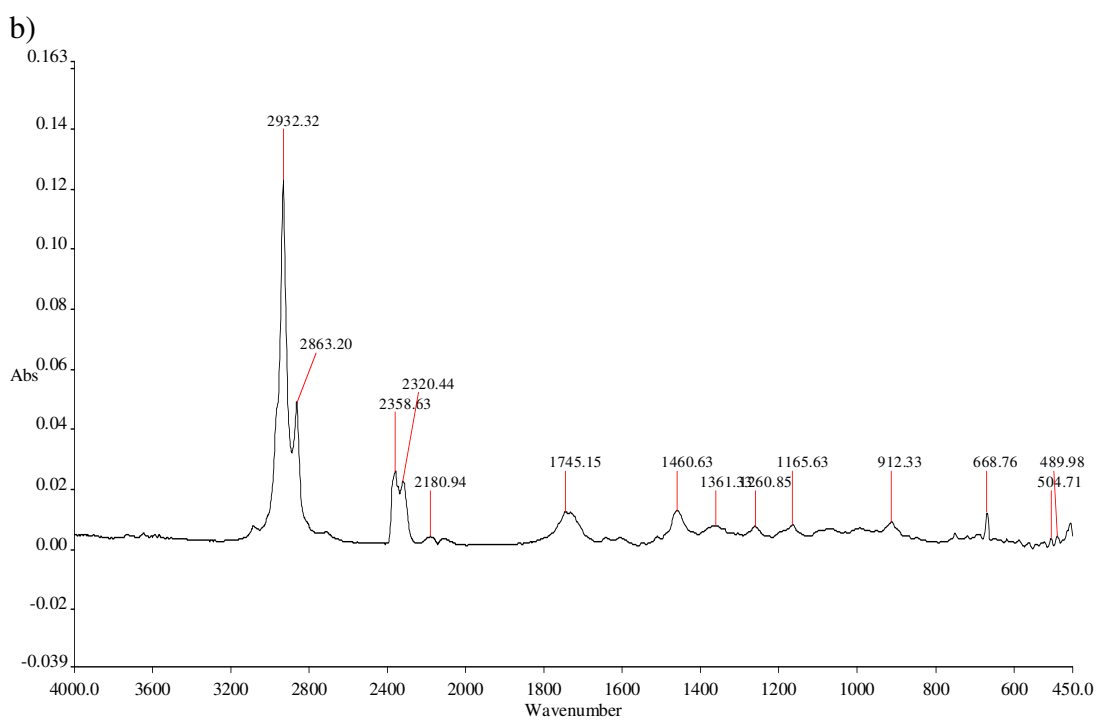


Figure 3.21.b and c. FTIR spectra of the decomposition products formed at b) 447°C, and c) 572°C during the heating of the product containing 13.66% poly(BPOCPA) in nitrogen

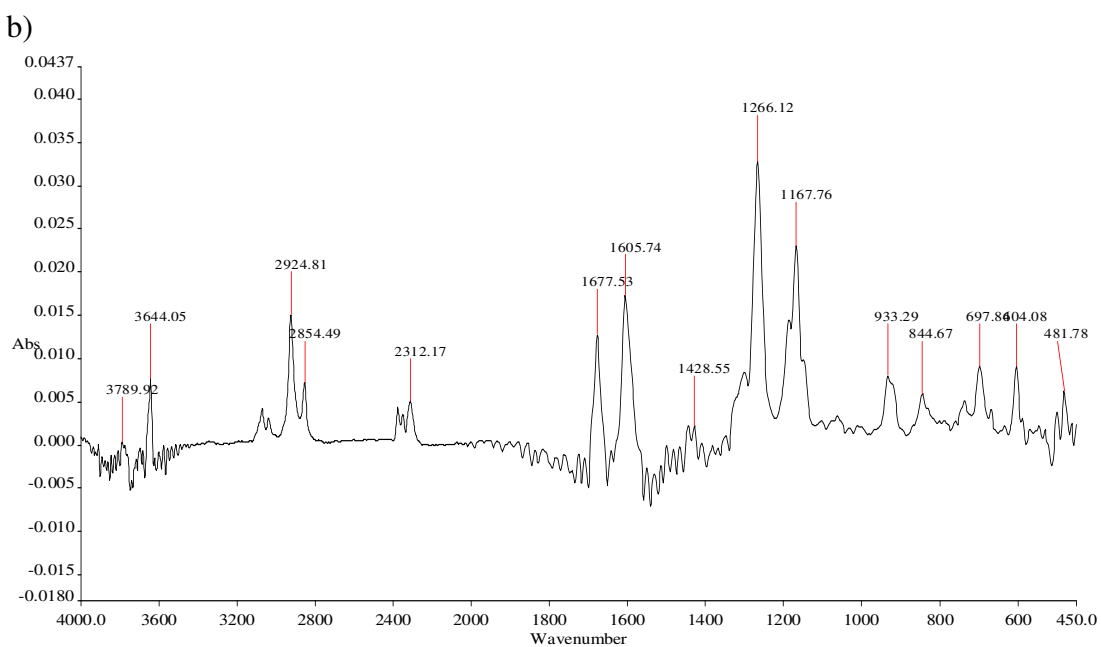
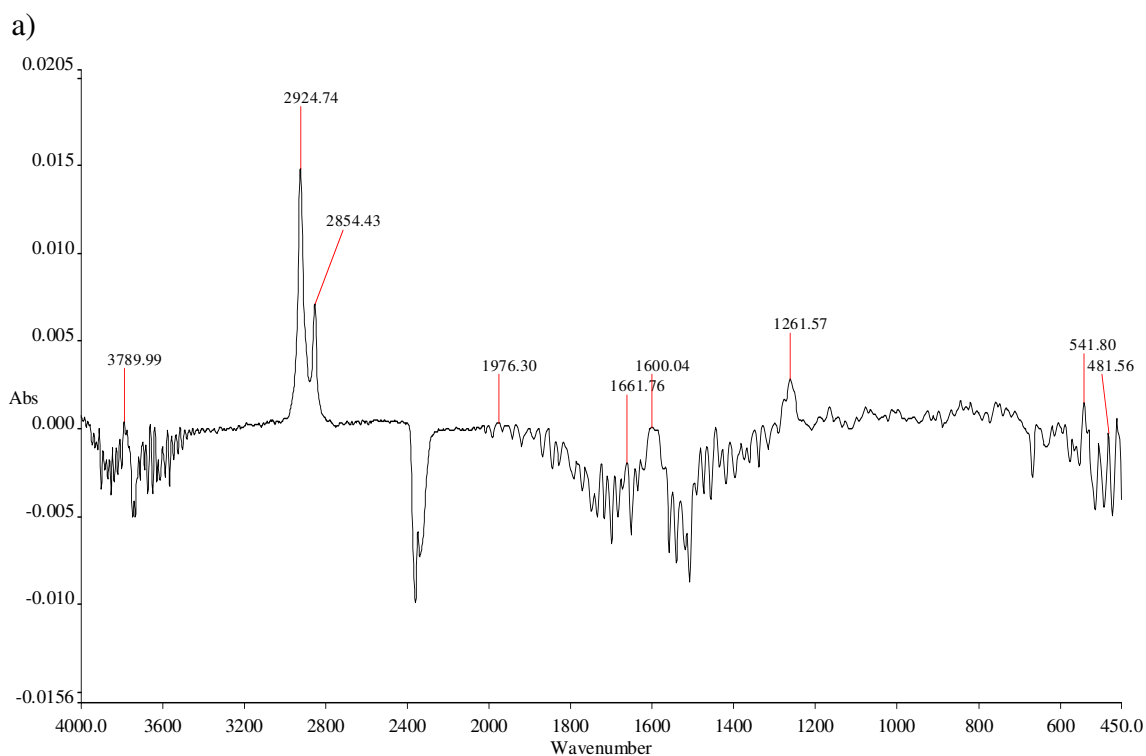


Figure 3.22.a and b. FTIR spectra of the decomposition products formed at a) 281°C, and b) 350°C during the heating of the product containing 39.10% poly(BPOCPA) in nitrogen

The TG/IR analysis of the graft copolymerization products with 13.66% and 39.10% poly(BPOCPA) were also carried out in air. The results indicated that the decomposition took place with the same mechanism and trend in air, Figure 3.23-26.

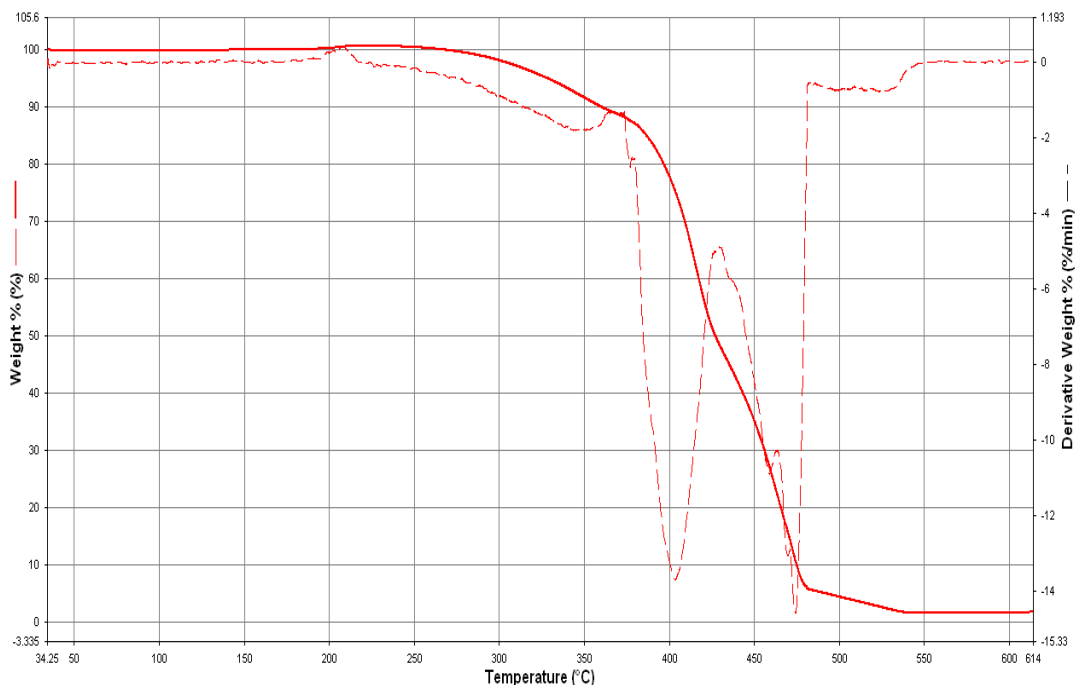


Figure 3.23. TGA thermogram of the product with 13.66% poly(BPOCPA) in air

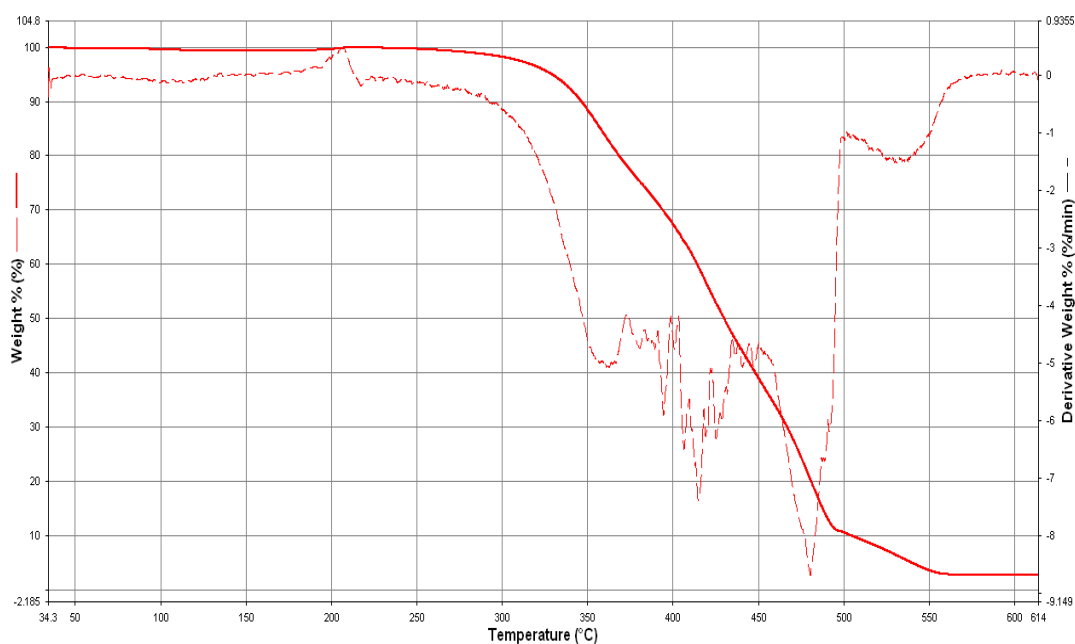


Figure 3.24. TGA thermogram of the product with 39.10% poly(BPOCPA) in air

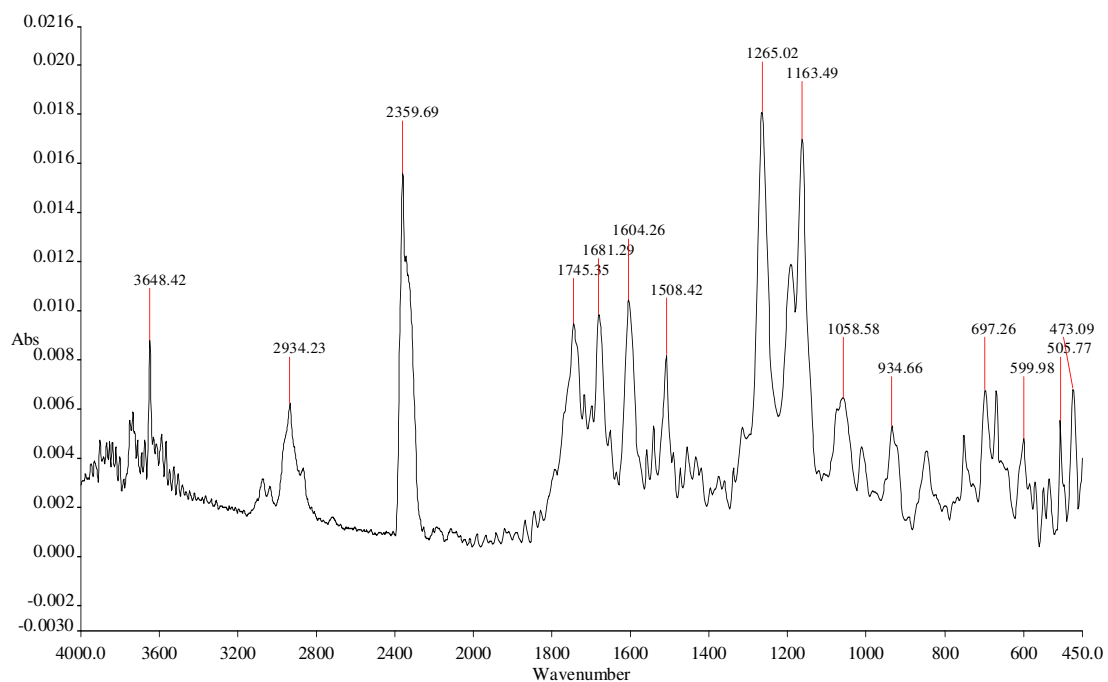


Figure 3.25. FTIR spectrum of the decomposition products formed at (326°C) during the heating of the product containing 13.66% poly(BPOCPA) in air

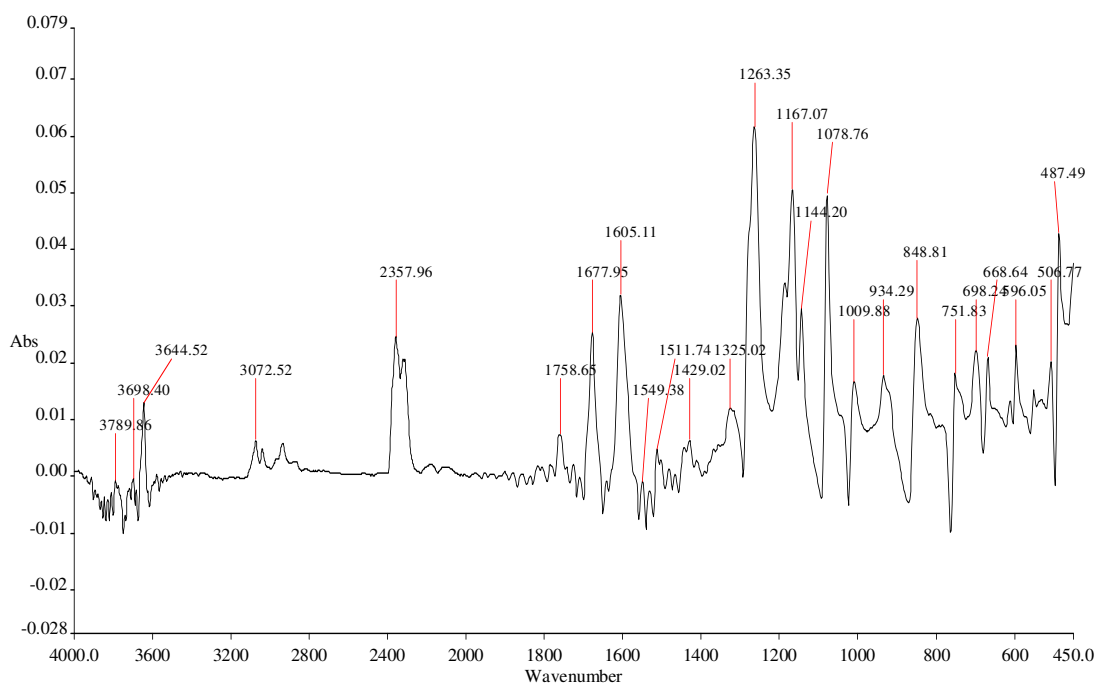


Figure 3.26. FTIR spectrum of the decomposition products formed at (381°C) during the heating of the product containing 13.66% poly(BPOCPA) in air

### **3.3. Mechanical Properties of the Polymers**

The mechanical properties of the graft copolymerization products were studied in order to find out the effect of poly(BPOCPA), a side chain liquid crystalline polymer present in the products as grafted and homopolymer, on the mechanical behavior of HDPE. The completely homogeneous structure and absence of phase separation in the products revealed from the SEM studies (section 3.5) indicated that the graft copolymer, poly(BPOCPA)-g-PE, formed in the reactions acted as a compatibilizer between PE and ungrafted poly(BPOCPA) homopolymer. Because, in case of blending alone, the different nature of poly(BPOCPA) from PE, with polar groups in its structure, would virtually have led to incompatibility between the components, PE and poly(BPOCPA), and thus resulted in a phase separation in the products.

The dogbone samples were prepared by micro-injection molding at 275°C in order to provide an ideal dispersion of reinforcing liquid crystalline polymer phase in the products. Although this processing temperature is well above the melting temperature of poly(BPOCPA) (231°C) and may be considered as the starting point of decomposition as revealed from TG/IR analysis, it became highly compulsory to process the injection mold samples at this temperature owing to gummy behavior of the samples. At lower temperatures the samples were very hard to process due to difficulties in the flow behavior of the melts. On the other hand, considerable and important improvements were observed in the mechanical properties of the products, particularly, in ultimate tensile strength and modulus. But, yield stress and percent elongation were lost in the products with higher contents of poly(BPOCPA), accordingly, these samples were mostly broken in brittle nature, while ductile failure with neck formation was observed at lower contents.

Stress-strain curve of virgin HDPE and of the products are illustrated in Figure 3.27. Although virgin HDPE showed a great extent of cold drawing or orientatiton, the products with 4.97% and 9.32% of poly(BPOCPA) failed during strain softening, the former at about 38% strain and the latter at about 29% stain. They exhibited ductile failure with neck formation. On the other hand, the product with 13.66% poly(BPOCPA) broke just after yield stress, while the products with higher contents of poly(BPOCPA) than 15% broken in brittle nature. Brittleness increased with poly(BPOCPA) content in the products, Figure 3.28.

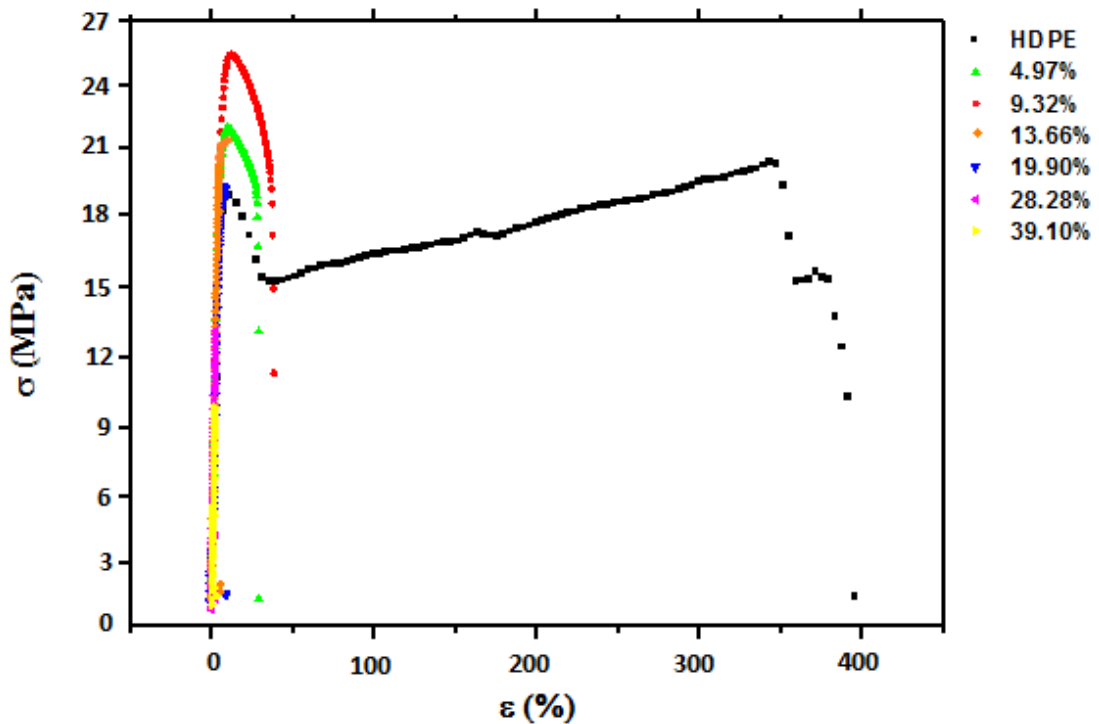


Figure 3.27. Stress-strain curve of HDPE and the graft copolymerization products with the content of 4.97, 9.32, 13.66, 19.90, 28.28 and 39.10% poly(BPOCPA)

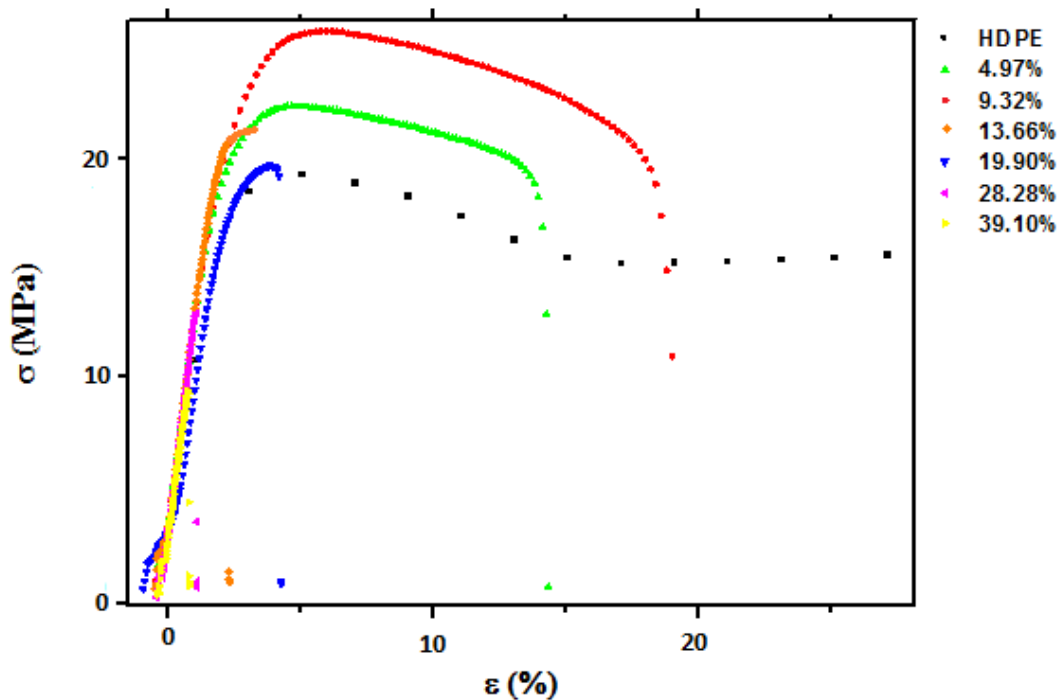


Figure 3.28. Magnified stress-strain curve of HDPE and the graft copolymerization products with the content of 4.97, 9.32, 13.66, 19.90, 28.28 and 39.10% poly(BPOCPA)

The results of tensile strengths of the graft copolymerization products are tabulated in Table 3.1 and drawn in Figure 3.29, which were determined with the elongation speed of 5 cm/min. The strength of the samples increased with the increase of poly(BPOCPA) percentage in the products. The maximum strength of 26.00 MPa, which was 38% greater than virgin PE (18.78 MPa), was achieved with 9.32% poly(BPOCPA). The maximum was then followed by a decrease. A similar trend was also observed in modulus, determined on the same samples during tensile tests. Modulus increased with poly(BPOCPA) content in the products. The maximum, 605 MPa, was attained also at 9.32% poly(BPOCPA), which was very high compared to modulus of virgin PE, 362 MPa, (67% greater), and then was



followed by a decrease with the content of poly(BPOCPA), Table 3.2 and Figure 3.30.

Table 3.1. Ultimate tensile strength of the products with % poly(BPOCPA) in samples

% Poly(BPOCPA)	4.97	9.32	13.66	19.90	28.28	39.10	PE
Ult.Strength(MPa)	21.86 ±3.86	26.00 ±5.5	21.65 ±5.07	18.86 ±1.18	12.13 ±2.99	9.13 ±0.86	18.78 ±3.15

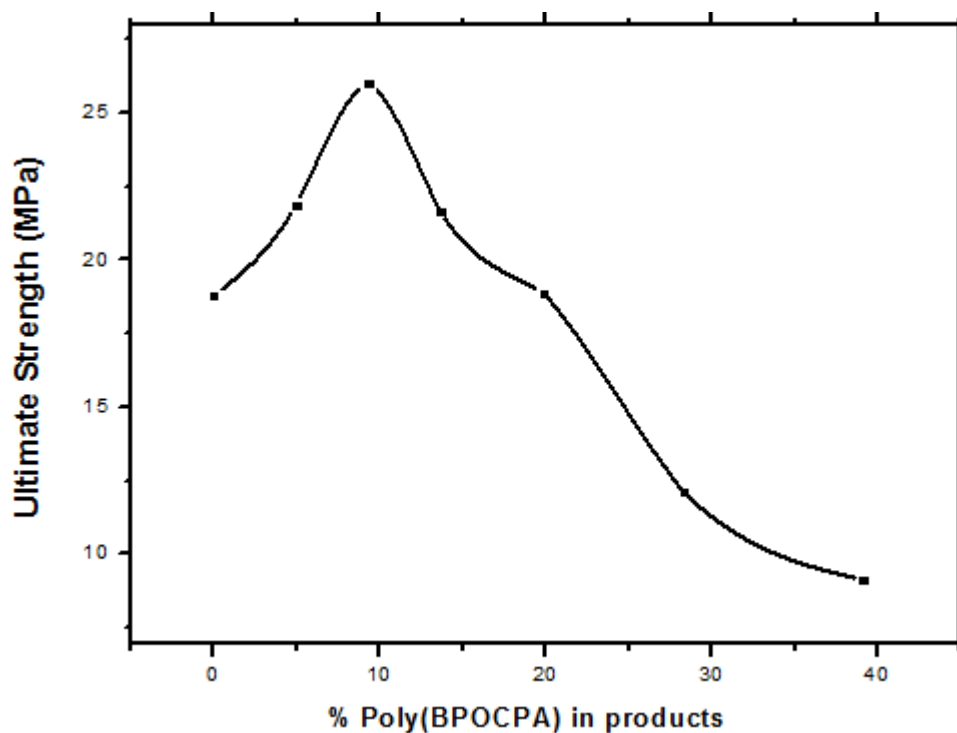


Figure 3.29. Dependence of ultimate strength of on content of poly(BPOCPA)

Table 3.2. Young's modulus of the products with % poly(BPOCPA) in samples

% Poly(BPOCPA)	4.97	9.32	13.66	19.90	28.28	39.10	PE
Modulus(MPa)	441	605	506	498	481	491	362

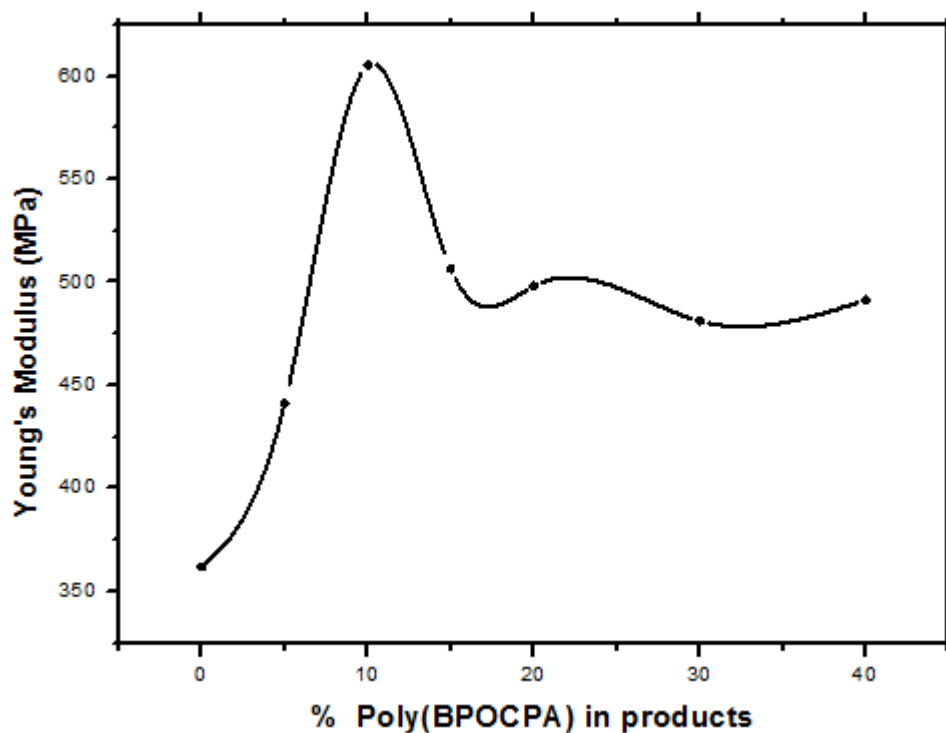


Figure 3.30. Dependence of Young's modulus on content of poly(BPOCPA)

The variation of impact strength with respect to poly(BPOCPA) content in the products is given in Table 3.3 and Figure 3.31. Because the PE and the products with 4.97% and 9.32% poly(BPOCPA) were not broken, their impact strengths could not be determined confidently. The measurements of impact strength of the other products displayed that the strength increased initially with the percentage of poly(BPOCPA), and the maximum strength, 52.39 kJm<sup>-2</sup>, achieved with 19.90% poly(BPOCPA), was followed by a dramatic decrease with the content, reducing to 17.85 kJm<sup>-2</sup> at 28.28% poly(BPOCPA). It can be stated that at higher contents, the products are obviously in brittle nature and brittleness increased with poly(BPOCPA) percentage, also as revealed with missing yield stress and increased brittleness in tensile tests.

Table 3.3. Impact strength of HDPE and the products with % poly(BPOCPA) in samples. NB denotes 'Not Broken' samples

BPOCPA%	4.97	9.32	13.66	19.90	28.28	39.10	PE
Impact Strength (kJ/m <sup>2</sup> )	NB	NB	48.02 ±9.28	52.04 ±2.55	27.83 ±7.85	21.90 ±3.22	NB

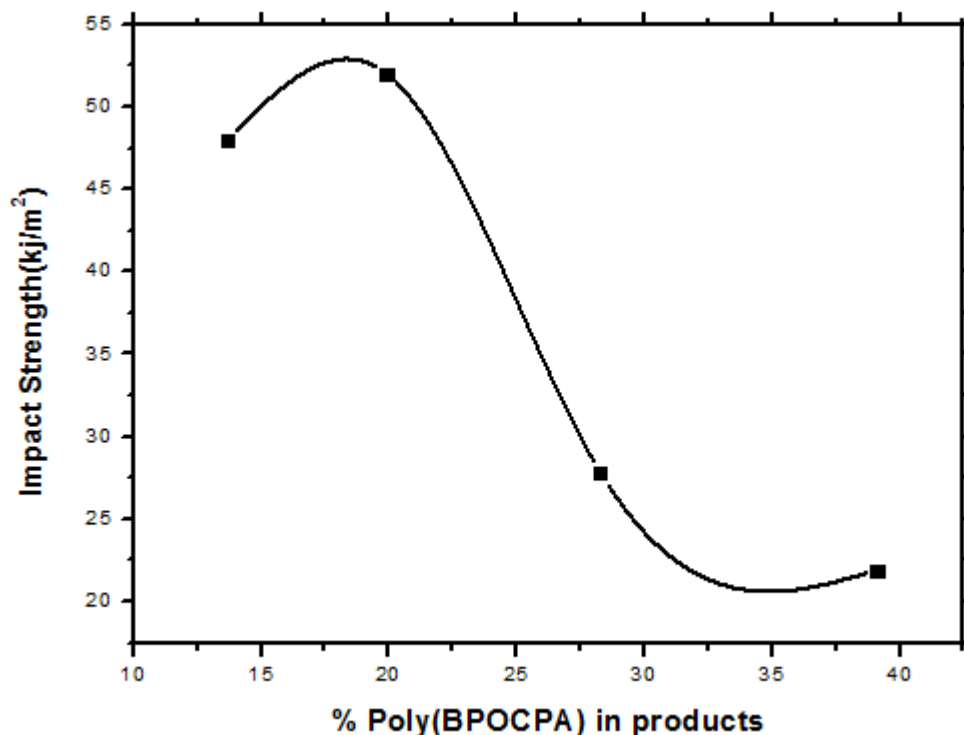


Figure 3.31. Dependence of impact strength on content of poly(BPOCPA)

### 3.4. SEM Analysis of the Polymers

The tensile and impact fractured surfaces of the products were shown in Figure 3.32-3.44. SEM photographs showed that the products displayed no phase separation and their structures were completely homogeneous in spite the graft units of poly(BPOCPA), with polar groups in its structure, were different from HDPE in nature. Furthermore, the products used in all characterizations and tests involved totally both grafted and ungrafted poly(BPOCPA) present as homopolymer. The absence of phase separation and completely homogeneous structure in the products confirmed the graft copolymerization of BPOCPA onto HDPE and indicated that the graft copolymer, poly(BPOCPA)-g-PE, formed in the reactions acted as a compatibilizer between PE and ungrafted poly(BPOCPA) homopolymer.

In general, the morphology of fracture greatly changed from ductile failure observed at low contents of poly(BPOCPA) to brittle nature seen at high contents. Tensile fractographs of the products with increasing poly(BPOCPA) content were given in Figure 3.32-39. We observed an extensive fibrillation broken in ductile at low contents of poly(BPOCPA), and the extent of ductility decreased with the increase of the content. The shortening of the extensions are clearly seen in Figure 3.32-37 where Figure 3.35 is the magnified version of the fractograph of the sample with 13.66% poly(BPOCPA) and showing a significant change in the morphology. In the sample with 28.28% poly(BPOCPA) although some fibrillar structure with smaller extensions were present, microcracks and openings started to appear, Figure 3.36-37. In this sample and at higher contents fractographs illustrated the cracks and holes showing brittle fracture, Figure 3.38-39, at which the tensile strength was found to be the lowest.

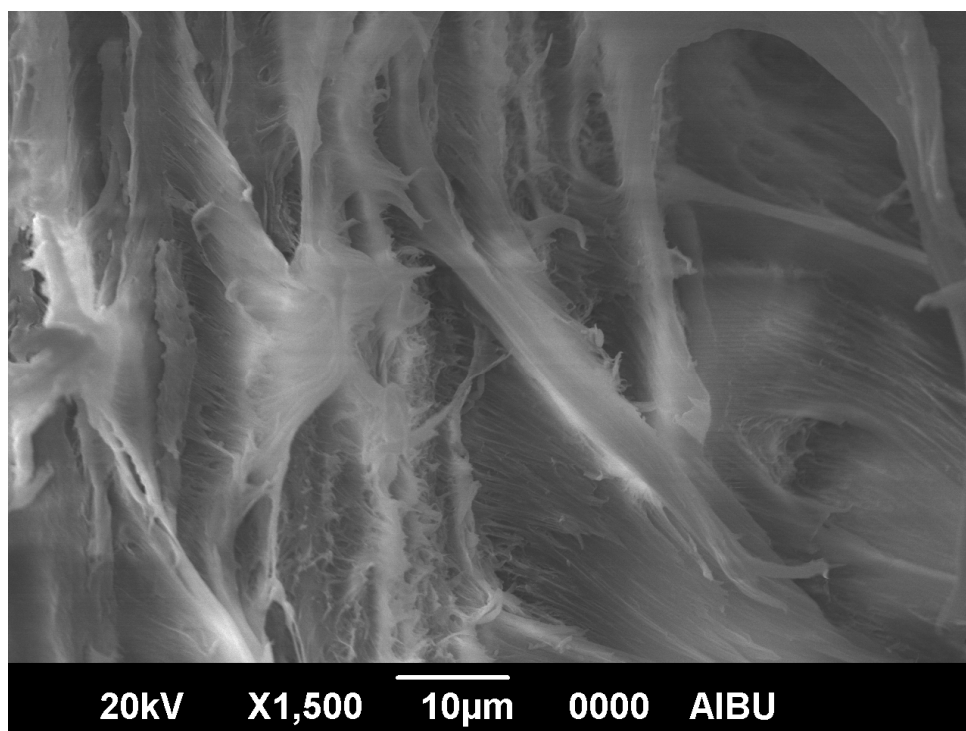


Figure 3.32. SEM photograph of the product with 4.97% poly(BPOCPA), after obtained from tensile test

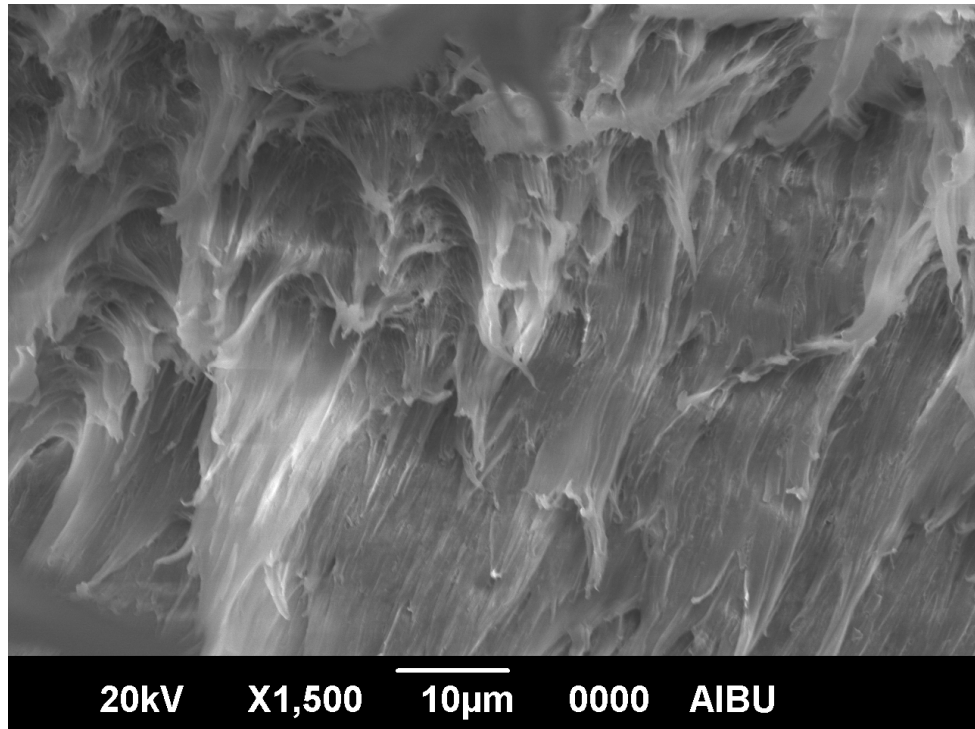


Figure 3.33. SEM photograph of the product with 9.32% poly(BPOCPA) after obtained from tensile test

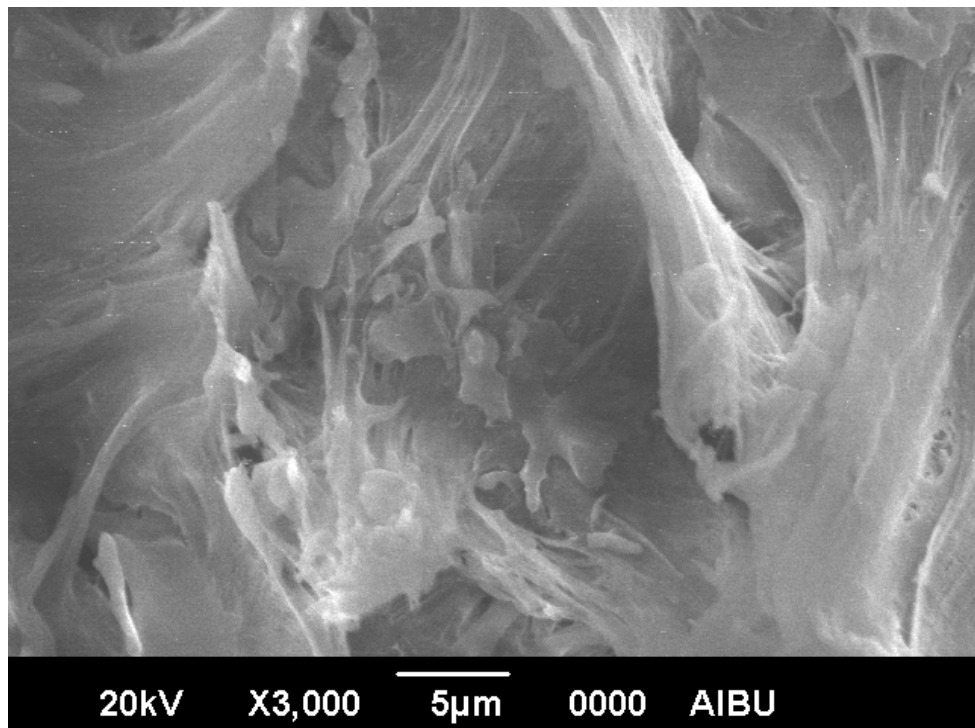


Figure 3.34. SEM photograph of the product with 13.66% poly(BPOCPA), after obtained from tensile test

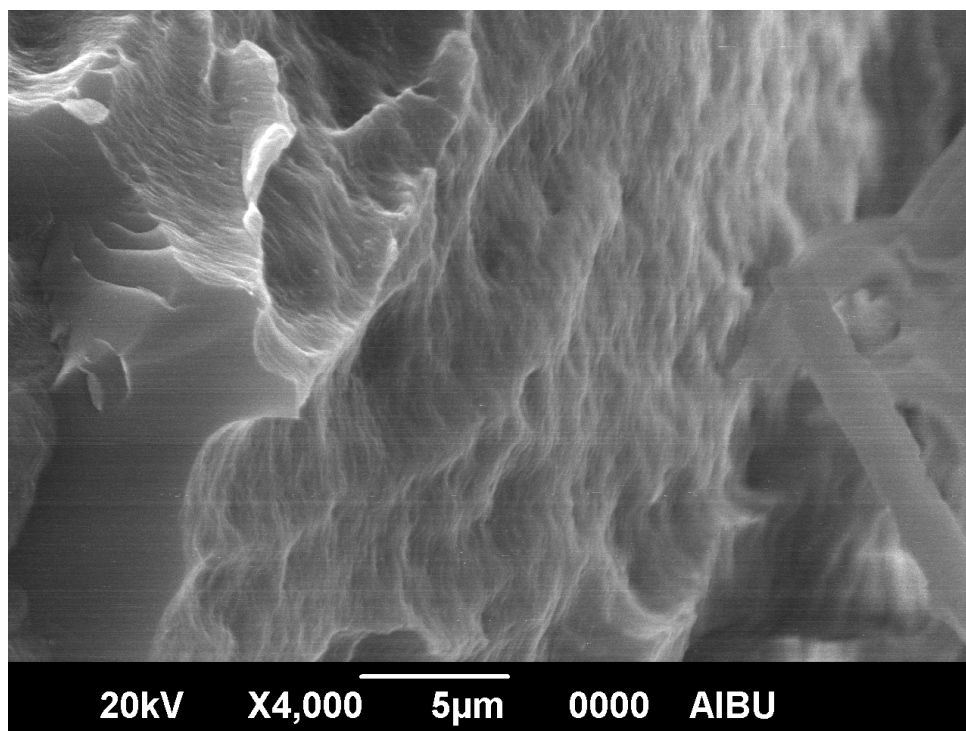


Figure 3.35. SEM photograph of the product with 13.66% poly(BPOCPA), after obtained from tensile test

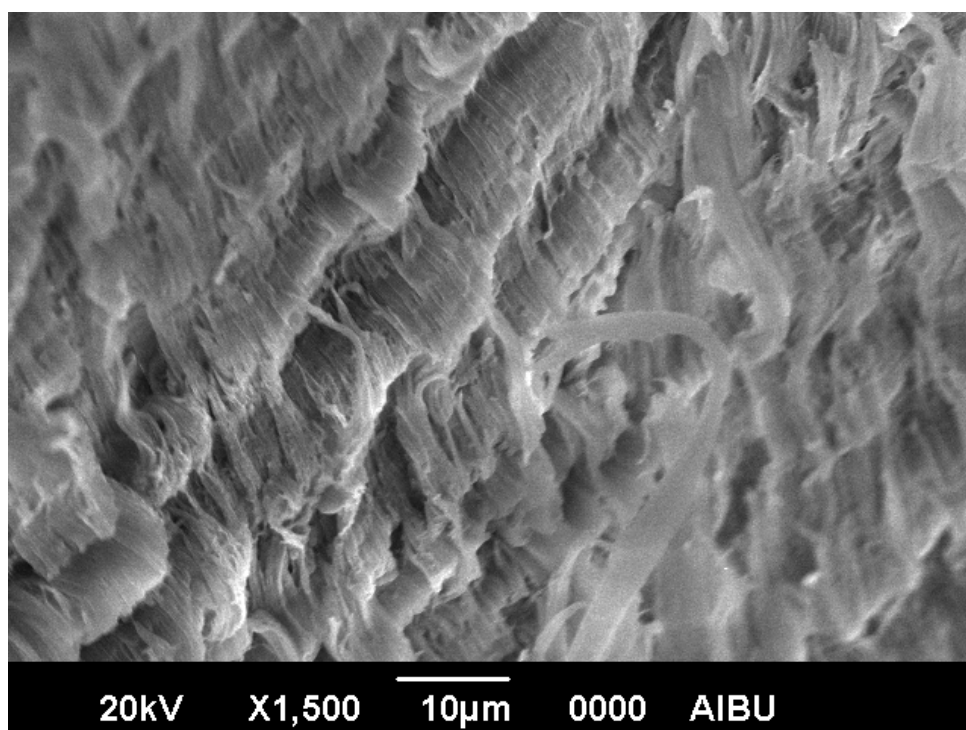


Figure 3.36. SEM photograph of the product with 19.90% poly(BPOCPA), after obtained from tensile test

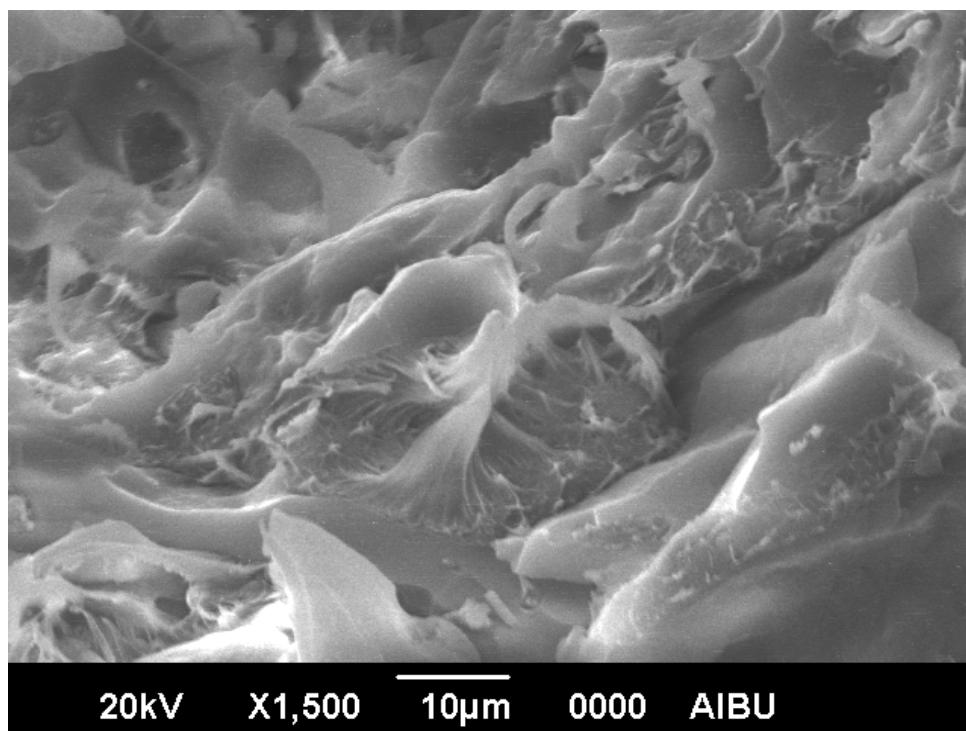


Figure 3.37. SEM photograph of the product with 28.28% poly(BPOCPA), after obtained from tensile test

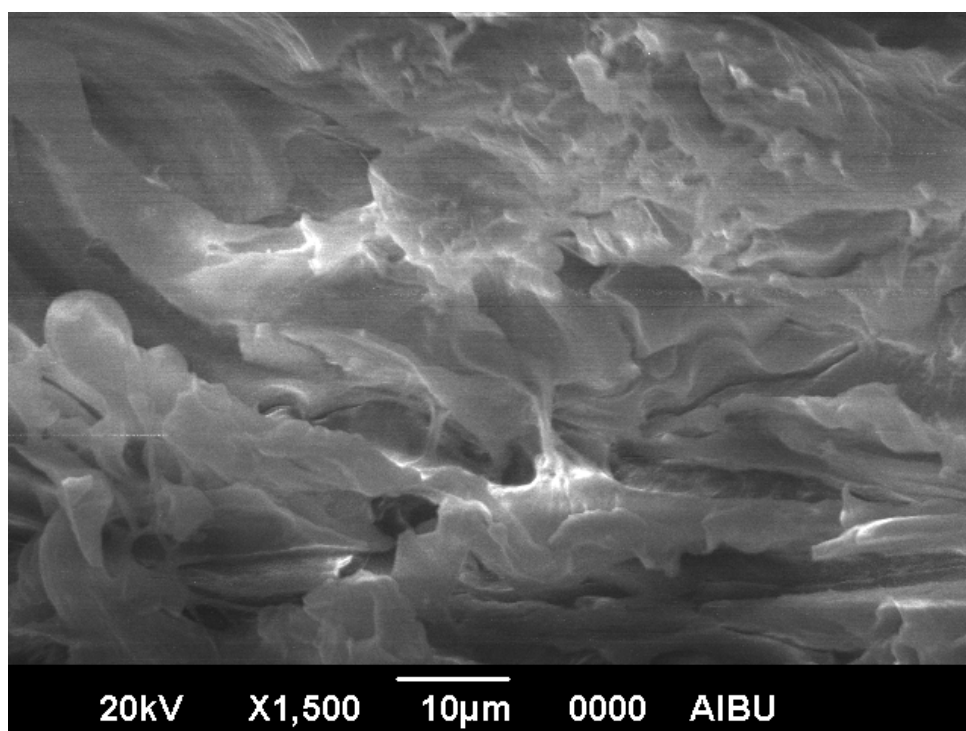


Figure 3.38. SEM photograph of the product with 28.28% poly(BPOCPA), after obtained from tensile test



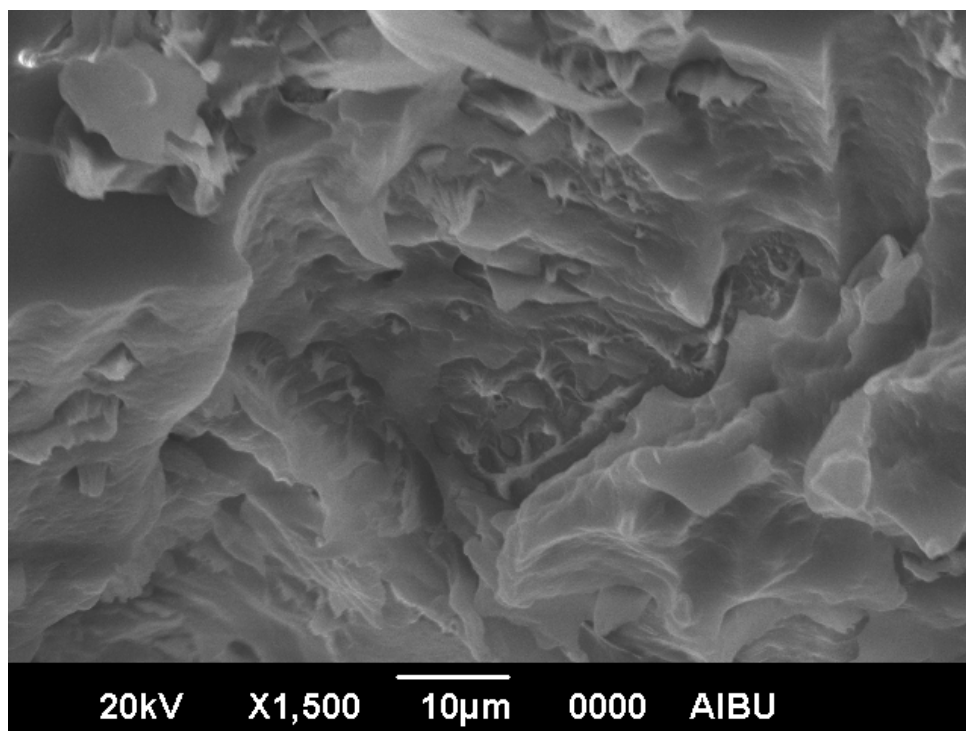


Figure 3.39. SEM photograph of the product with 39.10% poly(BPOCPA), after obtained from tensile test

Impact testing indicated that at higher contents of poly(BPOCPA) the products are in brittle nature and brittleness increased with poly(BPOCPA) percentage. In impact testing, a force is loaded onto the certain area of the test sample in a small time scale, and the time allowed for any orientation of polymer chains is very restricted, i.e. impact energy delocalization is prohibited. Therefore, the energy is localized in the weak regions of the structure of the material to form cracks and voids at the molecular level. However, despite this restriction of orientation of the chains and of impact energy delocalization in a short time, some fibrillation was observed in impact fractures, as short extensions in the sample with 13.66% poly(BPOCPA), Figure 3.40-41. On the other hand, the layered and tortuous structure in the products with the content of 13.66%, 28.28% and 39.10% poly(BPOCPA), Figure 3.42-44, revealed how cracks and voids were produced to failure, indicating the brittle nature in these samples.

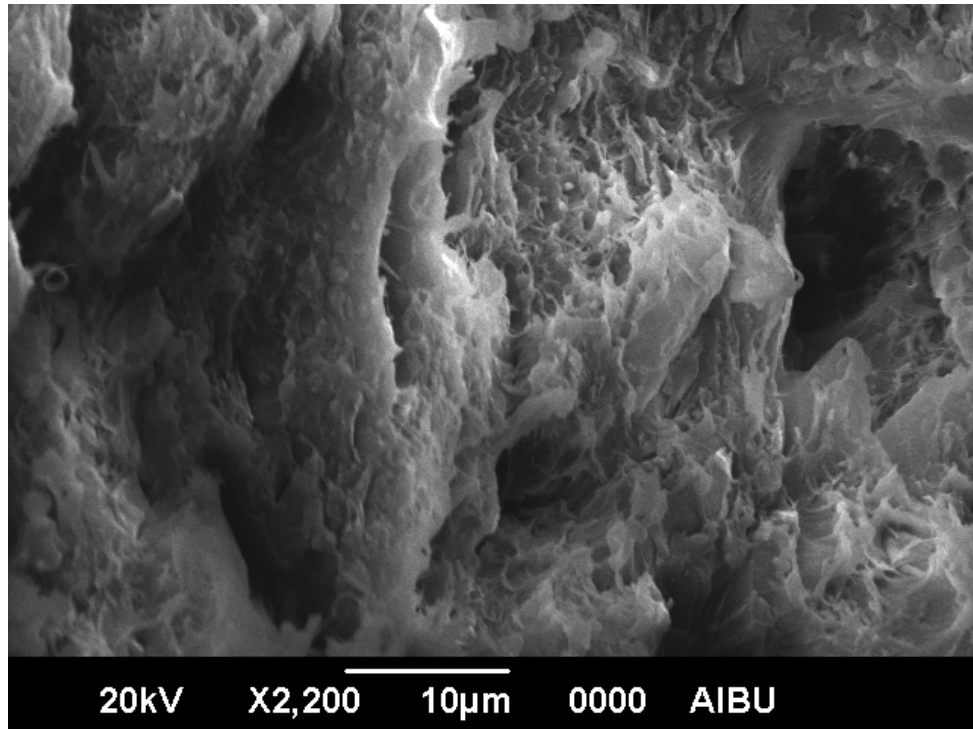


Figure 3.40. SEM photograph of the product with 13.66% poly(BPOCPA), after obtained from impact test

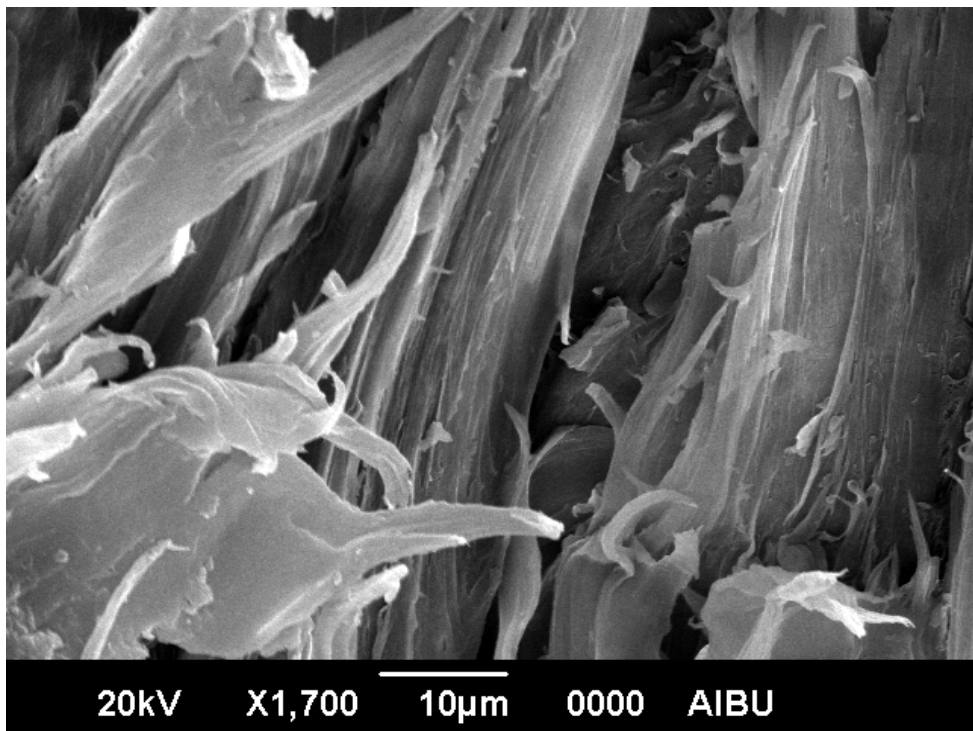


Figure 3.41. SEM photograph of the product with 13.66% poly(BPOCPA), after obtained from impact test

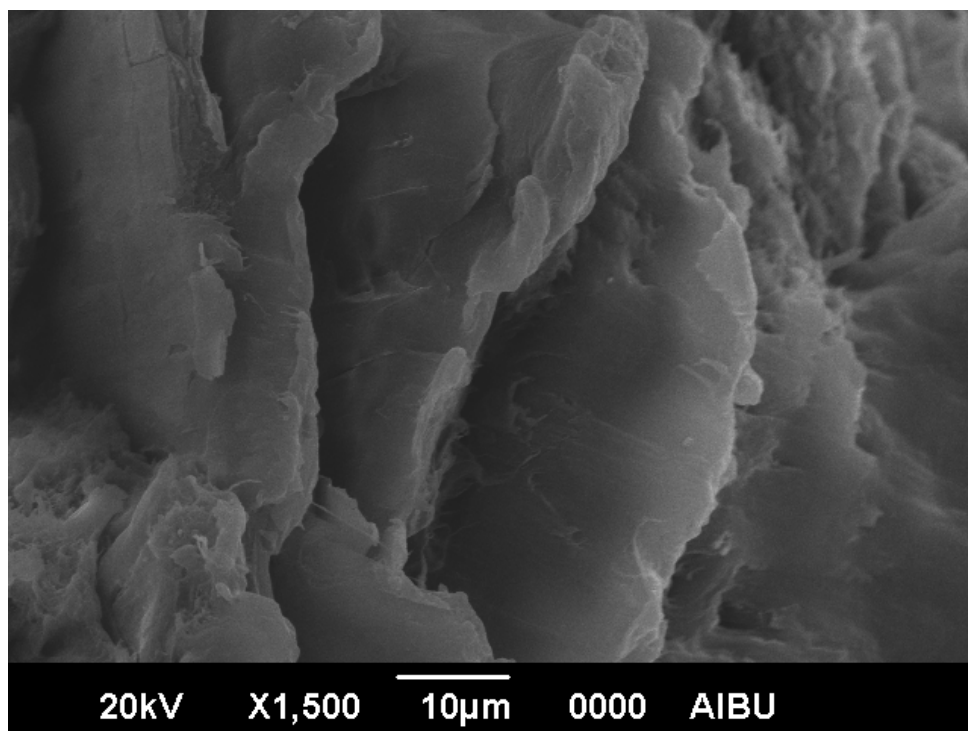


Figure 3.42. SEM photograph of the product with 13.66% poly(BPOCPA), after obtained from impact test

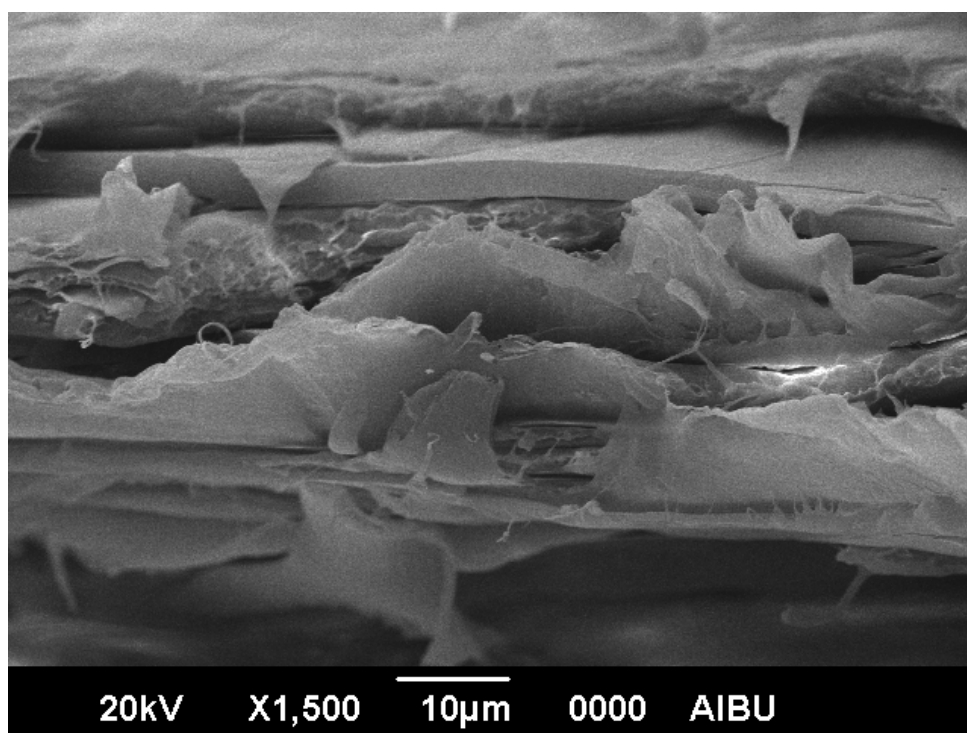


Figure 3.43. SEM photograph of the product with 28.28% poly(BPOCPA), after obtained from impact test

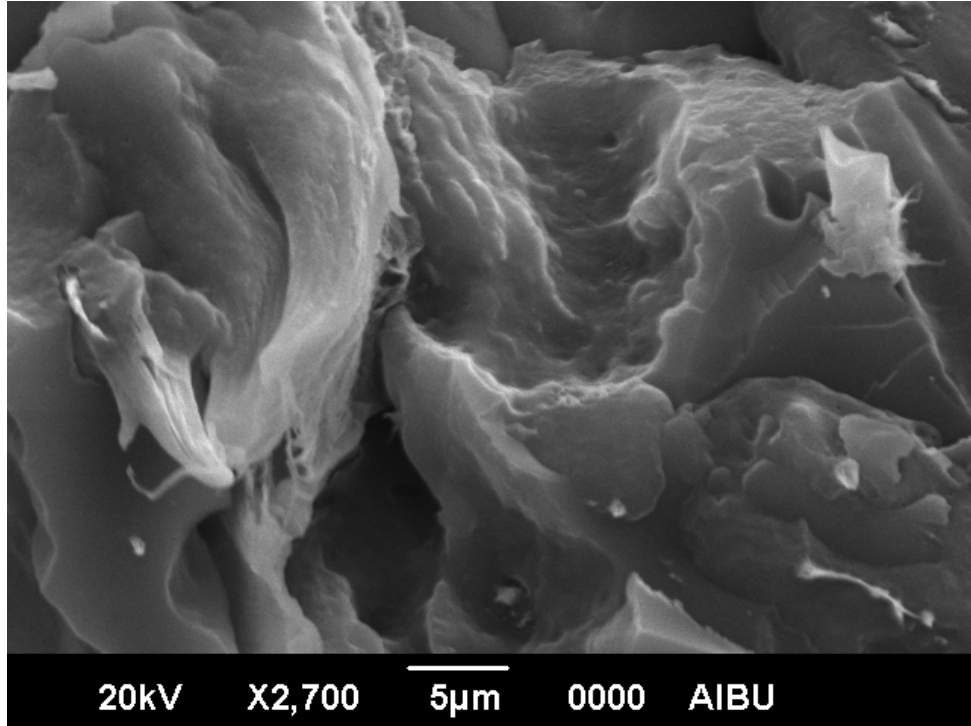


Figure 3.44. SEM photograph of the product with 39.10% poly(BPOCPA), after obtained from impact test

## CHAPTER 4

### CONCLUSION

Poly(BPOCPA) was obtained by solution and bulk melt polymerization of the monomer BPOCPA. The maximum conversion, 94.9%, was achieved by bulk melt polymerization with the initiation of DCP at 140°C.

Thermally induced graft copolymerization of BPOCPA onto HDPE was carried out at 140°C with varying concentration of the monomer (5, 10, 15, 20, 30 and 40%) in the reaction mixture. The amount of grafting increased with increasing concentration of the monomer and reached the maximum, 14.2% poly(BPOCPA), at 30% BPOCPA in the reaction medium.

The graft copolymerization resulted in increase of melting temperature of PE from 131°C to about 134-135°C in the products, while melting temperature of poly(BPOCPA), 231°C, was not observed in general. The only graft coproduct for which poly(BPOCPA) melting temperature was detected, as a weak endotherm at 235°C, was the sample containing 39.1% poly(BPOCPA).

Poly(BPOCPA) degrade, starting at about 275-280°C in both air and nitrogen atmosphere, predominantly by decomposition of side groups giving mainly carbondioxide, phenolic and vinylic groups. PE had a retardation effect in decomposition of the graft coproducts.

The improvement in the mechanical properties was obtained particularly in tensile strength and modulus. The impact strength of the products increased initially with the percentage of poly(BPOCPA), and then decreased dramatically with the content.

All the graft coproducts showed homogeneous structure. At low contents of poly(BPOCPA) the samples were mainly ductile while at high percentages they displayed brittle nature, with an increasing trend with the content.

Improvement of properties of polyolefins with mesomorphic polymers provides an important technique for the preparation of materials with superior properties.

## REFERENCES

- [1] Teegarden, D.M., *Polymer Chemistry: Introduction to Indispensable Science*, National Science Teachers Association, 2004.
- [2] Nwabunma, D., Kyu, T., *Polyolefin Blends*, Wiley, XV, 2008.
- [3] Çetin, S., PhD Thesis, METU, 2004.
- [4] Tice P., *Packaging Materials: 4. Polyethylene for Food Packaging Applications*, International Life Science Institute, 6-7, 2003.
- [5] Malpass, B.D., *Introduction to Industrial Polyethylene: Properties, Catalysts, Processes*, Wiley, 4-16, 2010.
- [6] Lepoutre, P. The Manufacture of Polyethylene (Company Report), Transpak Industries Ltd., 1-2, 1989.
- [7] Saunders K. J., *Organic polymer chemistry: an introduction to the organic chemistry of adhesives, fibers, paints, plastics and rubbers.*, Chapman&Hall, 58, 1994.
- [8] Azapagic A., Emsley A., Hamerton L., *Polymers, the environment and sustainable development*, Wiley, 2003
- [9] Billmeyer, F. W., *Textbook of Polymer Science*, Wiley, New York, 361-366, 1984.
- [10] Averill, B., Eldredge, P., *General Chemistry: Principles, Patterns, and Applications, 1*, 853-854, 2011.

- [11] Onogi, Y., White, J.L., Fellers, J.F., J. Non-Newton. Fluid, 7, 121-151, 1980.
- [12] Çağırıcı, S., Master Thesis, METU, 2006.
- [13] Wang, X.J., Zhou, Q.F., *Liquid Crystalline Polymers*, World Scientific, 6-10, 2004.
- [14] Suto, K., Shimamura, J., White L., Fellers, J.F., SPE ANTEC Tech. Papers, 28, 42, 1982.
- [15] Kenig, S., Polym. Eng. Sci., 27, 887-892, 1987.
- [16] Zachariades AE, Kanamoto T, Porter RS, *High Modulus Polymers: approaches to design and development*, New York, Marcel Dekker, 1-36, 1988.
- [17] La Mantia, F.B., Thermotropic Liquid Crystal Polymer Blends (Chung, T.S.), 185-207, 1993.
- [18] Kiss, G., Polym. Eng. Sci., 27, 410-423, 1987.
- [19] Barham, P.J., Keller A., J. Mater. Sci., 20, 2281-2302, 1985.
- [20] Arrighi, V., Higgins J.S., Polymer, 37, 141-148, 1996.
- [21] Done, D., Baird, D.G., Polym. Eng. Sci, 27, 816-827, 1987.
- [22] Tjong, S.C., Mat. Sci. Eng. A-Struct., 41, 1-61, 2003.
- [23] Qin, Y, Brydon, DL, Mather, RR, Wardman, R.H., Polymer, 34, 3597-3604, 1993.
- [24] Qin, Y, Brydon, DL, Mather, RR, Wardman, R.H., Polymer, 34, 1196-1201, 1993.
- [25] Nwabunma, D., Kyu T., *Polyolefin Blends*, Wiley, 502, 2008.



- [26] Becker, D., Roeder, J., Oliveira R.V.B., Soldi V., Pires A.T.N., *Polym. Test.*, 22, 225-230, 2003.
- [27] O'Donnell, H.J., Baird, D.G., *Polymer*, 36, 1331-3126, 1995.
- [28] Ide, Y., Ophir Z., *Polym. Eng. Sci.*, 23, 261-265, 1983.
- [29] Turek, D.E., Simon, G.P., *Polymer*, 34, 2750-2762, 1993.
- [30] Leng, Y., Chan, H.S., Gao, F., *Compos. Sci. and Technol.*, 62, 757-765, 2002.
- [31] Yan, F., Zhou, Jia., Tian, N., Zhou, Jin., *Polym. Test.*, 24, 270-274, 2005.
- [32] Nobile, M. R., Amendola, E., Nicolais, L., Acierno, D., Carfagna, C., *Polym. Eng. Sci.*, 29, 244-257, 1989.
- [33] Blizard, K. G., Baird, D. G., *Polym. Eng. Sci.*, 27, 653-662, 1987.
- [34] Pilatov, Y.S., *Polymer Reinforcement*, ChemTec. Publishing, 225, 1995.
- [35] Done, D., Biard D.G., *Polym. Eng. Sci.*, 30, 989-995, 1990.
- [36] Datta, A., Chen, H.H., Baird, D.G., *Polymer*, 34, 759-766, 1993.
- [37] Bretas, R.E.S., Baird, D.G., *Polymer*, 33, 5233-5244, 1992.
- [38] Weiss, R.A., Zhang, H., Kuder, J.E., Cangiano, D., *Polymer*, 41, 3069-3082, 2000.
- [39] Yang, W., Chen, J., Yu, G., Wang, M., Ni, H., Shen, K., *J. Mater. Process. Tech.*, 202, 165-169, 2008.
- [40] Albano, C., Perera, R., Catano, L., Karam, A., Gonzalez, G., *J. Mech. Behav. Biomed.*, 4, 467-475, 2011.
- [41] Faruk, O., Matuana, L.M., *Compos. Sci. and Technol.*, 68, 2073-2077, 2008.
- [42] Liu, H., Wu, Q., Zhang, Q., *Bioresource Technol.*, 100, 6088-6097, 2009.

- [43] Zhou, J., Yan, F., Polym. Test., 23, 827-833, 2004.
- [44] Thomas, S., Francis, B., Jose, S., Kocsis, J.K., Polymer, 47, 3874-3888, 2006.
- [45] Odian, G., *Principles of Polymerization* (Wiley-Interscience), 464, 2004.
- [46] Jenkins, A. D., Kratochvíl, P., Stepto, R. F. T., Suter, U. W., Pure Appl. Chem., 68, 2287-2311, 1996.
- [47] Yu, H.Y., He, J.M., Liu, L.Q., He, X.C., Gu, J.S., Wei, X.W., J. Membrane. Sci., 302, 235-242, 2007.
- [48] Zhao, J., Xie, Z., Guo, Z., Lang, G., Wang, J., Appl. Surf. Sci., 229, 124-131, 2004.
- [49] Spencera, M., Parent, J.S., Whitney, R.A., Polymer, 44, 2015-2023, 2003.
- [50] Mai, Y., Wang, X., Zhang, W., Li, Z., Appl. Surf. Sci., 257, 7600-7608, 2011.
- [51] Hsu, C.S., Prog. Polym. Sci., 22, 829-971, 1997.
- [52] Finkelmann, H., Ringsdorf, H., Wendorff, J.H., Makromol. Chem. Phys., 179, 273-276, 1978.
- [53] Collings, P.J., Hird, M., *Introduction to Liquid Crystals*, 1st Edition (Taylor & Francis: London, UK), 174-175, 1997.
- [54] Mihara, T., Tsutsumi, M., Koide, N., Mol. Cryst. Liq. Cryst., 382, 53-64, 2002.
- [55] Hsiue, G.H., Sha, Y.-A., Hsieh, S.-J., Jeng, R.-J., Kuo, W.-J., Liq. Cryst., 28, 365-374, 2000.
- [56] Ganicz, T., Stanczyk, W.A., Gladkova, N.K., Sledzinska, I., Macromolecules, 33, 289-293, 2000.

- [57] Ward M., *Structure and Properties of Oriented Polymers*, Chapman and Hall, 256, 1997
- [58] Wang, X.J., *Prog. Polym. Sci.*, 22, 735-764, 1997.
- [59] Menczel, J., Walsh, J. P. and Wunderlich, B. J., *J. Polym. Sci.*, 19, 837-847, 1981.
- [60] Blumstein, A., Blumstein, R. B., Clough, S. B. and Hsu, E. C., *Macromolecules*, 9, 243-249, 1976.
- [61] Çetin S., Tinçer T., *J. Appl. Polym. Sci*, 108, 414–422, 2008.
- [62] Sessa Sainath, A.V., Rao, A.K, Reddy, A.V.R., *J. Appl. Polym. Sci.*, 75, 465-474, 2000.
- [63] Sessa Sainath A.V., Inoue, T., Yonetaka, K., Koyama,K., *Polymer*, 24, 9859-9862, 2001.
- [64] Zhang, B.O., Hu, J.S., Zang, B.L., Zhou, A.J., *J. Appl. Polym. Sci.*, 88, 1936-1941, 2003.